# The role of the calcium sensing receptor as a modulator of smooth muscle cell mineralisation

*Presented for the degree of Master of Philosophy to Cardiff University*

**Siobhan Briody (0829409)**

**September, 2011**

## Declaration

**DECLARATION**

This work has not previously been accepted in substance for any degree and is not concurrently submitted in candidature for any degree.

Signed …… (candidate)

Date ……

**STATEMENT 1**

This thesis is being submitted in partial fulfillment of the requirements for the degree of MPhil

Signed …… (candidate)

Date ……

**STATEMENT 2**

This thesis is the result of my own independent work/investigation, except where otherwise stated. Other sources are acknowledged by explicit references.

Signed …… (candidate)

Date ……

**STATEMENT 3**

I hereby give consent for my thesis, if accepted, to be available for photocopying and for inter-library loan, and for the title and summary to be made available to outside organisations.

Signed …… (candidate)

Date ……

## Acknowledgments

I must first express my gratitude to my supervisors Dr. Daniela Riccardi and Prof. Paul Kemp for providing me with the opportunity to pursue a Master's program. Particularly to Daniela, I am very thankful for your support and patience throughout the project.

My thanks must also go to my supporting supervisors Dr. Donald Ward and Prof. Ann Canfield, University of Manchester, who invited me into their labs and, in every way, treated me as one of their own students. Without your expertise and guidance throughout the course of this research, this project would not have been possible.

In addition I'd also like to thank the members of the Riccardi, Kemp, Canfield and Ward labs who provided invaluable assistance along the way and made the experience an enjoyable one

Thanks also go to BBSRC and Amgen whose funding made this project possible.

Finally I would like to thank my family for their continued faith and patience. My parents taught me the value of education and to believe in myself, for which I can never thank them enough and my sister showed me anything is possible with hard work and a few sleepless nights.

## Table of contents


| | Page numbers |
|---|---|
| Abstract | viii |
| Abbreviations | ix |
| List of figures | xii |
| List of tables | xvi |
| **Chapter 1: Introduction** | 1 |
| 1.1 Vascular calcification in chronic kidney disease | 1 |
| 1.2 Mechanisms of vascular calcification in CKD | 4 |
| 1.2.1. Dysregulated mineral metabolism as a trigger for calcification in CKD | 6 |
| 1.2.1.1 Dysregulated mineral homeostasis in CKD | 6 |
| 1.2.1.2 Hyperphosphatemia as risk factor / contributor to vascular calcification | 9 |
| 1.2.1.3 Hypercalcaemia as risk factor / contributor to vascular calcification | 11 |
| 1.2.2. Inhibitors of vascular calcification | 12 |
| 1.3.1.1 Fetuin A | 13 |
| 1.3.1.2 Matrix γ-carboxyglutamic acid protein | 15 |
| 1.3.1.3 Osteopontin | 17 |
| 1.3.1.4 Pyrophosphate | 17 |
| 1.3.1.5 Osteoprotegerin | 18 |
| 1.3 Introduction to the calcium sensing receptor (CaSR) | 20 |
| 1.3.1 Structure of the CaSR and downstream signalling pathways | 21 |
| 1.3.2 Pharmacology of the CaSR | 24 |

1.4 Calcimimetics in vascular calcification 26
1.4.1 A systemic role for calcimimetics in the protection against vascular calcification 26
1.4.2 A protective role for calcimimetics on smooth muscle cells 27
1.4.2.1 CaSR expression in SMC 28
1.4.2.2 SMC CaSR and mineralisation 28

1.5 Aims of this research 30

**Chapter 2: Methods** 32
2.1 Cell culture 32
2.1.1 Isolation and culture of BAoSMC 32
2.1.2 Culture of human SMC 33
2.2 Immunofluorescence 33
2.2.1 α-smooth muscle actin (α-sma) staining 33
2.2.2 CaSR staining 34
2.3 Mineralisation assays 35
2.3.1 $Ca^{2+}$ experiments 35
2.3.2 Calcimimetic experiments 35
2.3.3 Alizarin red staining 36
2.3.4 $Ca^{2+}$ deposition assay 36
2.4 Alkaline phosphatase (ALP) activity 37
2.5 Assessment of protein content 38
2.6 Western blotting 38
2.6.1 ERK activation assay 38
2.6.2 CaSR western blotting 40
2.7 Bio-Plex phosphoprotein detection array 40
2.8 Adenoviral infection 44
2.9 RT-PCR 44
2.9.1 RNA isolation 44
2.9.2 First strand cDNA synthesis 45
2.9.3 PCR 46

2.10 Statistical analysis 46

**Chapter 3: Results** 50
3.1 Characterisation of explanted cells 50
3.2 Assessment of CaSR immunoreactivity in BAoSMC 55
3.3 Assessment of CaSR mRNA expression in BAoSMC 57
3.4 $Ca^{2+}$ increases mineralisation and osteogenic differentiation in BAoSMC in the presence of BGP 59
3.5 $Ca^{2+}$-induced mineralisation may, at least in part, be independent of the CaSR 63
3.6 The effect of calcimimetics on mineral deposition by BAoSMC 65
3.7 Signalling profile(s) induced by acute $Ca^{2+}$ and calcimimetic incubation 69
3.7.1 $Ca^{2+}$-induced signalling in HAoSMC 73
3.7.2 Calcimimetic-induced signalling in HAoSMC 75

**Chapter 4: Discussion** 77
4.1 Characterisation of explant cultures 77
4.1.1 α-sma expression and mineralisation potential 77
4.1.2 CaSR expression in BAoSMC 78
4.2 The effect of CaSR activation on SMC mineralisation 80
4.2.1 The effect of $Ca^{2+}$ on SMC mineralisation 80
4.2.1.1 Understanding the process of $Ca^{2+}$-induced mineralisation 82
4.2.2 The effect of calcimimetics on SMC mineralisation 84
4.2.2.1 Calcimimetic-induced signalling in SMC 84
4.2.2.2 Implications for mineralisation 86
4.5 Conclusions 87
4.6 Limitations of current work 87
4.7 Future research questions and directions 89

**Chapter 5: References** 92

**Chapter 6: Appendix** 117
6.1 Serum batch testing 117
6.2 Supplementary figures 117

## Abstract

Background: Vascular calcification is a common complication of advanced chronic kidney disease, contributing to increased cardiovascular mortality. Hypercalcaemia is a recognised risk factor for calcification, and calcimimetics show protective actions in vivo. In addition to its central role in $Ca^{2+}$ homeostasis, the calcium sensing receptor (CaSR) has been identified in smooth muscle cells, suggesting extracellular $Ca^{2+}$ and calcimimetics may have a more direct role in the modulation of mineralisation.

Methods and results: The presence of CaSR in bovine aortic smooth muscle cells (BAoSMC) is confirmed using immunofluorescence and western blot. In an in vitro model of calcification (i.e. β-glycerophosphate induction) $Ca^{2+}$ dose-dependently increases SMC mineralisation and induces alkaline phosphatase activity. Transfecting cells with a dominant negative CaSR does not attenuate $Ca^{2+}$-induced SMC mineralisation. Confirming previous reports, calcimimetics R-568 (1 nM) and AMG641 (10 pM, 100 pM and 1nM) delay the process of calcification. However S-568 (1 nM), an isomer of R-568 that shows little/no activity at the CaSR, fails to elicit any protective effects. The signalling pathways activated by R-568 (1nM), in the presence of 2.5 mM $Ca^{2+}$ are investigated in human aortic smooth muscle cells (HAoSMC) using a multibead phosphoprotein detection array. R-568 (1 nM) produces significant elevations in MEK and p90RSK phosphorylation. The relevance of these molecules in the mineralisation process is not investigated, although it is interesting to note that, elevations in MEK and p90RSK phosphorylation are not observed in HAoSMC incubated with $Ca^{2+}$ alone (i.e. 5 mM $Ca^{2+}$ vs. 0.5 mM $Ca^{2+}$).

Conclusions: These results suggest that the delay in mineralisation afforded by calcimimetics are mediated via the CaSR, whilst the increased mineralisation observed when cells are exposed to 1.8 mM $Ca^{2+}$ are, at least in part, independent of the CaSR.

## Abbreviations

| | |
|---|---|
| $1,25(OH)_2D_3$ | 1,25-dihydroxyvitamin D |
| 7TMD | 7 transmembrane domain |
| $25(OH)D_3$ | 25-hydroxyvitamin D |
| ADH | Autosomal dominant hypocalcaemia |
| ALP | Alkaline phosphatise |
| ApoE | Apolipoprotein E |
| α-sma | α-smooth muscle actin |
| BAD | Bcl-2 associated death promoter |
| BAoSMC | Bovine aortic smooth muscle cell |
| BGP | β-glycerophosphate |
| BMP-2 | Bone morphogenetic protein 2 |
| BMP-4 | Bone morphogenetic protein 4 |
| BSA | Bovine serum albumin |
| $Ca^{2+}$ | Calcium ion |
| cAMP | Cyclic adenosine monophosphate |
| Ca x P | Calcium-phosphate product |
| Cbfa1 | Core binding factor alpha 1 |
| CaSR | Calcium sensing receptor |
| cDNA | Complementary DNA |
| CKD | Chronic kidney disease |
| CREB | cAMP response element-binding |
| DAPI | 4',6-diamidino-2-phenylindole |
| DMEM | Dulbecco's Modified Eagle Medium |
| DMSO | Dimethyl sulfoxide |
| dnCaSR | Dominant negative CaSR |
| dp- | Dephosphorylated |
| ECD | Extracellular domain |
| ENPP1 | Ectonucleotide pyrophosphate/phosphodiesterase1 |
| ERK | Extracellular signal-regulated kinases |
| ESRD | End stage renal disease |

| | |
|---|---|
| FCS | Fetal calf serum |
| FGF-23 | Fibroblast growth factor 23 |
| FHH | Familial hypocalciuric hypercalcaemia |
| FITC | Fluorescein isothiocyanate |
| GPCR | G protein coupled receptor |
| GAPDH | Glyceraldehyde 3-phosphate dehydrogenase |
| HAoSMC | Human aortic smooth muscle cell |
| HBSS | Hank's balanced saline solution |
| HEK | Human embryonic kidney cell |
| HSP27 | Heat shock protein 27 |
| IIAC | Idiopathic infantile arterial calcification |
| IGF-1R | Insulin like growth factor 1 receptor |
| $IK_{Ca}$ | Intermediate conductance calcium-activated potassium channels |
| $IP_3$ | Inositol trisphosphate |
| JNK | Jun N-terminal kinase |
| MAPK | Mitogen-activated protein kinase |
| MGP | Matrix γ-carboxyglutamic acid |
| mRNA | Messenger RNA |
| Msx2 | Msh homebox 2 |
| MV | Matrix vesicles |
| NF- κβ | Nuclear factor – κβ |
| NSHPT | Neonatal severe primary hyperparathyroidism |
| OPG | Osteoprotegerin |
| OPN | Osteopontin |
| $PO_4^{3-}$ | Phosphate |
| p70 S6K | p70 S6 kinase |
| p90RSK | p90 ribosomal S6 kinase |
| PBS | Phosphate buffered saline |
| PDGF | Platelet derived growth factor |
| PIK4 | Phosphatidylinositol 4-kinase |
| Pit-1 | Phosphate transporter 1 |

| | |
|---|---|
| PKC | Protein kinase C |
| PLA2 | Phospholipase A2 |
| PLC | Phospholipase C |
| PLD | Phospholipase D |
| PPi | Pyrophosphate |
| PTH | Parathyroid hormone |
| R-568 | N-[3-[2-chlorophenyl]propyl]-[R]-α-methyl-3-methoxybenzylamine |
| ROS | Reactive oxygen species |
| RT | Room temperature |
| S-568 | S-[3-[2-chlorophenyl]propyl]-[R]-α-methyl-3-methoxybenzylamine |
| SHPT | Secondary hyperparathyroidism |
| siRNA | Small interfering RNA |
| SMC | Smooth muscle cell |
| TNAP | Tissue non-specific alkaline phosphatase |
| TNF | Tumour necrosis factor |
| Tyk2 | Tyrosine kinase 2 |
| uc- | Uncarboxylated |
| VDR | Vitamin D receptor |
| VFTD | Venus fly trap domain |
| WT | Wild type |

## List of figures


| | Page number |
|---|---|
| **Figure 1.1** Cardiovascular mortality rates (per 1000 person-years) in dialysis patients vs. the general population (GP) (adapted from de Jager et al. (2009)). | 1 |
| **Figure 1.2** Coronary artery calcification of a CKD patient (adapted from Amann K. (2008)). | 3 |
| **Figure 1.3** Mechanisms contributing to the initiation and promotion of vascular calcification. | 5 |
| **Figure 1.4** $Ca^{2+}$ and $PO_4^{3-}$ homeostasis (adapted from Renekema et al. (2008)). | 7 |
| **Figure 1.5** Time course of biochemical changes in rats with anti-GBM nephritis (adapted from Hasgawa et al. (2010)). | 8 |
| **Figure 1.6** Schematic illustrating the balance of inhibitors and inducers and the shift that results as patients move to CKD. | 13 |
| **Figure 1.7** Mineralised blood vessels in MGP deficient mice (taken from Luo et al. (1997)). | 16 |
| **Figure 1.8** Schematic representation of the CaSR (adapted from Saidak et al. (2009)). | 22 |
| **Figure 1.9** Protective effect of AMG641 in aortic mineralisation in adenine fed animals (taken from Henley et al. (2009)). | 27 |
| **Figure 1.10** Overexpression of the dominant negative calcium | 29 |

sensing receptor (dnCaSR) enhances mineralisation (taken from Alam et al. (2009)).

**Figure 2.1** Schematic diagram illustrating the structure of the aorta, showing the intima, media and adventita, and positioning of smooth muscle cells (taken from Ashley and Niebauer (2004)). 32

**Figure 2.2** The methodological processes and rationale underlying the Bioplex assay (adapted from Bioplex manual). 42

**Figure 2.3** Binding sites of primer sets on the Bos taurus CaSR sequence (NM_174002). 47

**Figure 3.1** Immunostaining of bovine aortic explanted cells (prep A-C) with α-sma. 51

**Figure 3.2** Mineralisation potential of explanted BAoSMC (prep A-C). 52

**Figure 3.3** Effect of 2.5 mM $Ca^{2+}$ and 5 mM BGP on cell morphology and distribution (prep A-C). 54

**Figure 3.4** CaSR immunoreactivity in BAoSMC. 56

**Figure 3.5** Calcium-sensing receptor (CaSR) mRNA expression was not detected in BAoSMC**.** 58

**Figure 3.6** $Ca^{2+}$-induced mineralisation requires the presence of BGP. 59

**Figure 3.7** Concentration-dependent effects of $Ca^{2+}_{o}$ on SMC mineral deposition. 61

**Figure 3.8** Alkaline phosphatase activity in BAoSMC is $Ca^{2+}$ dependent. 62

**Figure 3.9** Effect of overexpressing a dominant negative adenoviral CaSR on $Ca^{2+}$-induced mineralisation in BAoSMC. 64

**Figure 3.10** Effect of AMG641 on $Ca^{2+}$-induced mineralisation. 66

**Figure 3.11** Protective actions of R-568 on $Ca^{2+}$-induced mineralisation. 67

**Figure 3.12** S-568 does not delay $Ca^{2+}$-induced mineralisation. 68

**Figure 3.13** CaSR like immunoreactivity in human aortic SMCs. 70

**Figure 3.14** ERK phosphorylation in the presence of 0.5 mM or 5.0 mM $Ca^{2+}$ in CaSR-HEK and BAoSMC. 74

**Figure 6.1** Serum batch testing. 117

**Figure 6.2** CaSR immunoreactivity in BAoSMC (supplement to Figure 3.4). 118

**Figure 6.3** $Ca^{2+}$-induced mineralisation requires the presence of BGP (supplement to Figure 3.6). 119

**Figure 6.4** Concentration-dependent effects of $Ca^{2+}_o$ on SMC mineral deposition (supplement to Figure 3.7). 120

**Figure 6.5** Effect of AMG641 on $Ca^{2+}$-induced mineralisation (supplement to Figure 3.10). 121

**Figure 6.6** Protective actions of R-568 on $Ca^{2+}$-induced 122

mineralisation (supplement to Figure 3.11).

**Figure 6.7** S-568 does not delay $Ca^{2+}$-induced mineralisation (supplement to 3.12). 123

## List of tables


| | | Page number |
|---|---|---|
| **Table 2.1** | Phosphorylation sites targeted by Bioplex antibodies. | 43 |
| **Table 3.1** | $Ca^{2+}$-induced signalling in CaSR-HEK cells. | 72 |
| **Table 3.2** | $Ca^{2+}$-induced signalling in SMCs. | 73 |
| **Table 3.3** | R-568-induced signalling in SMCs. | 76 |

# Chapter 1: Introduction

## 1.1 Vascular calcification in chronic kidney disease (CKD)

Calcification of the cardiovascular system is associated with a number of diseases including metabolic syndrome, diabetes, hypertension and atherosclerosis. However, its most devastating manifestation is in patients with chronic kidney disease (CKD), the focus of this work. Patients with CKD, particularly end stage renal disease (ESRD), show a disproportionate burden of vascular calcification[1-4] which contributes to the markedly increased cardiovascular risk and mortality in these patients (Figure 1.1).


**Figure 1.1 Cardiovascular mortality rates (per 1000 person-years) in dialysis patients vs. the general population (GP) (adapted from de Jager et al. (2009)[5]).**

*de Jager DJ, Grootendorst DC, Jager KJ, van Dijk PC, Tomas LM, Ansell D, Collart F, Finne P, Heaf JG, De Meester J, Wetzels JF, Rosendaal FR, Dekker FW. Cardiovascular and noncardiovascular mortality among patients starting dialysis. Jama. 2009;302:1782-1789*

In general, the prevalence and intensity of vascular calcification increases as kidney function declines. Although calcification can be present at early stages of CKD[6, 7], increased calcification is observed prominently once a patient enters ESRD and requires dialysis treatment[1, 6, 8]. It has been suggested that dialysis may prime arteries to develop vascular calcification[9] as more rapid progression of vascular calcification is detected in dialysis patients compared to the general population[1, 10].

The majority of CKD patients who require dialysis die as a result of cardiovascular events, and the presence and extent of vascular calcification are independent predictors of cardiovascular disease and mortality[11]. Arterial

calcification leads to a number of adverse clinical outcomes i.e. myocardial infarction, congestive heart failure, valvular heart disease[3, 11, 12] that can cause cardiovascular disease or aggravate its severity.

Calcification can occur at two distinct sites in the vessel wall: the intima and the media and both types of arterial calcification can occur in CKD. Intimal calcification involves localised calcification in the vicinity of lipid or cholesterol deposits within an atherosclerotic plaque. Calcification can be detected on the shoulders and at the base of the plaque[13]. Intimal calcification is thought to be triggered by inflammatory processes[14]. In an in vivo model of atherosclerosis, accumulation of infiltrating macrophages was shown to be one of the earliest steps in the calcification processes, potentially acting as a trigger for further pro-calcifying actions[15].

Medial calcification (also known as Mönckeberg's sclerosis) is typically observed as a pipeline-like distribution and can occur all around the vessel[16]. In contrast to intimal calcification, it occurs in the absence of lipid or cholesterol deposits[17] and without macrophage infiltration suggesting that distinct mechanisms may underlie the development of these two types of calcification.

Intimal and medial calcification also differ in their clinical consequences. Medial calcification results in stiffening of the vasculature and reduced vascular compliance which is associated with increased pulse pressure[18, 19] and left ventricular hypertrophy[20]. Whereas, intimal $Ca^{2+}$ deposition may contribute to atherosclerotic plaque instability[21] which can cause myocardial infarction and thrombotic events.

**Figure 1.2 Coronary artery calcification of a CKD patient (adapted from Amann K. (2008)[17]).** Both intimal (*) and medial calcification (arrow) are observed in hematoxylin and eosin (H&E) stain (A) and Kossa stain (B).

*Amann K. Media calcification and intima calcification are distinct entities in chronic kidney disease. Clinical journal of the American Society of Nephrology : CJASN. 2008;3:1599-1605*

In CKD patients, one or both of intimal and medial calcification can be observed[4, 22] (Figure 1.2). Looking at a select subgroup of individuals with coronary artery disease and varying kidney function, Nakamuru et al. (2009) found that intimal calcification is observed in most cases of vascular calcification with CKD, across stages 1-5, whereas medial calcification is typically only present when more severe CKD ensues i.e. CKD stage 4/5 and haemodialysis patients[6]. Despite the delay in presentation, the development of medial calcification does not appear to be dependent on intimal calcification as medial calcification can be identified in segments that show no signs of intimal calcification[17].

Amongst haemodialysis patients the presence of predominantly intimal calcification has been shown to be associated with a relative higher risk in mortality compared to predominantly medial calcification[16]. Additionally within the dialysis population, patient characteristics influence the likelihood of developing intimal or medial calcification: intimal calcification is typically observed in older patients with a conventional atherosclerotic risk factors whereas medial calcification is observed in younger patients and is related to the time on dialysis and the Ca x P balance[16].

## 1.2 Mechanisms of vascular calcification in CKD

Knowledge of the mechanisms underlying vascular calcification have greatly increased in recent years. Thinking has evolved from the original hypothesis suggesting that vascular calcification is a passive degenerative process, to understanding vascular calcification to be a highly regulated, active, cell–mediated process that involves phenotypic change[23, 24]. The process shows many similarities to bone formation and cells with osteoblastic and chondrogenic potential have been identified in vascular tissue[25-28].

There is growing acceptance that smooth muscle cells (SMCs) undergo a phenotypic transition and act as the source of the osteochondrogenic precursors. SMCs are the predominant cell type found in the artery wall and unlike most cell types, retain phenotypic plasticity in response to injurious stimuli. With treatment of pro-calcifying stimuli, SMC cultures can be induced to express osteoblastic and chondrogenic transcription factors whilst in parallel showing reduced expression of SMC marker proteins (i.e. expression of α-smooth muscle actin and SM22α)[29, 30]. Evidence in favour of SMCs as the source of the osteochondrogenic precursors came with the findings by Speer et al. (2009) who, using genetic fate mapping of matrix Gla protein mutant mice (MGP -/-), identified that the chondrocytic cells identified in areas of calcification had differentiated from SMCs[29].

The onset of expression of bone marker proteins, and reduced expression of SMC markers, appears to be a trigger for mineralisation rather than a consequence, as these events precede calcification[29]. Moreover, a recent report by Speer et al. (2010) suggests that it is primarily the induction of the osteogenic transcription factors and not the loss of the SMC markers which promote mineralisation[30]. Loss of myocardin alone does not appear to drive an osteochondrogenic phenotype change or an increased propensity to mineralise[30]. Similarly, forced expression of SMC markers does not affect the calcification ability of SMCs when treated with the pro-calcifying factor, inorganic phosphate[30]. However, that is not to say that the reduced expression of SMC markers is just a consequence of SMC transdifferentiation as in cases of arterial injury, expression of SMC markers appears to be

protective. A recent study demonstrated that mice deficient in SM22α exhibit enhanced medial chondrogenesis in response to arterial injury compared to their wild type counterparts[31].

Of particular interest within these recent studies is data suggesting that SMC transdifferentiation may be reversible and cells can regain SMC properties[30]. When cultured in medium that favours SMC differentiation (i.e. supplemented with 20% FBS) vascular cells with an osteochondrogenic phenotype regained SMC properties showing increased expression of SMC marker proteins (i.e. SM22α and α-sma), in parallel to reduced expression of osteochondrogenic gene expression[30]. Additional support for the reversibility of vascular SMCs in the osteochondrogenic state is provided by data reporting that sevelamer (a phosphate binder) reduces established calcification in a mouse model of atherosclerosis and CKD[32]. Together these findings suggest that vascular calcification may be therapeutically treated and potentially reversed.

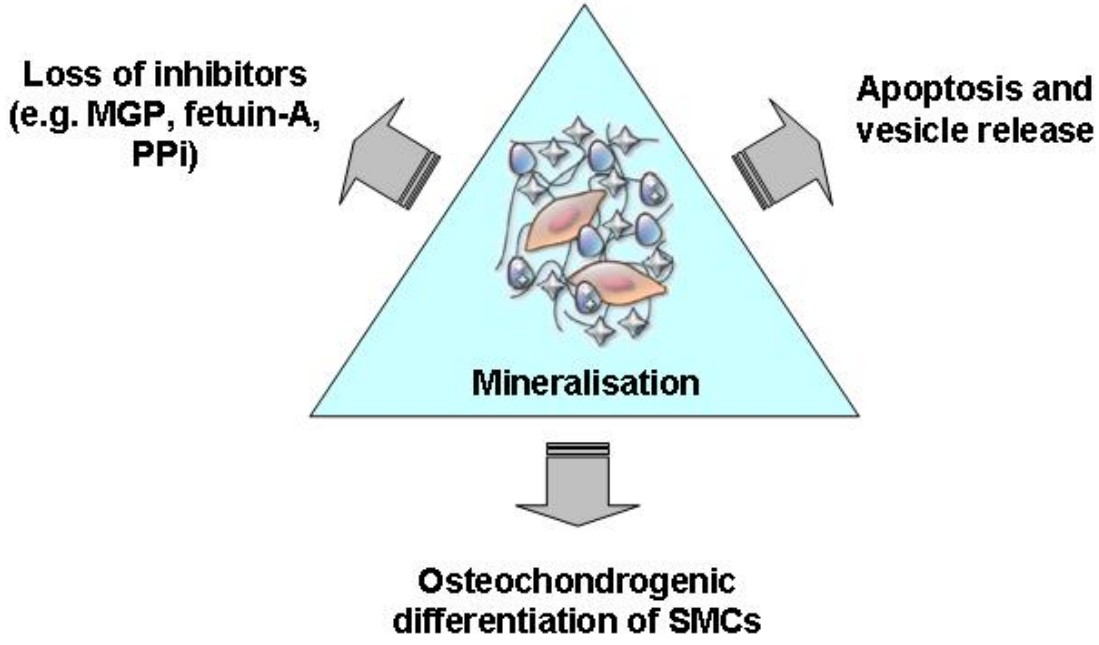


**Figure 1.3 Mechanisms contributing to the initiation and promotion of vascular calcification.** Loss of mineralisation inhibitors (for example, matrix Gla protein (MGP), fetuin-A and pyrophosphate (PPi)), cellular apoptosis and the production of calcifying matrix vesicles, and transdifferentiation of SMCs all contribute to process of mineralisation.

The complete mechanism underlying transdifferentiation and mineralisation is still under investigation. A number of key events contribute to vascular calcification initiation and progression (Figure 1.3), including dysregulated mineral metabolism, loss of local and systemic inhibitors of calcification, induction of apoptosis and matrix vesicle (MV) release, and development of a calcifiable extracellular matrix[26, 33].

### 1.2.1 Dysregulated mineral metabolism as a trigger for calcification in CKD

Abnormal regulation of mineral ion homeostasis is one of the major problems in patients with CKD and is strongly linked to the development of calcification. There is increasing evidence that hyperphosphatemia, hypercalcaemia, an increased Ca × P product and hyperparathyroidism may increase susceptibility to develop vascular calcification[34]. Direct actions of elevated levels of phosphate and $Ca^{2+}$ on SMCs have been shown and their contribution to calcification beginning to be unravelled, discussed in sections 1.2.1.2 and 1.2.1.3 respectively.

#### 1.2.1.1 Dysregulated mineral homeostasis in CKD

In normal physiology $Ca^{2+}$ and phosphate levels are under tight control via a number of hormonal regulators which work through concerted actions on the intestine, kidney and bone. Hormonal regulators of phosphate metabolism include parathyroid hormone (PTH), $1,25(OH)_2D_3$, FGF-23 and klotho. PTH, $1,25(OH)_2D_3$ and klotho are also regulators of $Ca^{2+}$ metabolism. The actions of these hormonal regulators are illustrated in Figure 1.4. The physiological role of calcitonin in humans remains unclear, although inhibition of bone resorption is detected at pharmacological doses underlying its use for Paget's disease, osteoporosis and hypercalcaemia of malignancy[35]. For detailed reviews on $Ca^{2+}$ and phosphate homeostasis see Bergwitz and Juppner (2010)[36], Renkema et al. (2008)[37].

**Figure 1.4 $Ca^{2+}$ and phosphate homeostasis (adapted from Renekema et al. (2008)[37]).** Mechanisms responsible for the control of $Ca^{2+}$ and phosphate (Pi) homeostasis are interlinked. The calcium sensing receptor (CaSR) in the parathyroid glands responds to free extracellular $Ca^{2+}$ and modulates PTH secretion. PTH acts directly, on renal $Ca^{2+}$ reabsorption, and indirectly, via stimulation of $1,25(OH)_2D_3$ production, to increase serum $Ca^{2+}$. Hyperphosphatemia also stimulates secretion of PTH, which acts directly to increase urinary excretion of phosphate whilst indirectly increases intestinal absorption via $1,25(OH)_2D_3$. Both PTH and $1,25(OH)_2D_3$ stimulate the FGF-23-klotho axis, increasing Pi excretion. To ensure tight regulation of $Ca^{2+}$ and Pi homeostasis numerous feedback loops exist – $1,25(OH)_2D_3$ inhibits PTH secretion, and FGF-23 inhibits the synthesis of $1,25(OH)_2D_3$ and PTH.

*Renkema KY, Alexander RT, Bindels RJ, Hoenderop JG. Calcium and phosphate homeostasis: Concerted interplay of new regulators. Annals of medicine. 2008;40:82-91*

In CKD, the mechanisms that normally ensure tight control of serum phosphate and $Ca^{2+}$ levels are dysregulated and cannot sufficiently compensate for changes in serum phosphate and $Ca^{2+}$. With renal insufficiency the ability of the kidney to excrete phosphate and generate $1,25(OH)_2D_3$ is compromised. Additionally, in CKD changes in the expression of the hormonal regulators, and the relationship between them, contribute to the mineral dysregulation observed and development of secondary hyperparathyroidism.

In humans, FGF-23 levels rise in parallel to declining renal function[38-40]. Stimulation of FGF-23 is typically triggered by elevations in serum phosphate or increased $1,25(OH)_2D_3$. However the trigger in early CKD remains unclear as FGF-23 levels appear to increase before the development of hyperphosphatemia [41, 42]. Using a model of progressive CKD in rats, Hasegawa et al. (2010) assessed the development of mineral dysregulation by evaluating different biochemical parameters in the serum over an extended

timeframe. Interestingly, significant elevations in FGF-23 were detected on day 10, while increased phosphate was not detected until day 30 (Figure 1.5). Although Hasegawa et al. (2010) described FGF-23 as the first biochemical change, it has also been shown that PTH is necessary for the initial elevation in FGF-23 levels, as a parathyroidectomy prevented the increase in FGF-23 in kidney failure rats[43]. Therefore the onset of events may be more complex than shown (Figure 1.5).

FGF-23 inhibits 1α-hydroxylase, a key enzyme in the development of $1,25(OH)_2D_3$ [44-47] and can also stimulate 24-hydroxylase, an enzyme involved in the inactivation of vitamin D metabolites[46]. Therefore, increased levels of FGF-23 result in reductions in $1,25(OH)_2D_3$, further confounded by the reduced capacity of the kidney to convert $25(OH)D_3$. With reduced generation of $1,25(OH)_2D_3$, and therefore reduced intestinal $Ca^{2+}$ absorption, hypocalcaemia ensues. Hypocalcaemia acts as a stimulus for PTH secretion, which acts on the bone to increase serum $Ca^{2+}$ and in doing so also increases serum phosphate. As the glomerular filtration rate declines in advanced CKD, inefficient urinary phosphate excretion combined with disordered bone remodelling results in hyperphosphatemia.

**This image has been removed by the author for copyright reasons.**

**Figure 1.5 Time course of biochemical changes in rats with anti-GBM nephritis (adapted from Hasegawa et al. (2010)[42]).** Progressive nephritis was induced in Wistar-Kyoto rats by injecting an anti-glomerular basement membrane antiserum. On days 0, 10, 20, 30 blood samples were collected and sera prepared. The figure illustrates the sequential changes in serum parameters compared to control rats (i.e. those injected with an equivalent volume of normal rabbit serum), at their first presentation. All changes shown are significantly different vs. control.

*Hasegawa H, Nagano N, Urakawa I, Yamazaki Y, Iijima K, Fujita T, Yamashita T, Fukumoto S, Shimada T. Direct evidence for a causative role of fgf23 in the abnormal renal phosphate handling and vitamin d metabolism in rats with early-stage chronic kidney disease. Kidney international. 2010;78:975-980*

With persistent hyperphosphatemia, $1,25(OH)_2D_3$ deficiency and hypocalcaemia, secondary hyperparathyroidism (SHPT) develops. Whilst abnormal parathyroid function is detected in only some patients with stage 2 CKD, it increases in prevalence with disease progression and most patients with stages 4 and 5 CKD show elevations in PTH[48, 49]. PTH elevations are accompanied by parathyroid hyperplasia which increases the capacity of the parathyroid gland to synthesise and secrete PTH. Additionally, expression of the "sensor" molecules on the parathyroid gland, the vitamin D receptor (VDR) and the calcium sensing receptor (CaSR), which normally act as part of a negative feedback loop, are decreased in renal failure[50] and SHPT[51, 52] respectively. It has also been suggested that in later stages of CKD the parathyroid gland may become resistant to the inhibitory signals produced by FGF-23, thus allowing high levels of FGF-23 and PTH to co-exist[53]. It has been suggested that down regulation of klotho and FGF receptor 1 underlie this change, as parathyroid tissue of chronic haemodialysis patients showed reduced expression of these receptors[54].

In the absence of correctly functioning negative feedback loops, levels of PTH continue to rise and hypercalcaemia can be observed in later stages of CKD. Additionally, the management of SHPT of CKD and $1,25(OH)_2D_3$ deficiency can involve calcium-based phosphate binders and vitamin D analogues[55] both of which contribute to the generation of hypercalcaemia.

#### 1.2.1.2 Hyperphosphatemia as risk factor / contributor to vascular calcification

Clear associations between serum phosphate and cardiovascular outcomes and mortality have been reported in haemodialysis patients[1, 56-61] and in the general population[62, 63]. The importance of phosphate regulation in the calcification process can also be observed in vivo by examining the phenotype of mice with a targeted deletion of either FGF-23[64, 65] or klotho[66] both of which show hyperphosphatemia accompanied by enhanced vascular calcification. Furthermore, in vitro it has been shown that culturing SMC in

conditions of elevated phosphate produces mineralisation[71-78]. A number of potential mechanisms underlying phosphates pro-calcifying effect exist including, apoptosis and initiation / promotion of osteochondrogenic differentiation, discussed below.

Phosphate has been shown to dose-dependently increase SMC apoptosis[67], known to be important in the regulation of SMC calcification[68]. Downregulation of Gas6 (growth arrest-specific 6), a known apoptosis inhibitor in SMCs[69], and its receptor Axl. is detected with exposure to increasing phosphate concentrations[67].

In response to increased phosphate, a number of authors have shown upregulation of osteochondrogenic gene expression (Runx2, osterix, alkaline phosphatase, osteopontin) accompanied by down regulation of SM lineage gene expression (including α-sma, SM22α) in SMC cultures[30, 70-73]. Phosphate-induced osteochondrogenic conversion has also been detected in vivo by El-Abbadi et al. (2009) showing upregulation of Runx2 and osteopontin with simultaneous down regulation of SM22α in uremic mice fed with a high phosphate diet[74].

The mechanisms underlying phosphate-induced calcification have been shown to involve a number of different proteins / pathways. Phosphate entry into SMCs, via Pit-1, has been shown to contribute to the process of phosphate-induced calcification[75]. Loss of Pit-1, in vitro, and therefore inhibition of phosphate uptake reduces calcification and prevents Cbfa1/Runx2 and osteocalcin expression[75].

Also, recent reports highlight BGP as an inducer of $H_2O_2$, and more specifically mitochondrial superoxide[76]. Blockade of mitochondrial ROS can abrogate β-glycerophosphate -induced calcification, and reduce expression of the osteogenic genes, Cbfa1 and Msx2[76]. Furthermore, in a rat model of dietary adenine-induced chronic renal failure, blockade of mitochondrial ROS by the use of MnTMPyP (Mn(III)tetrakis(1-methyl-4-pyridyl)porphyrin

pentachloride) reduces aortic ROS levels, p65 activation, and $Ca^{2+}$ deposition[76].

Additionally the presence of BMP-2 is required for phosphate-induced mineralisation. Addition of noggin, a BMP2 inhibitor, can block mineralisation[77] (for a more comprehensive review of the effects of phosphate on SMC calcification see Shanahan et al. (2011)[78]).

However, despite a seemingly key role for phosphate in vascular calcification, experiments performed using serum from uremic patients show that calcification occurs irrespectively of phosphate levels[73], suggesting that other factors are required to induce mineralisation in the vasculature.

#### 1.2.1.3 Hypercalcaemia as risk factor / contributor to vascular calcification

Hypercalcaemia has been shown to contribute to the increased morbidity in dialysis patients[58, 61, 79]. Treatment with calcium-based phosphate binders vs. calcium free phosphate binders has been shown to accelerate arterial calcification in randomized control trials[79, 80], however studies showing that calcium-based phosphate binders increase cardiovascular mortality are lacking in patients with ESRD[81].

The role of $Ca^{2+}$ in calcification has received less attention than phosphate. On the basis of in vitro findings it is still unclear if $Ca^{2+}$ can produce SMC mineralisation in the absence of phosphate, as contradictory reports exist[82-84]. Yang et al. (2004) reported $Ca^{2+}$-induced mineralisation under normal phosphate conditions but observed that increased phosphate levels accelerated mineralisation, suggesting independent and synergistic mechanisms[82], also observed by Reynolds et al. (2004)[84]. However, Alam et al. (2009) failed to detect any mineralisation without an external phosphate source, suggesting phosphate plays a permissive role[84]. Interestingly, when combined it appears that for a given Ca x P product elevated $Ca^{2+}$ is more potent at inducing SMC calcification than elevated P[85, 86].

Whether $Ca^{2+}$-induced mineralisation is mediated by osteochrondogenic differentiation remains unclear. Upregulation of alkaline phosphatase mRNA expression was detected in $Ca^{2+}$ treated SMCs[82], however a recent report shows that when $Ca^{2+}$ is added to high phosphate media the level of alkaline phosphatase activity detected decreases[86].

To date, the role of $Ca^{2+}$ as a promoter of calcification has largely focused on its effects on cell apoptosis and release of matrix vesicles. Apoptosis has been demonstrated to precede calcification, and apoptotic bodies can initiate calcification in a similar way to matrix vesicles (MVs)[68]. Matrix vesicles have been identified in mineralising tissues where they are believed to be released into the extracellular space and attach to matrix proteins initiating mineralisation[87]. Exposing SMCs to elevated levels of $Ca^{2+}$ promotes apoptosis and the release of matrix vesicles[83]. In addition to promoting their formation, $Ca^{2+}$ can also increase the mineralisation potential of MVs, increasing the level of $Ca^{2+}$ incorporation[83] and potentially the level of phosphate incorporation via upregulation of Pit-1[82].

Under normal conditions, MV contain inhibitors of calcification, fetuin-A and MGP (discussed in sections 1.2.2.1 and 1.2.2.2 respectively), preventing mineralisation, however in CKD / ESRD lower levels of inhibitors are detected[88]. Interestingly, $Ca^{2+}$ has been shown to increase fetuin-A uptake into matrix vesicles[83, 89, 90] and upregulate MGP production[91, 92] potentially as an adaptive response. However in the case of MGP it has been suggested that unprocessed MGP may be produced as a consequence of ER stress driven by prolonged exposure to elevated $Ca^{2+}$, and that MGP levels eventually deplete from MV[93].

### 1.2.2 Inhibitors of vascular calcification

The existence of inhibitors of calcification has long been suspected as serum, even of a healthy individual, is supersaturated with $Ca^{2+}$ and phosphate and thus a mechanism(s) to prevent the development and progression of

extraskeletal calcification must be in place. Even in CKD patients, a small subset of patients do not develop calcification despite exposure to a similar uremic environment[79].

A number of calcification inhibitors have been identified including fetuin-A, matrix Gla protein (MGP), osteopontin (OPN), pyrophosphate (PPi) and osteoprotegerin (OPG). Evidence suggests that these proteins may be deficient or non-functional in patients with CKD, and many have been correlated with calcification scores in CKD patients[88], therefore increasing the likelihood of calcification (see Figure 1.6). Our understanding of the role of these physiological inhibitors has been assisted by recent animal knockout models, discussed below.

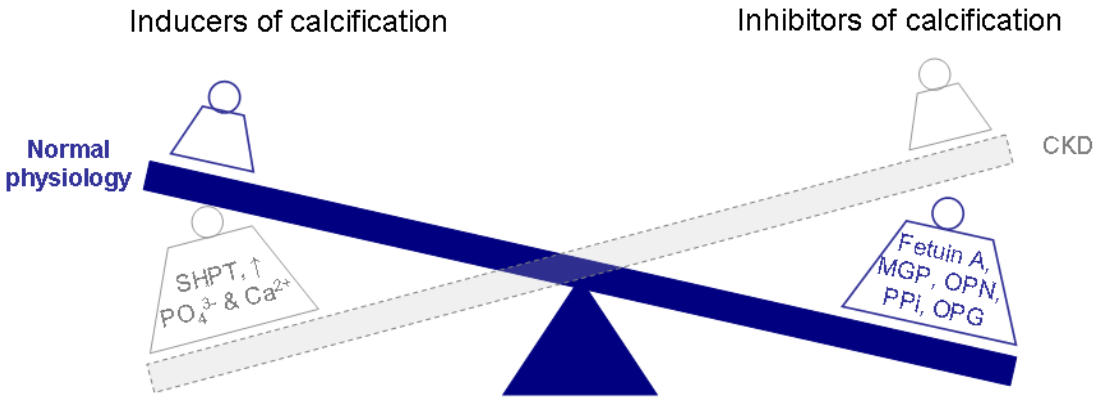


**Figure 1.6 Schematic diagram illustrating the balance of inhibitors and inducers in normal physiology and CKD.** In normal physiology, calcification inhibitors protect from spontaneous calcification. However, with reduced expression of inhibitors and additional drivers of calcification (hyperphosphatemia and hypercalcaemia) the balance shifts in CKD. MGP; matrix gla protein, OPN; osteopontin, PPi; pyrophosphate, OPG; osteoprotegerin, SHPT; secondary hyperparathyroidism.

### 1.2.2.1 Fetuin-A

Fetuin-A is a circulating serum protein that acts as a potent inhibitor of extraosseous calcification, accounting for ~50% of the calcification inhibitory capacity of serum[94]. This inhibition is achieved by formation of colloidal

spheres with $Ca^{2+}$ and $PO_4^{3-}$, referred to as calciprotein particles[95, 96] thereby preventing precipitation of basic calcium phosphate. Fetuin-A can also modulate the calcification process locally. Fetuin-A has been observed at sites of injury where it is internalised by SMCs, via an annexin-dependent mechanism[97], inhibiting apoptosis of smooth muscle cells (SMCs) and preventing mineral nucleation from MVs[89].

The role of fetuin-A as an important mineralisation inhibitor was demonstrated when examining animals with targeted disruption of the fetuin gene. Despite the mild calcification phenotype[98, 99] of fetuin-A knock out mice (Ahsg -/-), extensive calcification was observed when mice were either a) on a high phosphate and vitamin D diet or b) normal diet and crossed onto a strain of calcification-prone mice (DBA/2)[99]. Westenfield et al. (2004) produced an additional model, a double knock out of fetuin-A and apolipoprotein E (Ahsg -/-, ApoE -/-) and, in support of existing findings, confirmed that fetuin-A deficiency enhances calcification[100]. With induced CKD (i.e. a high phosphate diet and unilateral nephrectomy), these animals (Ashg -/- ApoE -/-) showed more extensive aortic calcification compared to their WT and ApoE-/- counterparts receiving the same treatment[100].

Clinically, the role of fetuin-A is more difficult to define as fetuin-A acts as an acute phase reactant and thus its production is down regulated with systemic inflammation. However, significantly lower levels of fetuin-A have been observed in dialysis patients (vs. normal population)[101], and associated with increased all-cause cardiovascular mortality[101, 102]. A polymorphism in the fetuin-A gene (T256S) predisposes patients to low levels of serum fetuin-A and is associated with increased mortality versus those patients carrying the alternative polymorphism[103, 104]. While none of these studies assessed the relationship between fetuin-A and the extent of vascular calcification, Moe et al. (2005) reported an inverse relationship between circulating levels of fetuin-A and coronary calcification scores, in CKD stage 5 patients[88]. Similar observations have also been noted in patients without CKD[105, 106]. Moreover, serum from dialysis patients shows a reduced capacity to inhibit Ca x P product precipitation in vitro versus serum from normal controls, an effect that

can be reversed by addition of purified fetuin-A to physiological concentrations[101].

#### 1.2.2.2 Matrix γ-Carboxyglutamic Acid Protein

Matrix Gla (γ-carboxyglutamic acid) protein (MGP) was the first calcification inhibitor to be characterised in vivo[107] and probably the most widely known. To produce its anti-calcification effects, MGP requires post translational gamma carboxylation[107]. Out of 5 of the glut residues, 4 need to be converted to gla, for MGP's inhibitory actions[108], a process which is dependent on the availability of vitamin K. Additionally, a second series of post translational modifications appear to be required to ensure successful secretion and functionality of MGP: phosphorylation of 3 serine residues[109].

MGP is expressed and secreted by SMCs [110, 111], and is found in high abundance in areas of calcification both in vitro[111] and in vivo[112, 113]. However it is the uncarboxylated form that is predominantly found in areas of calcification[114]. MGP is believed to work via 1) direct inhibition of $Ca^{2+}$ precipitation and crystalisation as a result of $Ca^{2+}$-binding to Gla motif[110, 115], and 2) antagonising bone morphogenetic protein 2 (BMP-2), which plays a role in osteoblast differentiation and thus bone formation[116-118] and bone morphogenetic protein 4[119]. Interestingly, the effect of MGP, in vitro, is dependent on the relative amounts of BMP-2 present and when BMP-2 is low MGP has been shown to promote calcification[120]. MGP has also been identified as being associated with matrix vesicles[83] however whether its mechanism of inhibition in matrix vesicles is the same as above, or MGP has other actions, is unknown.

**Figure 1.7 Mineralised blood vessels in MGP deficient mice (taken from Luo et al. (1997)[107]).**

4 week old MGP -/- mice show prominent calcification of the arteries. Calcified arteries resisted the alkaline digestion of soft tissues and show alizarin red staining, for mineral. *1 carotid artery, 2 cervical trunk, 3 anxillary artery, 4 unnamed, 5 aortic arch, 6 aorta, 7 intercostal artery, 8 coeliac artery, 9 renal artery, 10 iliac artery*

*Luo G, Ducy P, McKee MD, Pinero GJ, Loyer E, Behringer RR, Karsenty G. Spontaneous calcification of arteries and cartilage in mice lacking matrix gla protein. Nature. 1997;386:78-81*

Deletion of the MGP gene in mice results in extensive arterial calcification within a few weeks (Figure 1.7) and aortic rupture causing premature death[107]. Restoration of MGP expression in SMC can rescue the calcification phenotype[108]. Clinical data also suggest a role for MGP as a calcification inhibitor; an inverse association exists between serum MGP levels and calcification[121, 122]. Additionally, mutations in the MGP gene resulting in truncated forms of MGP, i.e. Keutel syndrome[123], produce widespread calcification in the tracheobronchial tree[123, 124]. However, unlike in vivo models, patients survive until adulthood, suggesting that the truncated forms of MGP may retain some biological activity. Additionally in CKD, an inverse relationship between total uncarboxylated MGP and vascular calcification is reported in haemodialysis patients[125-127]. However, recently in a report examining all CKD patients and focusing only on dephosphorylated and uncarboxylated MGP (dp-ucMGP), it was reported that plasma dp-ucMGP increases progressively with CKD stage and is positively association with the severity of arterial calcification[128] suggesting that the dephosphorylated and uncarboxylated form of MGP is regulated differently to the uncarboxylated form.

### 1.2.2.3 Osteopontin

Osteopontin (OPN) is a $Ca^{2+}$-binding, phosphorylated glycoprotein normally found in mineralised tissues where it is involved in bone remodelling: promoting osteoclast function through αvβ3 integrin[129] and inhibiting apatite crystal growth[130]. Whilst OPN is not normally present in soft tissues it is secreted by macrophages, T cells, haematopoietic cells, SMCs, fibroblasts, and myocardial cells[131].

Whilst loss of OPN alone does not cause spontaneous calcification, in the presence of pro-calcifying stimuli, deficiency of OPN in vivo results in accelerated calcification[132]. Similarly to MGP, the anti-calcification abilities of OPN are dependent on post translational modifications, its inhibitory effect being directly dependent on the number of phosphorylated sites[133].

In injured / atherosclerotic vessels, OPN is found in abundance[134-140] and plasma OPN levels are significantly higher in patients with coronary calcification[141]. OPN exists as a component of human atherosclerotic lesions[137, 142] and is observed in the arteries of MGP null mice[71]. In patients with coronary artery disease OPN correlates to disease severity, independent of conventional risk factors[143]. Whilst a protective action for OPN is assumed, data supporting the suggestion of an atherogenic role for OPN rather than a protective one also exist[144].

### 1.2.2.4 Pyrophosphate

Pyrophosphate (PPi) has demonstrated inhibition of mineralisation both in vivo[145] and in vitro[146], inhibiting hydroxyapatite formation via a direct physicochemical reaction[147]. It has been suggested that PPi may also play a role in stabilising the SMC phenotype and preventing transdifferentiation[148].

To maintain PPi levels, its generation and release is modulated via ectonucleotide pyrophosphatase/phosphodiesterase I (ENPP1) and Ank respectively, and its breakdown via tissue nonspecific alkaline phosphatase (TNAP). Studies in vivo and ex vivo report that deficiencies in ENPP1[149] or

Ank, a pyrophosphate transporter[150], or overexpression of TNAP[149] results in extensive calcification. Idiopathic infantile arterial calcification (IIAC) results from a genetic deficiency of pyrophosphate and in most cases this is related to deficiencies in ENPP1[151]. These patients exhibit severe medial arterial calcification at an early age[151, 152], and often die as a result of heart failure soon after birth highlighting the importance of pyrophosphate control.

In vivo, upregulation of TNAP has been demonstrated in the aorta of uremic animals[153] which may lead to vascular deficiency of PPi in CKD. In fact, PPi levels are reported to be reduced in haemodialysis patients[154], and a negative association with the severity of vascular calcification exists[155]. Administration of exogenous PPi shows substantial inhibition of vascular calcification in uremic rats, without detrimental effects on bone[156]. Despite the short half life of pyrophosphate, inhibition of calcification was achieved with small, transient elevations in plasma PPi and therefore PPi has been suggested as a therapy for uremic vascular calcification[156].

#### 1.2.2.5 Osteoprotegerin

Osteoprotegerin (OPG) is a member of the tumour necrosis factor (TNF)-related family and is involved in bone metabolism. In mice, the importance of OPG in vascular calcification is clear with OPG null mice (OPG -/-) showing both severe osteoperosis and spontaneous calcification[157]. In vivo, loss of OPG results in markedly increased calcification when animals are subjected to pro-calcifying stimulus[158] or pro-atherogenic conditions[159]. Additionally, treatment with OPG can reduce the extent of calcification in animals prone to develop atherosclerosis[159, 160] and calcification[161].

However the role of OPG in humans appears to be different. Clinical studies have consistently reported that serum OPG levels are positively associated with the progression of coronary calcification[88, 162-164]. Whilst it's possible that OPG may be upregulated in response to vascular damage to exert its protective role, detrimental effects on the vasculature have also been

documented[165, 166], however further work is required to complete our understanding.

### 1.3 Introduction to the calcium sensing receptor

The calcium sensing receptor (CaSR) is central to the calcium homeostatic mechanism. The CaSR senses free extracellular calcium ions and couples this information to intracellular signalling pathways enabling the cell to respond to increases in extracellular $Ca^{2+}$ concentrations. It is highly expressed in the parathyroid chief cells where it acts as the sensor modulating the synthesis and secretion of PTH. High levels of extracellular $Ca^{2+}$ activate the CaSR, which in turn inhibits the expression and secretion of PTH as well as inhibiting parathyroid cell proliferation[167]. In contrast, when a fall in serum $Ca^{2+}$ is sensed by the CaSR, increased release of preformed PTH is detected and, within hours, increased transcription of pre-pro-PTH mRNA[168]. CaSR has also been shown to be highly abundant in the kidney[169] and thyroidal cells[170] where it further contributes to $Ca^{2+}$ homeostasis; controlling urinary $Ca^{2+}$ excretion (reviewed by Riccardi and Brown (2010)[171]) and the release of calcitonin, respectively.

The importance of CaSR in $Ca^{2+}$ homeostasis is highlighted by the phenotype resulting from CaSR mutations in humans, including familial hypocalciuric hypercalcaemia (FHH; inactivating), neonatal severe primary hyperparathyroidism (NSHPT; inactivating), autosomal dominant hypocalcaemia (ADH: activating) and Bartter syndrome type V (activating). Heterozygous inactivating mutations of the CaSR gene typically cause FHH and homozygosity of the mutation manifests as NSHPT. Patients present with hypercalcaemia and relative hypocalciuria. The hypercalcaemia of FHH is mild to moderate, whereas children with NSHPT can develop severe hypercalcaemia and without quick intervention neurodevelopmental damage or fatality may result. ADH is characterized by hypocalcaemia accompanied by hypercalciuria and an inappropriately low concentration of PTH. Patients with activating CaSR mutations and features of Bartter syndrome additionally exhibit hypokalemia with renal potassium wasting, hyperreninemia, and hyperaldosteronemia. CaSR autoantibodies have also been identified that can be activating or inactivating in nature, mimicking ADH[172] and FHH[172-174], respectively.

### 1.3.1 Structure and signalling of the CaSR

The CaSR is a G-protein coupled cell surface receptor (GPCR), originally cloned from bovine parathyroid gland, and is well conserved showing a large degree of homology between different species. The human CaSR gene is located on chromosome bands 3q13.3-21. The cDNA has a coding region of 3234 bp, producing a 1078aa protein. Several splice variants have been reported[175-177] however for many of these the functional significance is unknown.

The CaSR belongs to family 3 (or C) G-protein coupled receptors. Family 3 represents a small subfamily of GPCRs including metabotropic glutamate receptors (mGluR1-8), $GABA_B$ receptors, GPRC6A responsible for sensing basic amino acids, sweet taste receptors (T1R1-3) and putative pheromone receptors (V2Rs). Figure 1.8 shows the topology of the CaSR with its large extracellular domain (ECD) (612 residues), a transmembrane domain (TMD) of 250 amino acids containing the 7 membrane spanning helices, and an intracellular C-terminal domain (ICD) of 216 amino acids.

Characteristic of family 3 GPCRS, the CaSR possesses an unusually large N-terminal extracellular domain (ECD). The ECD contains a bi-lobed venus fly trap domain, cysteine-rich domain and several N-linked glycosylation sites. The venus fly trap domain shows homology to the bacterial periplasmic binding protein[178]. Based on the crystal structure of mGluR1 it has been suggested that the VFTD can exist in open and closed confirmations and agonist binding is thought to stabilise the closed confirmation[179, 180]. The cysteine-rich domain is a second characteristic feature of family 3 GPCRs, present in all except orphan and $GABA_B$ receptors, and in the case of the CaSR has been shown to be critical for CaSR mediated signalling[181]. Upon cloning of the CaSR, 11 putative N-linked glycosylation sites were identified and since, mutagenesis studies have highlighted the importance of glycosylation in cell surface expression of the CaSR[182].


**Figure 1.8 Schematic representation of the CaSR (adapted from Saidak et al. (2009)[183]).** Predicted $Ca^{2+}$ bindings sites are illustrated in purple, yellow, pink, green and blue[184]. Residues involved in both calcimimetic and calcilytic binding are shown in black, and those only involved in calcilytic binding in orange[185-187].
*Saidak Z, Brazier M, Kamel S, Mentaverri R. Agonists and allosteric modulators of the calcium-sensing receptor and their therapeutic applications. Mol Pharmacol. 2009;76:1131-1144*

Thirdly, all family 3 GPCRs function as dimers. Dimerisation occurs in the endoplasmic reticulum through intermolecular disulfide bonds involving cysteines 129 and 131, and non-covalent interactions[188-191]. The cell-surface CaSR is typically present in a homodimeric configuration, however instances of heterodimerisation of CaSR with other family 3 receptors has also been reported[192-194].

As a GPCR, the CaSR coordinates its signalling cascades via heterotrimeric G proteins. The nature of the signalling pathways activated, i.e. the G proteins recruited, in response to CaSR activation varies depending on cell type and the CaSR has been labelled as a pleiotropic GPCR that can couple to more than one type of G-protein[195]. A large amount of work has focused on the signalling in HEK cells transfected with the CaSR (CaSR-HEKs). Activation of the CaSR can stimulate phospholipase $A_2$ ($PL_2A$), C (PLC) and D (PLD)[196]. Stimulation of PLC leads to the production of $IP_3$ and activation of protein kinase C (PKC). $IP_3$ binds to $IP_3$ receptors on the endoplasmic reticulum membrane, which causes $Ca^{2+}$ mobilisation within the cell. In parallel to activation of PLC, activation of the CaSR stimulates phosphatidylinositol 4-kinase (PIK4), involved in the first step in inositol lipid biosynthesis, via $G\alpha_q$. The CaSR not only interacts with $G\alpha_q$, but can also

signal via $G\alpha_i$, which results in the inhibition of adenylate cyclase and thus reduction of cyclic adenosine monophosphate (cAMP) levels[197]. Finally, another important group of signalling molecules that can be activated by CaSR is the mitogen activated protein kinases (MAPK)[198]; which often result in changes in gene expression. Whilst by no means an exhaustive list, genes known to be induced by MAPK signalling include COL1A1 (coding collagen 1)[199, 200], EGR1 (coding early growth response protein 1)[201, 202], FOS[203], HSPA5 (coding heat shock 70 kDa protein 5)[204], HSPB1 (coding heat shock 27 kDa protein)[205], JUN[206] and MYC[207].

Phosphorylation of the CaSR can alter the receptors signalling potential. At least 5 PKC sites exist (T646, S794, T888, S895 and S915) )[208] and 2 predicted protein kinase A (PKA) sites (S899 and S900)[209]. PKA phosphorylation is believed to contribute only a minor role in the regulation of CaSR[209], however the effects of PKC phosphorylation on PTH secretion and $Ca^{2+}$ mobilisation in the parathyroid were well known prior to the discovery of CaSR[210, 211]. Mutation of each PKC site highlighted the importance of Thr888 in the regulation of CaSR signalling; producing a substantial shift in EC50, whilst the other sites produces little (S895 and S915) or no change (T646 and S794)[212]. PKC mediated inhibition of CaSR signalling can be stimulated by receptor activation, allowing for a negative feedback loop[213].

CaSR signalling has also been shown to be influenced by the presence of filamin A. Filamin A is a cytoskeletal scaffold protein that has been shown to be important for CaSR mediated ERK activity[214-216], Rho signalling[217, 218] and JNK activation[215]. In addition to its role in signalling, filamin A may also allow for greater stability of the CaSR at the plasma membrane[219]. CaSR expression was shown to double in M2 cells when filamin A, not a natural expression, was transfected[219]. Other binding partners of the CaSR include the inwardly rectifying $K^+$ channels Kir4.1 and 4.2, dorfin, involved in the ubiquitination of the CaSR, the receptor activity-modifying proteins (RAMP) RAMP-1 and RAMP-3 involved in receptor trafficking and β-arrestins regulating internalisation and degradation (reviewed in detail by Huang and Miller (2007)[220]).

### 1.3.2 Pharmacology of the CaSR

A considerable number of ligands modulate CaSR activation and can be divided into 2 groups: orthosteric modulators which act on the CaSR directly or allosteric modulators, which modulate the effects of orthosteric modulators. Moreover the CaSR is responsive to changes in ionic strength[221] and pH[222].

Whilst $Ca^{2+}$ is the primary orthosteric agonist of the CaSR, many other orthosteric agonists exist. A number of divalent and trivalent cations can activate the CaSR i.e. $Gd^{3+}$, $Al^{3+}$, $Sr^{2+}$, $Mn^{2+}$, $Ni^{2+}$, $Ba^{2+}$, and $Mg^{2+}$ [223], however $Ca^{2+}$ and $Mg^{2+}$ are the only endogenous divalent agonists. Other orthosteric agonists, which are all positively charged, include polyamines and aminoglycoside antibiotics[223].

The hill co-efficient for CaSR indicates that 3–5 $Ca^{2+}$ ions bind cooperatively[224] and initial work by Huang et al. (2007) identified 2 regions, amino acids 222–235 and 383–408, which when removed from the CaSR altered intracellular responses to $Ca^{2+}$. Additionally, insertion of these sequences into non-$Ca^{2+}$ binding scaffold proteins gave the new protein the ability to bind $Ca^{2+}$[225]. More recent modelling work by the same group, utilised the crystal structure of mGluR1, and identified 5 potential $Ca^{2+}$ binding sites in the ECD[184]. Whilst binding of CaSR's other cation agonists was not examined at each of the potential sites individually, $Mg^{2+}$ and $La^{3+}$ were shown to bind within select subdomains of the CaSR ECD containing 2-3 of the potential binding sites and competition between the agonists visible. Whilst, the ECD is believed to possess the primary extracellular ion binding site(s), it is not the only site for orthosteric binding. Ray and Northup et al. (2002) report a response to $Ca^{2+}$, $Mg^{2+}$ and $Gd^{3+}$ in a CaSR mutant lacking the ECD (T903-Rhoc), suggesting at least one other site within the TMD also participates in cation sensing[226].

Allosteric modulators independently have no effect on receptor activity (in the case of the physiological CaSR) but in the presence of an orthosteric agonist

can influence receptor activity i.e. shift the dose-response curve. Both positive and negative allosteric modulators have been identified that can potentiate or attenuate the response to orthosteric agonists respectively.

L-amino acids, in particular aromatic L-amino acids have been demonstrated to act as positive allosteric modulators of the CaSR[227]. In addition to endogenous positive allosteric modulators, small molecule drugs (NPS R-568, AMG641, AMG073, Cinacalcet), also known as calcimimetics, have been developed. Most calcimimetics are phenylalkylamines and are derived from $Ca^{2+}$ channel blockers. Cinacalcet is approved for use in hyperparathyroid states (i.e. primary and secondary hyperpathyroidism and parathyroid carcinoma). Interestingly, further potential for calcimimetics may exist as recent reports suggest the possibility of using calcimimetics to rescue CaSR mutants[228].

Despite their common actions, the binding sites for L-amino acids and calcimimetics appear to be distinct. A chimeric receptor was developed in which the CaSR TMD was replaced with that of the rat mGluR1 receptor. While L-Phe enhanced the sensitivity of the chimeric receptor to $Ca^{2+}$, R-467, a calcimimetic, produced no effect. However, when assessed in an N-terminally truncated CaSR R-467, but not L-Phe, increased receptor sensitivity[229].

Negative allosteric modulators of the CaSR, known as calcilytics, have also been developed (SB-751689, SB-423557). As with the calcimimetics, the calcilytics are believed to bind in the 7TMD[185, 187], and in some cases the binding site may overlap with the calcimimetics[187]. No calcilytic is currently approved for use, however their potential as bone anabolic agents are being investigated for the treatment of osteoporosis.

## 1.4 Calcimimetics in vascular calcification

The central role of CaSR in SHPT makes it an interesting target to attempt to restore mineral imbalance and potentially reduce risk factors for vascular calcification in CKD. Currently calcimimetics represent the only available treatment of SHPT in CKD stage 5 patients which allows control of high PTH levels in the absence of a concomitant increase in serum $Ca^{2+}$ and phosphate[230, 231] and have been shown to be effective in this patient group. Therefore it was hypothesised that calcimimetics may also contribute to slowing the progression of vascular calcification in the setting of CKD.

### 1.4.1 A systemic role for calcimimetics in the protection against vascular calcification

Whilst clinical data are currently lacking to confirm or refute the ability of calcimimetics to attenuate vascular calcification in CKD patients, it is an area actively being researched and data from small scale studies emerging. Existing data report that cinacalcet treatment reduces cardiovascular-related hospitalization (39%) in haemodialysis patients with uncontrolled hyperparathyroidism[232] and prospective studies investigating cardiovascular events in dialysis patients are ongoing (EVOLVE study; Evaluation of Cinacalcet HCl Therapy to Lower CV Events)[233]. More specifically, attention is now also focused on vascular calcification as a primary endpoint. A small scale, prospective, observational study has reported the ability of cinacalcet to reduce arterial stiffness of SHPT with CKD[234] and the effect of cinacalcet plus low dose vitamin D on vascular calcification in CKD patients receiving dialysis is being addressed in the ADVANCE study[235]. However, as we await robust clinical data, strong support for a protective role of calcimimetics comes from numerous in vivo studies.

A number of uremic animal models exist including 5/6 nephrectomy and adenine-induced uremia. Treatment of uremic animals with calcitrol and/or a high phosphate diet can be used to accelerate calcification in these models. The effect of calcimimetics in vivo have been investigated by a number of groups, and consistently show reduced vascular calcification and increased

survival[236-239]. This benefit has been shown with different calcimimetic compounds including cinacalcet[237], R-568[238] and AMG641[236, 239](Figure 1.9) eluding to a class effect. As expected these actions are accompanied by alterations in serum biochemistry i.e. reductions in serum $Ca^{2+}$ [92, 236, 237, 239], phosphate[236, 239] and PTH[236, 237] towards levels of non-uremic animals. Reduction in serum PTH is also accompanied by reductions in parathyroid gland volume in the order of around 50%[236, 237].

### 1.4.2 A protective role for calcimimetics on smooth muscle cells

For the most part the beneficial actions of calcimimetics in vascular calcification have been attributed to reducing levels of the non-traditional risk factors (i.e. $Ca^{2+}$, phosphate, PTH), supported by the observation that a parathyroidectomy can also suppress calcification[237]. However, Ivanovski et al. (2009) surprisingly showed that R-568 not only to reduced intimal and medial calcification in uremic artherosclerotic mice, but also the progression of atherosclerosis[240]. R-568 reduced the atherosclerotic plaque area fraction suggesting R-568 may have a more direct action on the vasculature responsible for eliciting this protection. Moreover, with the identification of the CaSR in the vasculature, the possibility of a more direct effect of the calcimimetics also emerged.

**This image has been removed by the author for copyright reasons.**

**Figure 1.9 Protective effect of AMG641 in aortic mineralisation in adenine fed animals (taken from Henley et al. (2009)[236]).** Von Kossa-stained sections of aortas showing mineralisation from animals fed adenine (0.75%) for 4 weeks and treated for 4 weeks with either (A) AMG-641 (3 mg/kg, p.o.); (B) 10% captisol-vehicle for AMG 641 (1 ml/rat, p.o.) *Henley C, Davis J, Miller G, Shatzen E, Cattley R, Li X, Martin D, Yao W, Lane N, Shalhoub V. The calcimimetic amg 641 abrogates parathyroid hyperplasia, bone and vascular calcification abnormalities in uremic rats. Eur J Pharmacol. 2009;616:306-313*

### 1.4.2.1 CaSR expression in SMCs

CaSR has been convincingly shown to be expressed in the vascular endothelium[241], where upon activation it is responsible for an increase in intracellular $Ca^{2+}$ and thus opening IKCa channels, suggestive of a role in controlling arterial blood pressure. In addition in areas of calcification, phagocytic cells expressing the CaSR have been identified in uremic rats[239]. However it is the identification of the CaSR in SMC[84, 92, 242-244] that has attracted the most attention.

The presence of CaSR in SMCs was once a controversial topic. Within the literature, some groups have failed to detect CaSR[91, 245, 246]. However, CaSR, both in its protein and mRNA form, has been demonstrated in rat, bovine and human SMC[84, 92, 242-244]. Interestingly, in 2 reports failing to detect CaSR, only the presence of CaSR mRNA was investigated[91, 246], known to be in low abundance in SMC. Additionally CaSR expression has been shown to be sensitive to culture conditions; $Ca^{2+}$ concentrations of 1.8 mM present in normal DMEM (Dulbecco's Modified Eagle Medium) can result in reduced CaSR expression[84]. Recently the use of knock down technologies has confirmed the presence of a functional CaSR in SMC[84, 247].

Limited information exists as to the function of CaSR in SMC. So far, CaSR activation has been shown to increase proliferation via the MEK / ERK signalling pathways[242-244] and protect against apoptosis[242], however the relevance of CaSR in these processes in vivo have not yet been shown.

### 1.4.2.2. SMC CaSR and mineralisation

Evidence exists supporting a role for the SMC CaSR in the process of vascular calcification. Reduced expression of CaSR is observed in calcified human arteries versus non-calcified arteries and loss of the CaSR in vitro has been convincingly shown to be increase SMC mineralisation[84]. Transfection of BAoSMCs with a dominant negative construct of CaSR resulted in accelerated mineralisation, data shown in Figure 1.10[84]. In vitro findings show that constant exposure to high extracellular $Ca^{2+}$, a promoter of calcification,

results in reduced expression of the CaSR[84]. Similarly, arteries of ESRD patients, who are typically exposed to a high extracellular $Ca^{2+}$ concentrations, also show reduced levels of CaSR expression vs. general population[243]. Decreased expression of the SMC CaSR may be one of the changes in ESRD patients that increase their susceptibility to the development of vascular calcification.


**Figure 1.10 Overexpression of the dominant negative calcium sensing receptor (dnCaSR) enhances mineralisation (taken from Alam et al. (2009)[84]).**

*Alam MU, Kirton JP, Wilkinson FL, Towers E, Sinha S, Rouhi M, Vizard TN, Sage AP, Martin D, Ward DT, Alexander MY, Riccardi D, Canfield AE. Calcification is associated with loss of functional calcium-sensing receptor in vascular smooth muscle cells. Cardiovasc Res. 2009;81:260-268*

In vitro, treatment of SMC with R-568 has been shown to delay the process of calcification[84, 240]. These actions have been attributed to activation of the SMC CaSR as introduction of CaSR siRNA abolished this effect[240]. Whilst the downstream mechanism contributing to the protective actions of calcimimetics on mineralisation is still under investigation, in vitro studies with a second calcimimetic, AMG641, show increased CaSR expression in BAoSMC[92]. It is possible that by restoring CaSR expression, cells regain some protection against mineralisation. Additionally, stimulation of CaSR with AMG641 in vitro has recently been shown to increase MGP expression by SMCs[92], which may underlie their protective actions on mineralisation.

## 1.5 Aims of this research

Our understanding of the role of the CaSR in the modulation of calcification is by no means complete. Whilst evidence points to a protective role for the CaSR, it is well established that high concentrations of $Ca^{2+}$, the major physiological agonist for the CaSR can trigger mineralisation of SMC, whereas positive allosteric modulation of the receptor appears to be protective. Distinct mechanisms of $Ca^{2+}$ and calcimimetics must be at play, however the level of involvement of the CaSR in each of these processes is unknown.

Whilst the activity of $Ca^{2+}$ is certainly not limited to CaSR and calcification could be induced via a CaSR-independent mechanism, it is interesting that $Gd^{3+}$ a second orthosteric agonist has also been shown to promote calcification in BAoSMC[84]. Furthermore, common downstream actions are reported upon SMC treatment with $Ca^{2+}$ or calcimimetics i.e. elevated MGP expression[92], suggesting at least some shared mechanisms.

Our understanding has, to some extent, increased recently as it has been shown that chronic stimulation with $Ca^{2+}$ and $Gd^{3+}$ result in down regulation of the SMC CaSR[84] whereas AMG641 can increase SMC CaSR expression[92], however the mechanisms involved in these differential process, and their relative contribution to SMC mineralisation, is unknown.

Aims of research:

1) To produce an explant culture of BAoSMC and in vitro model of calcification using methods described by Alam et al. (2009)
2) Understand the relative involvement of CaSR in the effects of $Ca^{2+}$ and calcimimetics on mineralisation:
    a. Test the differential effects of $Ca^{2+}$ and calcimimetics on SMC mineralisation
    b. Test the hypothesis that the protective actions mediated by calcimimetics are related to their activity at the CaSR using pharmacological tools (research was performed prior to publication of data using siRNA to demonstrate CaSR mediated mechanisms)

3) Examine the signalling pathways activated by $Ca^{2+}$ and calcimimetic treatment in attempt to
    a. Better understand the cellular consequences of CaSR activation in SMCs
    b. Evaluate the potential overlap between $Ca^{2+}$- and calcimimetic-induced activities
    c. Identify potentially protective signalling pathways mediated by the calcimimetics through CaSR activation

# Chapter 2: Methods

## 2.1 Cell culture

### 2.1.1 Isolation and culture of BAoSMC

Bovine aorta was obtained from freshly slaughtered animals from a local abattoir. The aorta was cut open longitudinally and a 2 $cm^2$ section taken from the luminal face of the vessel wall, 20 cm below the left subclavian artery. The structure of the vessel wall is shown in Figure 2.1. After thorough washing with sterile Hank's balanced saline solution (HBSS; Invitrogen Ltd, Paisley, UK), the adventitia was removed by blunt dissection before removing the endothelial layer using a scalpel blade. The aortic section was then further dissected, removing 2 $mm^2$ sections of the medial layer and placing them luminal side down in a sterile 100 $mm^2$ petri dish.

**This image has been removed by the author for copyright reasons.**

**Figure 2.1 Schematic diagram illustrating the structure of the aorta, showing the intima, smooth muscle cell containing media and adventita (taken from Ashley and Niebauer (2004)[248]).**

*Ashley A.E. and Niebauer J (2004). Cardiology explained. London, Remedica*

Aortic explants were cultured in Dulbeccos Modified Eagles Medium (DMEM) without $CaCl_2$ (Invitrogen Ltd, Paisley, UK) containing 10% fetal calf serum (FCS), 100 U/mL penicillin, 100 μg/mL streptomycin, 2 mM L- glutamine, 1 mM sodium pyruvate and 1% non-essential amino acids. To match physiological $Ca^{2+}$ conditions, $Ca^{2+}$ free medium was supplemented with 1 M $CaCl_2$ to produce a final concentration of 1.2 mM $CaCl_2$. Amphotericin (1 μg/ml; Invitrogen Ltd, Paisley, UK) was included in culture media for the first 2 weeks to prevent fungal infections developing from the primary culture. With

the exception of those stated all cell culture reagents were purchased from Lonza (Lonza Biologics plc, Tewkesbury, UK).

Nine 2 $mm^2$ sections were arranged within one Petri dish and medium was initially added dropwise to the fresh explants. The following day, 15 ml of medium was added to the culture. BAoSMCs were first seen to migrate from the tissue explant at 5–7 days, at which point explants were removed. Cells were maintained at 37 °C and 5% $CO_2$ and medium renewed every 2–3 days. Cells were used between passages 3–10 with medium changed every second day.

### 2.1.2 Culture of human SMC

Proliferating human aortic SMC (HAoSMC), and all culture media for human cell culture, were purchased from Promocell (Heidelberg, Germany) and used for signalling experiments. HAoSMC were cultured in smooth muscle cell growth media containing 5 % FCS, 5 µg/ml insulin, 0.5 ng/ml epidermal growth factor and 2.0 ng/ml basic fibroblast growth factor (basal $Ca^{2+}$ concentration equals 1.6 mM). Cells were maintained at 37 °C and 5 % $CO_2$ and medium renewed every 2–3 days. Cells were used between passages 3–8 and split with a ratio of 1:2. Subcultivation was performed with DetachKit (Promocell) which utilises a trypsin/EDTA solution to promote detachment and a serum-free trypsin neutralisation solution to inactivate the trypsin.

## 2.2 Immunofluorescence

### 2.2.1 α-smooth muscle actin (α-sma) staining

BAoSMC at passage 3 were plated on 4-well chamber slides (Thermo Scientific Inc, Essex, UK) at a density of 1 x $10^4$ cells/$cm^2$. The next day cells were fixed in 50% methanol (2.5 min), 100% methanol (2.5 min) and 50% methanol (2.5 min). After washing, BAoSMCs were incubated with α-sma monoclonal antibody (Sigma-Aldrich Co, Dorset, UK) 1:400 in 1% rabbit serum (Dako, Glostrup, Denmark) for 1 hr at RT. After washing three times

with phosphate buffered saline (PBS), cells were incubated with rabbit anti-mouse fluorescein isothiocyanate (FITC) 1:100 (Dako, Glostrup, Denmark) for 40 min at RT in the dark. From this point onwards all experimental procedures were performed in the dark. Cell nuclei were stained with 4',6-diamidino-2-phenylindole (DAPI; final concentration 4 μg/ml) for 30 sec, before washing and mounting with Vectashield (Vector Laboratories Ltd., Peterborough, UK). Immunostained BAoSMCs were viewed with an upright microscope (Olympus BX51, Olympus, Essex, UK) and images captured using a high-resolution camera (Coolsnap ES camera (Photometrics, Arizona, US) with MetaVue Software (Molecular devices, California, USA)). Specific band pass filter sets for DAPI and FITC were used to prevent bleed through from one channel to the next. Control experiments were performed where the primary antibody was replaced with mouse immunoglobulin (IgG2a) (1:400) (DakoCytomation, Cambridgeshire, UK).

### 2.2.2 CaSR staining

BAoSMC (passage 4–6) and HAoSMC (human aortic smooth muscle cells; passage 4–5) were plated at 1 x $10^4$ cells/$cm^2$ on a 4-well chamber slide. Cells were fixed for 20 min with 4% formaldehyde in PBS. Non-specific binding was prevented by blocking with 4% rabbit serum (Dako, Glostrup, Denmark) in 0.2% bovine serum albumin (BSA; Sigma-Aldrich Co, Dorset, UK) in PBS for 1 hr at RT. SMCs were incubated with CaSR antibody (Affinity BioReagents MA1-934, Rockford, Illinois, USA), diluted in 4% rabbit serum in 0.2% bovine serum albumin at 1:200, overnight at 4 °C. After washing three times, cells were incubated for 1 hr at RT with rabbit anti-mouse FITC (BAoSMC and HAoSMC), goat anti-mouse Alexa Flour 488 and 568 (Molecular Probes, Oregon USA) (HAoSMC) all diluted in 4% rabbit serum in 0.2% bovine serum albumin at 1:40. Coverslips were mounted using Vectashield (Vector Laboratories Ltd., Peterborough, UK) and sealed with nail varnish. Alternatively, as control experiments, the CaSR primary antibody was replaced with a mouse IgG2a (DakoCytomation, Cambridgeshire, UK) or removed completely and cells incubated with the secondary antibody alone.

Immunostained SMCs were viewed and images captured as above but including a band pass filter set for texas red.

### 2.3 Mineralisation assays

#### 2.3.1 $Ca^{2+}$ experiments

BAoSMC (passage 5–8) were plated in 6-well plates (Corning Inc., New York, USA) at 1 x $10^4$ cells/$cm^2$ in 10% FCS-DMEM. The following day medium was changed to 5% FCS-DMEM. Upon confluence (~day 5) the incubation medium was switched to calcification medium i.e. medium supplemented with 5 mM β-glycerophosphate (BGP) (Sigma-Aldrich Co, Dorset, UK). The first day of culture in the calcification medium was defined as day 0. For $Ca^{2+}$ experiments, BAoSMCs were incubated with different $Ca^{2+}$ concentrations (1.2, 1.8 and 2.2 mM). Treatment medium was changed every 2–3 days. Time to onset of mineralisation was variable between preparations and individual experiments. Mineralisation was visualised using alizarin red dye which stains $Ca^{2+}$ deposits red (see section 2.3.3) and quantified by dye elution (see section 2.3.3).

#### 2.3.2 Calcimimetic experiments

BAoSMC (passage 6–9) were plated and maintained as above. Upon confluence, cells were treated with medium supplemented with 5 mM β-glycerophosphate (BGP) containing different $Ca^{2+}$ concentrations (1.2 mM, 1.8 mM, 2.2 mM), as indicated, with or without the calcimimetic R-568 (N-[3-[2-chlorophenyl]propyl]-[R]-α-methyl-3-methoxybenzylamine; 1 nM) or its isomer S-568 (1 nM). The first day of culture in the calcification medium was defined as day 0. Functional responses to calcimimetics have been previously shown to be elicited in SMC within the range of baseline $Ca^{2+}$ concentrations used in this study (1.8 mM or 2.2 mM $Ca^{2+}$)[84, 92]. The dose-dependent effects of AMG641 (10 pM, 100 pM, 1 nM) were also investigated. All calcimimetic compounds were provided by Amgen, Thousand Oaks, California. R-568 and S-568 were diluted in distilled water and AMG641 in

1:1000 DMSO for the most concentrated solution (1 nM). Upon formation of nodules and deposition of mineral, calcification was visualized by alizarin red staining which stains $Ca^{2+}$ deposits red (see section 2.3.3) and quantified by dye elution (see section 2.3.3).

### 2.3.3 Alizarin red staining

To visually detect mineralisation, alizarin red staining was used which identifies calcium-rich deposits in culture by staining them red. To perform the staining, first, medium was aspirated, BAoSMCs washed with PBS and fixed with 2% formaldehyde and 1% sucrose in PBS for 20 min. After washing BAoSMCs with PBS, 40 mM Alizarin Red (pH 4.1–4.2) was applied to cells for 20 min. Excess stain was removed using by washing the BAoSMCs with distilled $H_20$ (pH 7.0) for 20 min. After drying by evaporation at RT, the BAoSMCs were viewed with an inverted microscope (Olympus IX51, Olympus Optical, London, UK) and images captured using an Olympus digital camera and analySIS imaging software (Olympus soft imaging systems, Munster, Germany).

To quantify mineralisation the dye was eluted. This was performed by treating stained BAoSMCs with 800 µl of 10% acetic acid to each well for 30 min while shaking to extract the $Ca^{2+}$. Cells were detached from the plate using a plastic scraper and the resulting solution (yellow) was collected and vortexed. Mineral oil was added to prevent evaporation and the solution heated to 85 °C for 10 min. The solution was cooled on ice before centrifuging at 20,000 x g for 15 min. The supernatant was transferred to a clean 1.5 ml eppendorf tube and 200 µl 10% ammonium hydroxide added to neutralise the acid. 150 µl of the resulting solution (pH should be 4.1–4.2) was added to a 96 well plate (Corning Inc., New York, USA) in triplicate and absorbance measured at 405 nm.

### 2.3.4 $Ca^{2+}$ deposition assay

To verify results generated with alizarin red staining a second method of $Ca^{2+}$ detection was also employed. The $Ca^{2+}$ assay described detects total calcium

using the o-Cresolphthalein-calcium reaction which produces a vivid purple product that is absorbed between 560 and 590nm.

BAoSMCs (passage 5–7) were plated in 6-well plates (Corning Inc., New York, USA) at 1 x $10^4$ cells/$cm^2$ and $Ca^{2+}$ deposition assays performed in parallel to mineralisation assays. Upon mineralisation, medium was aspirated and BAoSMCs washed twice with PBS. Then, 500 µl 0.6 N HCl was added to each well and the plates incubated on a rotating platform overnight at 4 °C. The following day the HCl was removed from the wells and transferred to fresh 1.5 ml eppendorf tubes and kept for $Ca^{2+}$ quantification. BAoSMCs were then washed with PBS before adding 500 µl 0.1 M NaOH and shaking for 30 min. Cells were scraped from the culture dish using a cell scraper and assayed for protein content using a BCA assay (Thermo Scientific Inc, Illinois, US) (see section 2.5). Protein concentration was used to normalise the $Ca^{2+}$ detected through the cresolphthalein method.

HCl samples were assayed for $Ca^{2+}$ quantification. Samples (5 µl) were incubated in a 96-well plate along with 100 µl colour reagent containing HCl, O-cresolphthalein complexone powder, hydroxyquinoline (stored in the dark and at 4 °C) and 100 µl AMP buffer (AMP reagent (2-amino-2-methyl-1-propanol) dissolved in water and pH adjusted to 10.7, stored at 4 °C in dark) for 15 min and absorbance read at 570 nm. A $Ca^{2+}$ gradient was also included to create a standard curve for comparison. A stock $Ca^{2+}$ standard (50 mg/dl) was created using dry $CaCO_3$ dissolved in water and concentrated HCl and stored in brown bottle at RT. Stock $Ca^{2+}$ solution was diluted to create $Ca^{2+}$ standards at 5, 7.5, 10, 12.5 and 25 mg/dl $Ca^{2+}$ which were assayed along with the samples. All reagents unless otherwise stated are from Acros Organics, Thermo Fisher Scientific, Geel, Belgium.

### 2.4 Alkaline phosphatase (ALP) activity

Alkaline phosphatase (ALP), a phenotypic marker of osteoblasts, has been shown to be present at sites of vascular calcification and its activity implicated in the process of SMC mineralisation[72, 249, 250]. Therefore its activity was

evaluated as one factor suggestive of osteogeogenic differentiation within SMC cultures.

BAoSMC (passage 7–9) were plated in a 6-well plate (Corning Inc., New York, USA) at 1 x $10^4$ cells/$cm^2$. Upon confluence, BAoSMCs were incubated with 5% FCS-DMEM and 5 mM BGP in the presence of 1.2 mM or 1.8 mM $Ca^{2+}$. Protein was harvested from cultures on day 3 and day 5 by aspirating the medium and washing BAoSMCs twice in ice cold PBS. Cells were lysed using 0.1% Triton X-100 in 0.9% NaCl and detached from the plate with a plastic scraper. Alkaline phosphatase activity was measured colorimetrically by the conversion of p-nitrophenyl phosphate (pNPP; Sigma-Aldrich Co, Dorset, UK (colourless) to p-nitrophenol (pNP; yellow) and phosphate. Cell lysate (10 µl) was added to 200 µl pNPP, incubated at 37 °C for 20 min and the absorbance read immediately at 405 nm. A standard curve of pNP (10 mM – 10 nM) (Sigma-Aldrich Co, Dorset, UK) was used to correlate absorbance readings to conversion to pNP, representing ALP activity. Protein concentration was measured using a BCA assay (Thermo Scientific Inc, Illinois, US) (see section 2.5).

### 2.5 Assessment of protein content

Protein content was assessed using the Pierce BCA assay, according to the manufacturer's instructions. Protein standards ranging 25–2000 µg/µl were used (diluted in lysis buffer appropriate to sample). Samples and standards, 15 µl, were loaded onto a 96-well plate (Corning Inc., New York, USA). BCA reagents A and B were prepared at a 1:50 ratio and 200 µl added to each well before incubation at 37 °C for 30 min. Absorbance was read at 562 nm.

### 2.6 Western blotting

#### 2.6.1 ERK activation assay

BAoSMCs (passage 6–10) and CaSR-HEKs (HEK293 expressing human CaSR; passage 12–14) were seeded in 35 mm culture dishes (Corning Inc., New York, USA) in 10% FCS-DMEM (1.2 mM $Ca^{2+}$). Cells were washed with

PBS heated to 37 °C before being exposed to a low $Ca^{2+}$ solution (0.5 mM) for 20 min for equilibration (these and subsequent incubations were conducted at 37 °C). 0.5 mM $Ca^{2+}$ solution consisted of 20 mM HEPES (pH 7.4), 125 mM NaCl, 4 mM KCl, 0.5 mM $CaCl_2$, 0.5 mM $MgCl_2$ and 5.5 mM glucose. After this time equilibration medium was removed the cells treated with a low (0.5 mM) or high (5 mM) $Ca^{2+}$ solution for 5 min (BAoSMC) or 10 min (CaSR-HEK). When the concentration of $CaCl_2$ was increased to 5 mM, the concentration of NaCl was reduced accordingly to keep the total osmolarity constant. Timings for SMC incubation were selected in line with findings by Molostvov et al. (2007). After incubation, treatments were removed and cells washed with ice cold PBS and stored on ice. Cells were lysed with ice cold RIPA buffer; 12 mM HEPES (pH 7.6), 300 mM mannitol, 1% (v/v) Triton X-100, 0.1% (w/v) SDS, 1 mM EDTA and 1 mM EGTA with freshly added phosphatase inhibitors (100 µM sodium vanadate and 1 mM NaF) and protease inhibitors (250 µM sodium pyrophosphate, 1.25 µM pepstatin, 4 µM leupeptin and 4.8 µM phenylmethylsulfonyl fluoride; Sigma-Aldrich Co, Dorset, UK).

Lysates were transferred to fresh 1.5 ml eppendorf tubes and centrifuged at 2500 x g for 15 min to pellet the cell debris and nuclear fraction. Lysates were mixed with 5x Laemmli buffer and heated to 95 °C for 3 min. Proteins were separated on a 10% polyacrylamide gel and transferred to nitrocellulose membrane (Amersham, GE Healthcare, Buckinghamshire, UK). The protein equivalency of the samples was confirmed by ponceau-staining the blot before immunoblotting. Membranes were blocked with Tris-buffered saline Tween-20 (TBST; 150 mM Tris-HCl, 1.5 mM NaCl, 0.1% Tween 20) containing 2% BSA before incubation with a rabbit polyclonal antibody (1:5000) targeting the active forms of ERK1 and ERK2 (Promega UK Ltd., Hampshire, UK) at RT for 1 hr on a shaker. The primary antibody preferentially targets the dually phosphorylated form of ERK1 and ERK2 corresponding to residues $Thr^{183}$ and $Tyr^{185}$. After serial washes immunoblots were developed with a horseradish peroxidase-conjugated anti-rabbit mouse secondary antibody from DakoCytomation (Ely, Cambridgeshire, UK) for 1 hr at RT and the antigen-antibody reaction analysed by enhanced

chemiluminescense using a commercially available kit (ECL plus; Amersham, GE Healthcare, Buckinghamshire, UK).

### 2.6.2 CaSR western blotting

BAoSMC (passage 6–8) and HAoSMC (passage 4-5) were grown in 75 $cm^2$ culture flasks in 10% FCS-DMEM (1.2 mM $Ca^{2+}$) until confluence. Upon confluence, SMCs were lysed on ice with RIPA buffer supplemented with protease and phosphatase inhibitors (as above; section 2.6.1) with the addition of 1 mM N-ethylmaleimide. Lysates were spun at 2500 x g for 20 min, pelleting the cell debris and cell nuclei. The post nuclear supernatant was then spun at 17,000 x g for 30 min at 4 °C. After resuspension total protein concentration of the samples were determined as detailed in section 2.5.

Membrane preparations were mixed with 5x Laemmli buffer and heated at 65 °C for 3 min prior to immunoblotting. Proteins were separated on a 5% polyacrylamide gel and transferred to nitrocellulose membrane. Immunoblots were blocked with 2% BSA in TBST for 1 hr at 37 °C and probed with an anti-CaSR moloclonal antibody (Affinity BioReagents MA1-934, Rockford, Illinois, USA), raised to amino acids 214–235 of the extracellular domain of the human parathyroid CaSR. Primary antibody was diluted 1:5000 in 2% BSA in TBST and incubated for 1 hr at RT. Immunoblots were washed for 20 min with periodic changes of TBST and incubated with the secondary antibody, a horseradish peroxidase-conjugated anti-rabbit antibody (DakoCytomation, Cambridgeshire, UK) for 1 hr at RT. After washing, immunoblots were incubated with enhanced chemiluminescence (ECL plus; Amersham, GE Healthcare, Buckinghamshire, UK) to detect binding of the secondary antibody to the primary anti-CaSR antibody.

## 2.7 Bio-Plex phosphoprotein detection array

HAoSMC (passage 4–6) were plated at 2 x $10^5$ cells/$10cm^2$. All materials, including Bio-Plex kits, were from BioRad (BioRad Laboratories Inc, Hempstead, UK) unless otherwise stated. The following day (day 1) medium was changed to DMEM/F:12 (1:1) (Invitrogen, Paisley UK) with sterilized 0.2%

BSA and cells incubated overnight. On the day of the experiment (day 2) the medium was aspirated and HAoSMCs washed briefly with PBS heated to 37 °C. HAoSMCs were equilibrated in low $Ca^{2+}$ buffer (0.5 mM, as described in section 2.6.1) for 20–30 min. For $Ca^{2+}$ experiments: after equilibration, low $Ca^{2+}$ buffer was aspirated and cells incubated with 0.5 mM $Ca^{2+}$ (control) and 5 mM $Ca^{2+}$ for 5 min, consistent with the time-dependent elevation in $Ca^{2+}$-induced signalling in HAoSMC demonstrated by Molostvov et al. (2007). For calcimimetic experiments: after equilibration, low $Ca^{2+}$ buffer was aspirated and cells incubated with 2.5 mM $Ca^{2+}$ in the presence and absence (control) of R-568 (1 nM). Following the 5 min incubation, HAoSMCs were washed with ice cold wash buffer and lysed using 250 µl lysis buffer supplemented with factor 1 (250x), factor 2 (500x) (Bio-Plex cell lysis kit) and phenylmethylsulfonyl flouride (Sigma-Aldrich Co, Dorset, UK) dissolved in DMSO (500 mM), in accordance with manufacturer's instructions. HAoSMCs were incubated with the lysis buffer on a rotating platform at 300 rpm for 20 min at 4 °C after which they were removed using a plastic scraper. Lysates were collected in 1.5 ml eppendorf tubes and centrifuged at 4,500 x g for 20 min at 4 °C. The supernatant was collected and diluted 1:1 using assay buffer (Bio-Plex phosphoprotein detection reagent kit).

The Bioplex assay was performed following the manufacturer's protocol (BioRad, BioRad Laboratories Inc, Hempstead, UK), and summarised in Figure 2.2. The target phosphoproteins examined and the binding sites of the antibodies used are shown in Table 2.1. Firstly, the 96-well filter plate (Bio-Plex phosphoprotein detection reagent kit) was pre-wet with assay buffer. Then, 1 µl of each phosphoprotein bead solution (50x) was diluted in wash buffer (Bio-Plex phosphoprotein detection wash buffer) and added to each well. Excess liquid was removed by aspiration. After two washes, 50 µl of cell lysate (final concentration 200–900 µg/mL) was added to each well and incubated overnight at RT on a shaking platform at 300 rpm. The following day, any unbound proteins were removed by washing with wash buffer. Biotinylated detection antibodies (25x), specific to each phosphoprotein bead, were prepared using the detection antibody diluent and 25 µl added to the reaction. The plate was vortexed before a 30 min incubation. After further

washes and vacuum filtration, Streptavidin-Phycoerythrin (Strept-PE) (100x; Bio-Plex phosphoprotein detection reagent kit) diluted to a 1x solution with wash buffer to a final volume of 50 µl was then added and incubated for a further 10 min in the dark. Strept-PE was removed by vacuum filtration and a further series of washes . The beads were resuspended in 125 µl of resuspension buffer, incubated for 30 seconds at 1,100 rpm on a shaking platform and analysed using the Luminex 100 system. The Luminex system identifies beads for specific phosphoproteins by the bead region, the ratio of the internal red and green fluorescent dyes. Data are expressed as % change from control.


**Figure 2.2 The methodological processes and rationale underlying the Bioplex assay (adapted from Bioplex manual).**

**Table 2.1 Phosphorylation sites targeted by Bioplex antibodies**

| Phosphoprotein | Amino acid site |
|---|---|
| Akt | $Ser^{473}$ |
| BCR-Abl | $Tyr^{245}$ |
| c-Jun | $Ser^{63}$ |
| CREB | $Ser^{133}$ |
| ERK 1/2 | $Thr^{202}/Thr^{204}$<br>$Thr^{185}/Thr^{187}$ |
| GSK-3α/ß | $Ser^{21}/Ser^{9}$ |
| HSP27 | $Ser^{78}$ |
| IGF-1R | $Tyr^{1131}$ |
| I-κB | $Ser^{32}/Ser^{36}$ |
| JNK | $Thr^{183}/Tyr^{185}$ |
| MEK | $Ser^{217}/Ser^{221}$ |
| PDGF | $Tyr^{751}$ |
| p38 | $Thr^{180}/Thy^{182}$ |
| p53 | $Ser^{15}$ |
| p70 S6K | $Thr^{359}/Ser^{363}$ |
| p90 RSK | $Thr^{421}/Ser^{424}$ |
| Src | $Tyr^{416}$ |
| Stat3 | $Tyr^{705}$ |
| Tyk2 | $Tyr^{1054}/Tyr^{1055}$ |

## 2.8 Adenoviral infection

A recombinant adenovirus (RAd) encoding the full length human CaSR with an arginine to glutamine substitution at position 185 (pacAd5CMV/dnCaSR), resulting in a dominant negative form, was generated under the direction of Dr. Beverly Davidson at the University of Iowa Gene Transfer Vector Core and has been characterised previously[84]. A multiplicity of infection (MOI) of 150 pfu/cell and viral titre of 3 x $10^{10}$ plaque-forming units/µl was used and transfection efficiency confirmed using a CaSR Western blot.

BAoSMCs (passage 9) were transfected at 80% confluence (typically day 4). 48 hrs following infection (day 6), BAoSMCs were induced to calcify with medium containing 5% FCS-DMEM and 5 mM BGP with either 1.2 mM or 1.8 mM $Ca^{2+}$. BAoSMCs were maintained in this media for the remainder of the experiment. Overexpression of the transgene was maintained by re-infection of the cultures on day 8. Alizarin red staining was performed on day 12.

## 2.9 RT-PCR

### 2.9.1 RNA isolation

RNA from freshly isolated bovine parathyroid gland was kindly provided by Donald Ward (University of Manchester). RNA was isolated from cultured BAoSMCs (passage 6–8), at 90% confluence, using Trizol reagent (Invitrogen, Paisley, UK). Medium was removed, BAoSMCs washed with ice cold PBS and cells lysed directly in the culture flask. 1 ml Trizol/T75 flask was added and cells detached using a cell scraper. The Trizol solution was removed and placed in a 1.5 ml eppendorf tube where 0.2 ml chloroform (0.2 ml to 1 ml Trizol) was added. The lysates were vortexed vigorously for 15 sec and centrifuged at 12,000 x g for 10 min at 4 °C. Following centrifugation, the mixture separates into a lower red, phenol-chloroform phase, an interphase, and a colourless upper aqueous phase. RNA remains exclusively in the aqueous phase.

The clear aqueous solution (upper level) was transferred to a clean 1.5 ml eppendorf tube. To precipitate the RNA, the aqueous phase was mixed with

0.5 ml isopropanol for 2 min before being centrifuged at 12,000 x g for 10 min at 4 °C. The RNA precipitate forms a small pellet on the bottom/side of the tube. The RNA pellet produced was washed with 75% ethanol and further centrifuged at 12,000 x g for 5 min. All leftover ethanol was removed and the pellet left to air-dry. RNA was dissolved in diethylpyrocarbonate (DEPC)-treated water (Ambion, Warrington, UK) and stored at -80 °C until use.

RNA was quantified using a Nanodrop (Nanodrop ND-100 v3.3 Spectrophotometer, Thermo Scientific, Delaware, USA) and the quality of the RNA assessed by running 1 µl on a 2% agarose gel and ethidium bromide staining. Contaminating genomic DNA appears as a weak band of high molecular weight. If present, contaminating genomic DNA was removed using Turbo DNase (Ambion inc, Huntingdon, UK). The reaction was incubated at 37 °C for 30 min before adding the inactivation reagent. The inactivation reagent was removed from the sample by centrifugation.

### 2.9.2 First strand cDNA synthesis

Reverse transcription of total RNA was carried out using SuperScript first strand synthesis kit (Invitrogen, Paisley, UK), according to manufacturer's instructions. Total RNA was mixed with 50 ng/µl random hexamers, 10 mM dNTP mix, 10 µl DEPC-treated water and incubated at 65 °C for 5 min. Following incubation the RNA/primer mixture was placed on ice for 1 min. The cDNA synthesis mix was prepared by adding 10 X reverse transcriptase buffer, 25 mM $MgCl_2$, 0.1 M dithiothreitol (DTT), 40 U/µl RNaseOUT and 200 U/µl Superscript III RT. To this, the RNA/primer mixture was added, mixed gently and incubated for 10 min at 25 °C followed by 50 min at 50 °C. The reaction was terminated by heat inactivation of the enzyme at 85 °C for 5 min and samples chilled on ice. Finally, 1 µl of RNase H was added to each tube and the samples were incubated at 20 min at 37 °C before storing at -20 °C. Control reactions were performed in which the reverse transcription step was omitted.

### 2.9.3 PCR

PCR amplification of CaSR complementary DNA (cDNA) was attempted using 2 different primer sets; primer 1 designed to amplify 2198–2253 and primer 2 4755–4951 of NM_174002. The binding sites of each primer set is shown in Figure 2.3. Primer 1 was designed using Primer3[251], and the reverse primer bridges the exon6-exon7 junction. Primer 2 was kindly provided by Dr. Masih Alam (University of Manchester), and is positioned within the 3' downstream sequence. Amplification was performed using Immomix Red (Bioline, London, UK) using the Eppendorf MasterCycler Gradient (Eppendorf, Cambridge, UK). Each PCR amplification was performed under the following conditions: an initial denaturation step at 95 °C for 10 min, followed by a total of 35 cycles of 95 °C (30 sec), 58 °C (30 sec ), and 72 °C (30 sec) and a final elongation step of 72 °C. Control PCR was carried out using primers specific for bovine glyceraldehyde 3-phosphate dehydrogenase (GAPDH), amplifying 572–626 of NM_001034034, to produce a PCR product of 54 bp. As a negative control and to prevent amplification of contaminating genomic DNA, control samples which were treated without reverse transcriptase were also included. RT-PCR products were separated on a 1% agarose gel.

## 2.10 Statistical analysis

For paired comparisons, paired t-tests were performed. For multiple comparisons a one way anova with tukey's post hoc test was used. Signalling data were analysed comparing raw data from control vs. test samples. In instances where multiple control samples were included in one experiment the average of the control samples was used.

cggaaaaaaaaaaaaagttccccactctagtacagagaaggttggcagagtcgtaagcccccaacctctt
aaacttctctgcatctccaaggagaaggagggaagaggggttctttccgacctgaggagctggatctgggg
tccgagaaccccaaggtagcaccggaaagaacagcacaggaggcgagagcgtggccggtggccggg
agaaccagacccgacgcgcggtcctcggcgccggggtcccggggactcagctcagcacgactgggaa
gccgaaagtactacacacggtctctgcatgatgtgacttctgaagactcaagagccacccacttcactagtc
tgcaatggagaaggcagaaatggaaagtcaaaccccacggttccattctattaattctgtagacatgtgccc
ccactgcagggagtgagtcgcaccaaggggaaagtcctcaggggcccccagaccaccagcgcttga
gtccctcttcctggagagaaagcagaact**atg**gcactttatagctgctgttggatcctcttggctttttctacctg
gtgcacttccgcctatgggcctgaccagcgagcccaaaagaaaggggacattatcctcgggggctctttc
ctattcattttggggttgcagtgaaagatcaggatctaaagtcgaggccggagtccgtggagtgtatcaggta
taatttccgaggatttcgctggttacaagctatgatatttgccatagaggaaataaacagcagtccagcccttc
ttcccaacatgaccctgggatacaggatattcgacacttgtaacaccgtctctaaagccttggaggccaccct
gagttttgtggcccagaacaaaattgactctttgaaccttgatgagttctgcaactgctcagagcacatcccct
ctaccatcgcagtggtgggagctactggctcgggcatctccacagcagtggccaacctgctggggctcttct
acatcccccaggtcagctatgcctcctccagcagactcctcagcaacaagaatcaattcaagtccttcctcc
gcaccatacccaatgatgaacaccaggccacggccatggctgacatcatcgagtacttccgctggaactg
ggtgggcacaattgcagctgacgatgactatggccggccagggatcgagaagtttcgagaggaagctga
ggagagggacatctgcatcgacttcagcgagctcatctcccaatactctgatgaggaaaagatccagcag
gtggtggaggtgatccagaattccaccgccaaagtcattgtcgtcttctccagcggcccagacctggaaccc
ctcatcaaagagatcgtccggcgcaatatcacaggcaggatctggctggccagcgaggcctgggccagc
tcttccctgattgctatgcccgagtatttccatgtggtcggaggcaccattgggtttggtttgaaagctgggcag
atcccaggcttccgggaattcctgcagaaagtccaccccaggaagtctgtccacaatggttttgccaagga
gttttgggaagaaacatttaactgccacctgcaagagggtgctaaaggcccattaccggtggacaccttcct
gagaggtcacgaagaaggaggtgccaggttaagcaacagtcccactgccttccgacctctgtgcactggg
gaggagaacatcagcagtgtcgagactccttacatggattatacacatttacggatatcctacaacgtctact
tagccgtctactccattgctcatgccctacaagatatatacacctgcatacctgggagagggctcttcaccaa
cggttcctgcgcagatatcaagaaggttgaagcttggcaggtcctgaaacacctgcggcacctaaattttac
cagcaatatgggggagcaagtaactttcgatgaatgtggagacctggcagggaactattccatcatcaact
ggcacctctccccagaggacggctccatagtgtttaaggaagttggatattacaatgtctatgccaagaaag
gagagagactcttcatcaatgatgaaaaaattctgtggagtggattctcaagggaggtgcctttctccaactg
cagtcgagactgcctggcagggaccaggaaaggaatcattgaggggagcccacctgctgctttgagtgt
gtggaatgtcctgatggggagtacagcgacgagacag*atgcaagtgcctgtgataagtgccctgatgact
tctggtccaatgagaaccacacttcctgcatcgccaaggagatcgagtttctgtcgtggaccgagcccttcg
ggatcgcactcacgctctttgctgtgctgggcattttcctcacagccttcgtgctgggcgtcttcatcaagttccg

caacacgcccatcgtcaaggccaccaaccgggagctctcctatctccttctcttctccctgctctgctgcttctc
cagctccctgttcttcatcggggagccccaggactggacgtgccgcctgcgccagccggcctttggcatca
gcttcgtgctctgcatctcgtgcatcctggtgaaaaccaatcgggtcctcctggtgtttgaggccaagattccc
accagcttccaccggaagtggtgggggctcaacctgcagttcctgctggtcttcctctgcaccttcatgcagat
tgtcatctgtgccatttggctcaatacagcgcccccctcggctaccgcaaccacgagctggaggacgagat
catcttcatcacctgccacgagggctcgctcatggcgctgggcttcctgatcggctacacctgcttgctggcc
gccatctgcttcttcttcgccttcaagtcccggaagctgccagagaacttcaatgaagccaagttcatcacctt
cagcatgctcatcttcttcatcgtctggatctctttcatccccgcctacgccagcacttacggcaagttcgtctctg
ccgtggaggtgatcgccatcctggcggccagctttggcttgctggcctgtatcttcttcaacaaggtctacatc
atcctcttcaagccttcccggaacaccatcgaggaggtgcgctgcagcaccgcggcacacgccttcaagg
tggccgcccgagccacgctgcgccgcagcaacgtctcccgccagcggtccagcagcctaggggctcc
acgggatccacccctcctcctccatcagcagcaagagcaacagcgaggacccgttccctcagcagcag
ccgaagaggcagaagcagccgcagccgctggccctgagcccgcacaacgcgcagcagccacagcc
gcggccaccctcgaccccacagccgcagccacagtcgcagcagccgccccgatgcaagcagaaggtc
atcttcggcagcggcaccgtcaccttctcgctgagctttgacgagcctcagaagaccgccgtggctcacag
gaattccacgcaccagacctccctggaggcccagaaaaacaatgacgccctgaccaaacaccaggcgt
tgctcccgctgcagtgcggagagacggactcagaattgacctcccaggagacaggcctgcagggccctg
tgggtgaggaccaccagctagagatggaggaccccgaagagatgtccccggcacttgtagtgtctaattcc
cggagctttgtcatcagtggcggaggcagcactgttacggaaaacatgctgcgttctta**aaa**gggaaggag
aaagccagttcaggggaatccaggcagtttccccgggatgaccttctccaaagggatgaggaactgccc
ccccacccccacccccttcctccaggaaggagggataagacccaccaaatgcttggaacttagttgcact
gctataaacgacagtgaatgaaataatgtccccctaaaattaaaaagaggggagcggtgtgcttctgtggt
taggtttatcagagtgctgagatccctatagtcaggttcgcctttcctatccctgcttccattctcctcttctgttctat
cccatccaacagtccagagataaaaccatggctttaagatacccacctattccccctagggtcttatttgttgtt
tttgttgctgttgttttggtttgatttttgtttttaatgttgaaacgtctgccctgaactttgcagacagcctggtccaaa
aacaaacctgtgcagagtgacaggacctcctatgggcaccactagagttgagtgcgaaagacagaatgt
cgccagcgctgcccaacaccttgacagtgggaagaacttgaaatgtccagagctgtaagatgaatgtgtcc
cctcctatttatgaaaaatgttaaatatgtggtttcctacttgctgctgctgtcacgtgacatggagaaggttagc
atccatcctccagcagtatgtctgatcttgtccagagtgtgatggtgatgccacgtttagattccaatatctcagg
aatcacctcagcctgcatgaatccaatgagctgtatctgtaattaatattgtcatatgtagctttatccttaagaa
aatgtgtttgttttaatagtccgtggaaaatataagctggaaaaaatgtcccagtctggttgatataaggcagta
ttattgagtcccgttttctttgcccgccccaccacccacaccccaatgagctaagccctaaatgagccctttca
gggcccaggatccagaagctccctctttctccaccccaaacgcttcctgaagtcagatccatgcctttccct
gtgaagaataagctcccagtctctgacctcctaccagtttctggggtaagaacacgtggttccaagagagct

ctcatgggatattactcttggcacccccaatgccatacttaggttccctccagcagtgggatctgcccatggg
tagttacaagattgaacgttgaatggcatactgctgaacagtcagttctggagctagagaggcctggggtca
agtgctgggtttgtcactcacaagttgggtgaccacaggcagggaaccttgacctcactcagccccagcttc
tttgtgtctaaaatggaggtaataatcatccttttcccgcagagctcttatgtgggttaaatgagataaatgtatgt
aaagtattttagcatggtgcctagcccatagtaagcacgcaataaatattagttaatatta

**Figure 2.3 Binding sites of primer sets on the Bos taurus CaSR sequence (NM_174002).** Positioning of the two primer sets demonstrated in yellow (Primer 1) and pink (Primer 2). The start and stop codons, highlighting the translated region, are bolded. * represents positioning of intron 6–7.

# 3.0 Results

## 3.1 Characterisation of explanted cells

Three preparations of cells were explanted from bovine aorta (as described in section 2.1.1), named preparation A – C. Immunofluorescent staining using a monoclonal α-sma antibody, was used to characterise the explanted cells. A mouse IgG2a replaced the primary antibody and served as a negative control. Cells explanted from the aorta showed appropriate morphology for smooth muscle cells and positive α-sma staining of the actin filaments in each preparation (Figure 3.1, left panel) whilst no staining was observed when the primary antibody was replaced with mouse IgG (Figure 3.1, right panel).

To further characterise each SMC preparation, the mineralisation potential was assessed. SMCs can be induced to undergo mineralisation when cultured in the presence of β-glycerophosphate (BGP)[72]. The mineralisation potential of prep A-C was evaluated in response to 5 mM BGP in the presence of 1.8 mM $Ca^{2+}$ (Figure 3.2). In the presence of 1.8 mM $Ca^{2+}$ and 5 mM BGP, all preparations showed an increase in mineralisation confirmed using alizarin red staining (Figure 3.2, right panel). In preparations A and C, cells retracted into multicellular nodular structures which stained with alizarin red, whilst mineralisation in preparation B appeared more diffuse and widespread throughout the cell population.

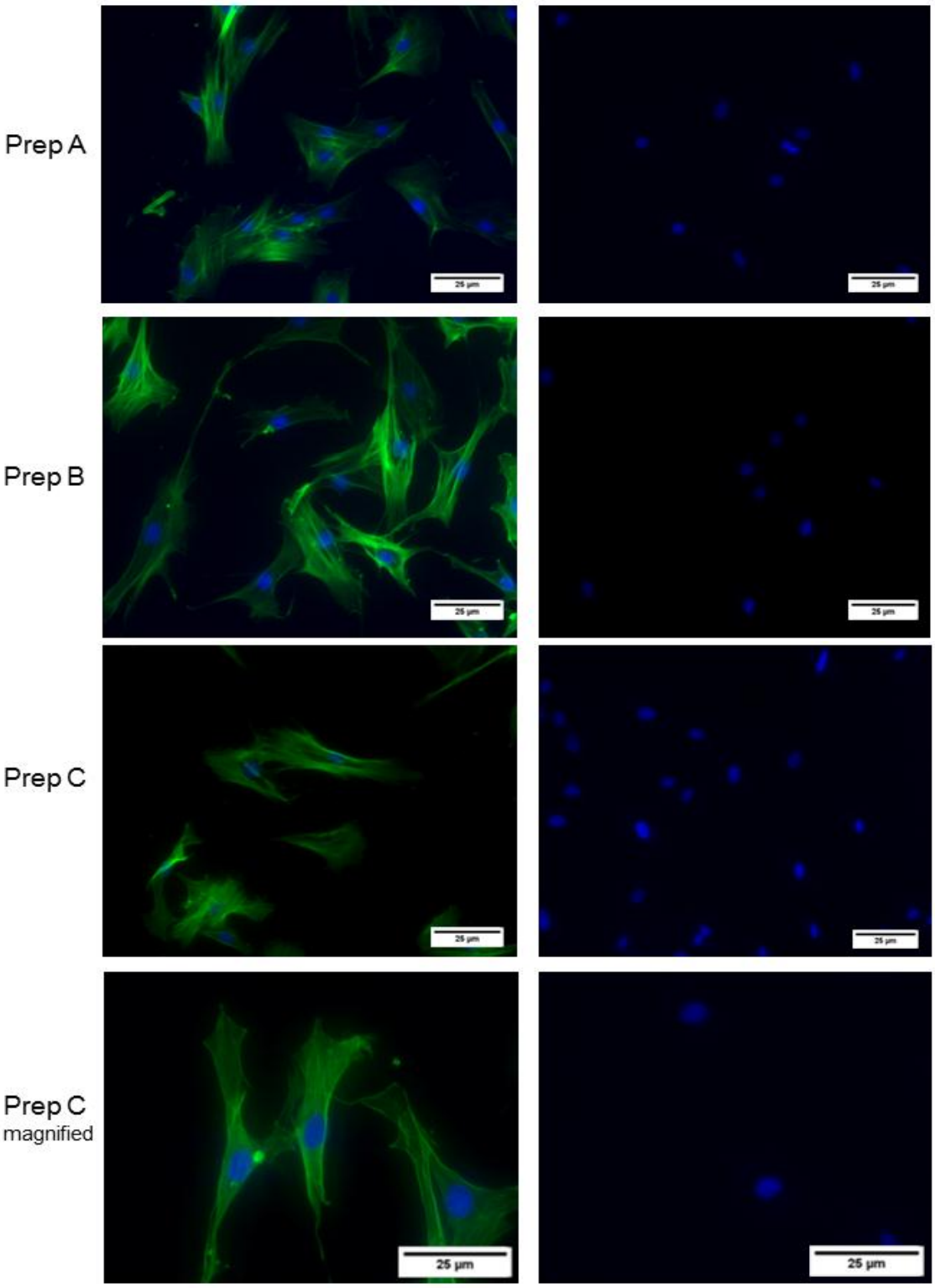


**Figure 3.1 Immunostaining of bovine aortic explanted cells (prep A-C) with α-sma.** BAoSMC (passage 3) were cultured in 10% FCS-DMEM in the presence of 1.2 mM $Ca^{2+}$. Images show immunofluorescence staining with α-smooth muscle actin (1:400) and fluorescein isothiocyanate (FITC) secondary (1:100) in cultured explanted BAoSMCs (left panel). As a control, the α-sma primary antibody was replaced with mouse IgG2a (right panel). Nuclei were counterstained using the DNA specific dye DAPI (blue). Bar = 25 µm.

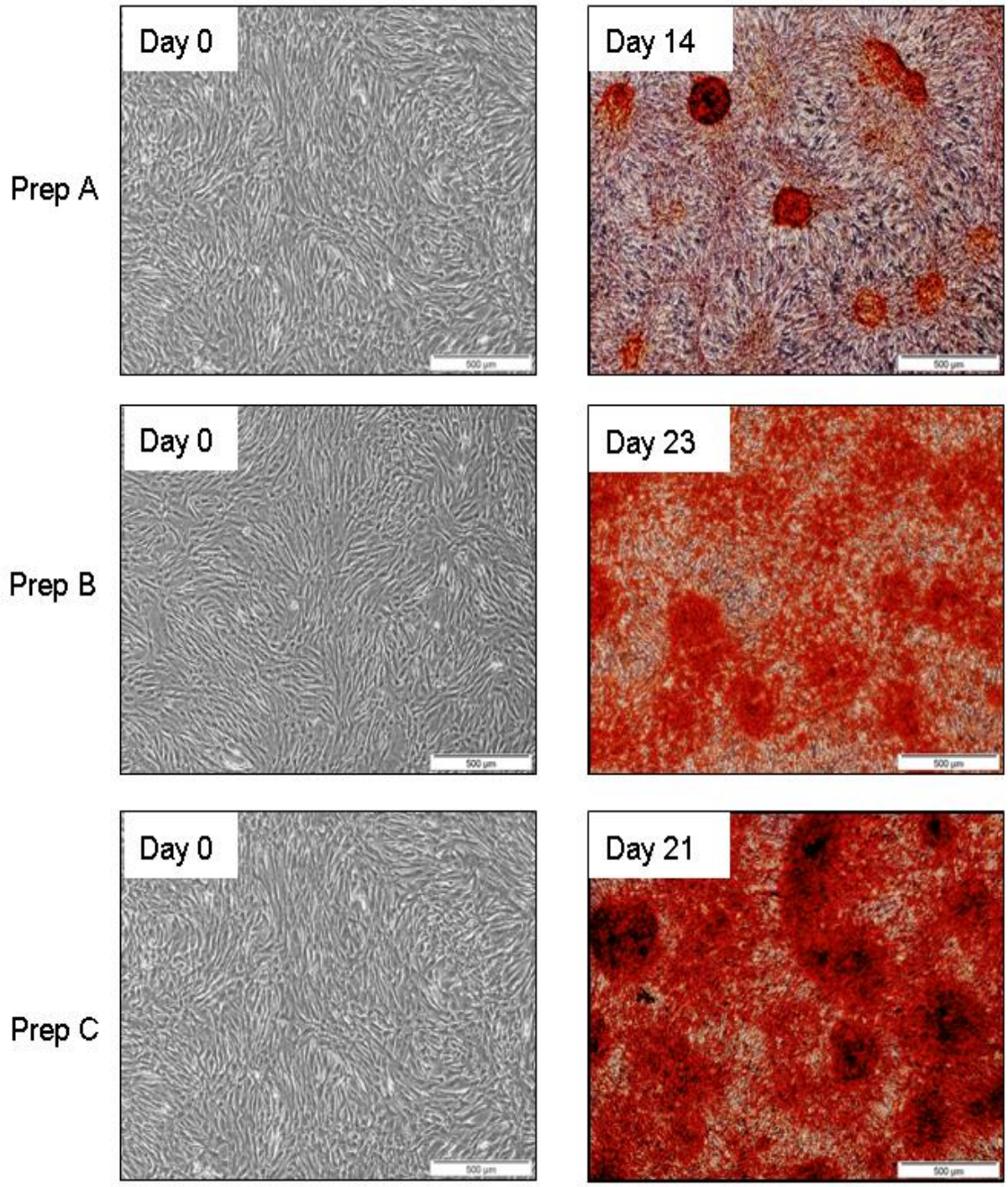


**Figure 3.2 Mineralisation potential of explanted BAoSMC (prep A-C).** Explanted BAoSMC (passage 3) were incubated from confluence (day 0) with calcifying medium (5% FCS-DMEM with 5 mM BGP) in the presence of 1.8 mM $Ca^{2+}$. Mineral deposition was detected with alizarin red staining at variable time points (right hand panel). Bar = 500 µm.

The different preparations of BAoSMCs showed variability in their response to incubation with 2.5 mM $Ca^{2+}$ in the presence of BGP (Figure 3.3). At day 9, BAoSMCs incubated with 5 mM BGP and 2.5 mM $Ca^{2+}$ from preparation A remain healthy, however by day 14 the cell monolayer had detached (image not shown). With preparation B, detachment of the cell monolayer was detected earlier in the course of the experiment with complete detachment detected by day 9 (Figure 3.3). Preparation C BAoSMCs did not show cell monolayer detachment but by day 9 rapid nodule formation was detected alongside cell loss.

For consistency only one preparation of BAoSMCs were used in all future experiments. On the basis of these initial results, any of the preparations shown would have been suitable for follow on experiments (all showing positive α-sma staining and the ability to undergo mineralisation), however preparation C was selected. Additionally, a maximum $Ca^{2+}$ concentration of 2.2 mM was used for experiments requiring chronic incubation.

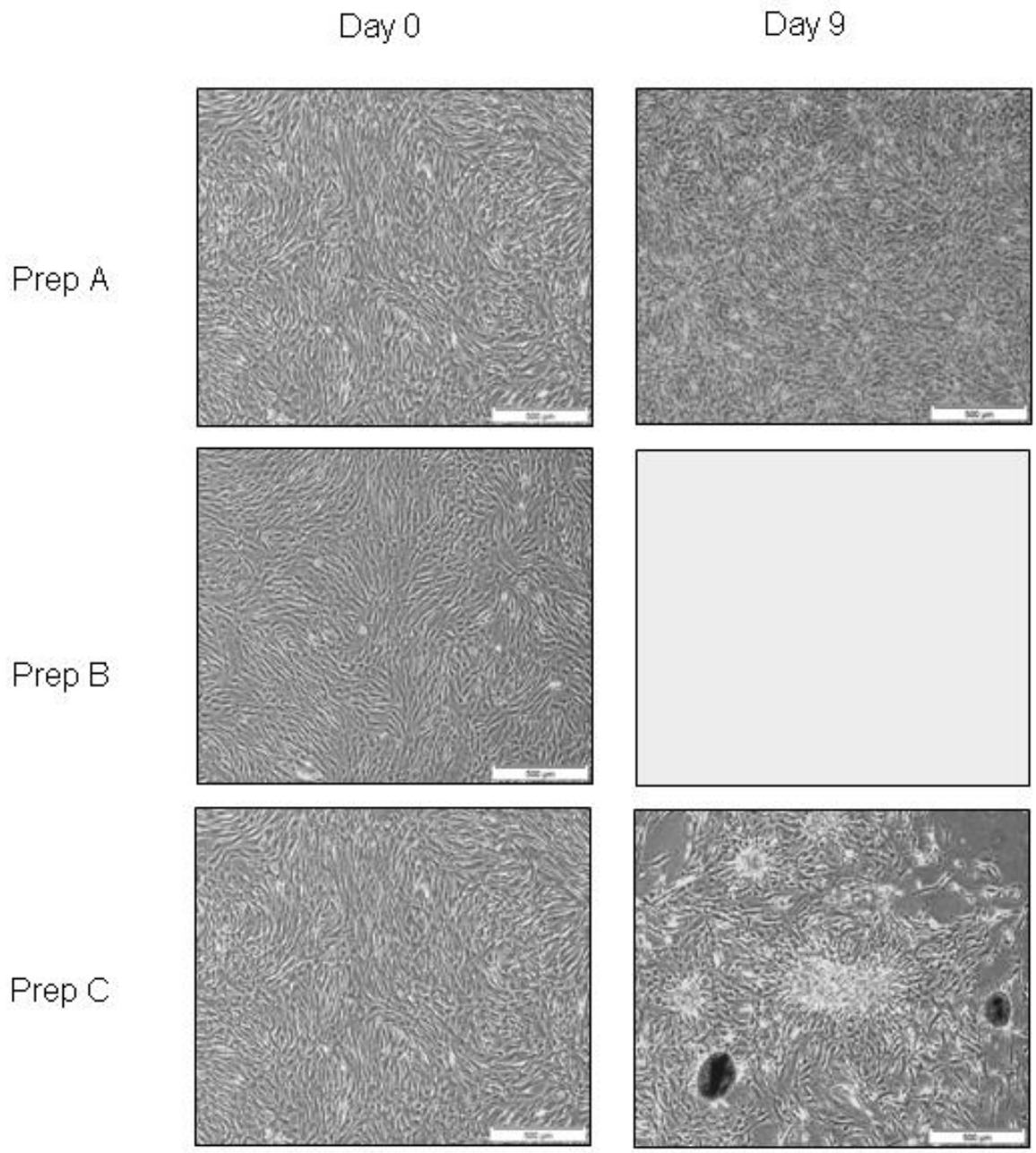


**Figure 3.3 Effect of 2.5 mM $Ca^{2+}$ and 5 mM BGP on BAoSMC morphology and distribution (prep A - C).** Explanted BAoSMC (passage 3) were incubated from confluence (day 0) with 5% FCS-DMEM with 5 mM BGP in the presence of 2.5 mM $Ca^{2+}$. Images were captured at day 0 and day 9. No image is presented for preparation B at day 9 as the cell monolayer had detached from the culture flask. Cell morphology in the presence of 1.8 mM $Ca^{2+}$ from the same experiment is shown in Figure 3.2. Bar = 500 µm.

### 3.2 Assessment of CaSR immunoreactivity in BAoSMC

To examine the expression of the CaSR in BAoSMC methods to investigate both protein and messenger RNA (mRNA) expression were used. Alam et al. (2009) previously examined the protein expression of CaSR in BAoSMC, successfully demonstrating CaSR-like immunoreactivity[84]. Therefore to confirm that preparation C BAoSMC also expressed CaSR, immunofluorescence and western blot analysis were employed. Immunostaining BAoSMC with an anti-CaSR antibody raised against residues 214–235 of the human CaSR, produced positive staining (Figure 3.4Ai). Whilst positive staining was detected in the majority of BAoSMCs (additional images shown in Figure 6.2B), a few cells showed no expression (Figure 3.4Ai, arrow). Replacing the primary antibody with mouse IgG2a (ii) or omitting the primary antibody (iii) resulted in the absence of immunoreactivity.

CaSR-like immunoreactivity in BAoSMC was also demonstrated using SDS PAGE and Western blotting of BAoSMC membrane preparations (Figure 3.4B). Under reducing conditions 3 major bands were detected with apparent Mw's of ~160, ~200 and ~250 kDa. The ~160 kDa polypeptide corresponds to the expected position of the glycosylated form of the full length CaSR while the 250 kDa band is likely to represent the dimeric form. In human embryonic kidney cells (HEK293) induced to stably express human CaSR (CaSR-HEK), 4 major bands were detected; with bands at ~160 kDa and ~200 kDa corresponding to those seen in SMCs and a doublet at ~280 / 300 kDa (Figure 3.4C). A comparison of the immunoreactivities produced by CaSR-HEK and SMC samples is shown in Figure 6.2A.

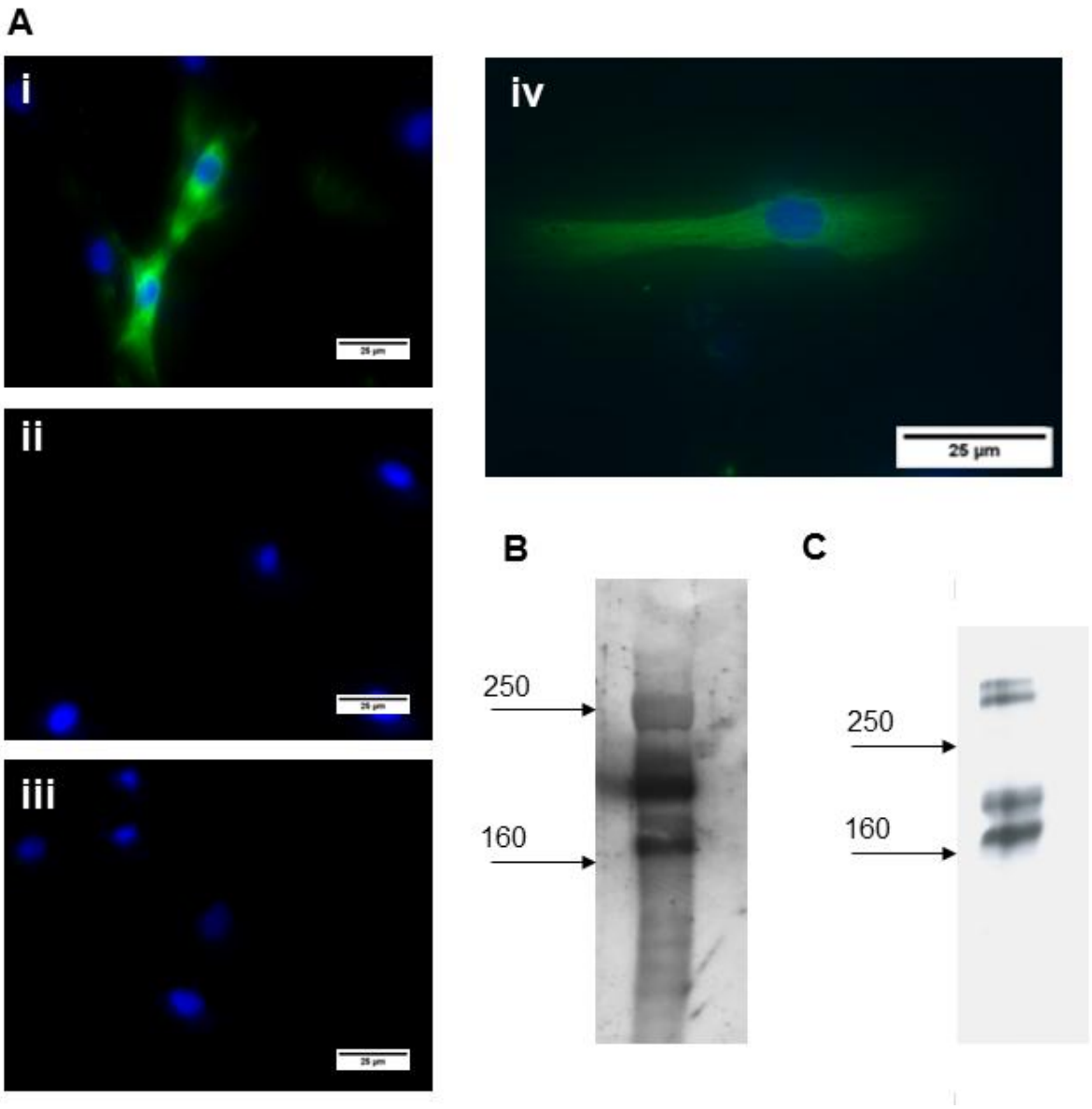


**Figure 3.4 CaSR immunoreactivity in BAoSMC.** A: BAoSMC (prep C; passage 4) grown on chamber slides for 24 hrs in 10% FCS-DMEM (1.2 mM $Ca^{2+}$) were fixed with 4% formaldehyde before incubation with a polyclonal antibody against human CaSR (1:200). A fluorescein isothiocyanate (FITC)-conjugated secondary antibody (green; 1:40) and DAPI (blue) was used to visualise the CaSR and nuclear staining (i). Arrows used to highlight BAoSMCs with negative staining. Control cells were stained with either mouse IgG2a (ii) or secondary antibody alone (iii). (iv) shows BAoSMC stained with anti-CaSR (as above) at a higher magnification. Bar = 25 µm. B: Membrane preparations from cultured BAoSMC (passage 6) were separated using 5% SDS-PAGE and CaSR immunoreactivity detected by Western blotting using a CaSR antibody (1:5000). Exposure time 3 min. Lysate from CaSR-HEK cells (C) were used as a positive control. Exposure time 10 sec. Size (in kDa) of molecular weight markers is indicated on the left.

### 3.3 Assessment of CaSR mRNA expression in BAoSMC

To investigate whether CaSR mRNA is expressed in cultured BAoSMC, RT-PCR was performed on complementary DNA (cDNA) synthesized from total RNA. Amplification of CaSR from BAoSMC and parathyroid cDNA (from freshly isolated bovine parathyroid gland) was performed with two distinct primer sets (detailed in section 2.9.3 and illustrated in Figure 2.3). PCR products of the expected size for each primer set were demonstrated with parathyroid cDNA, 55 bp and 196 bp respectively (Figure 3.5A). No products were detected in the absence of reverse transcriptase. However, RT-PCR of BAoSMC cDNA did not yield any CaSR amplicons, despite the acceptable quality of the cDNA demonstrated with successful amplification of GAPDH, a house keeping gene (Figure 3.5B). Despite the negative result, the presence of CaSR cannot be confirmed or denied as amplification of CaSR was not attempted in other tissues with reported low expression of CaSR (e.g. lung).

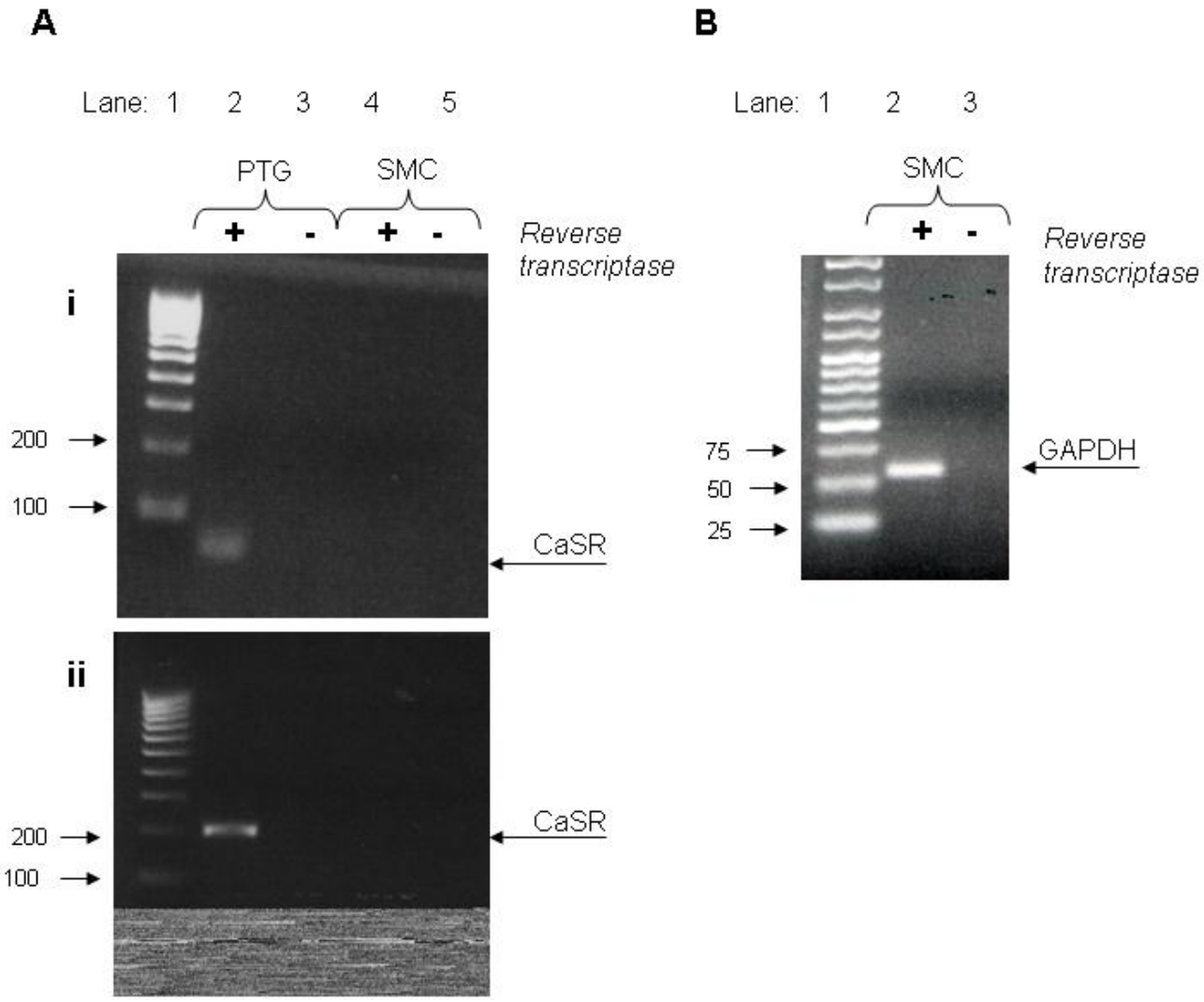


**Figure 3.5 Calcium-sensing receptor (CaSR) mRNA expression was not detected in BAoSMC**

RT-PCR was carried out using cDNA synthesized from total RNA from cultured BAoSMC (prep C; passage 6) and freshly isolated bovine parathyroid gland (provided by Donald T Ward). A: Two distinct primer sets for CaSR (described in section 2.9.3) were used (Ai-ii). *Lane 1: Hyperladder IV, Lane 2: PTG (+ reverse transcriptase (RT)), Lane 3: PTG (-RT), Lane 4: SMC (+RT), Lane 5: PTG (-RT).* B: A control PCR to demonstrate successful reverse transcription of BAoSMC RNA was conducted using bovine GAPDH primers. *Lane 1: Hyperladder V, Lane 2: SMC (+ RT), Lane 3: SMC (-RT).*

### 3.4 $Ca^{2+}$ increases mineralisation and osteogenic differentiation in BAoSMC in the presence of BGP

The effect of $Ca^{2+}$, a typical CaSR agonist, on BAoSMC mineralisation was investigated. No mineralisation was detected in BAoSMC treated with different concentrations of $Ca^{2+}$ (1.2 mM, 1.8 mM and 2.2 mM) in the absence of BGP, however retraction of cells into nodular formations was observed (Figure 3.6).

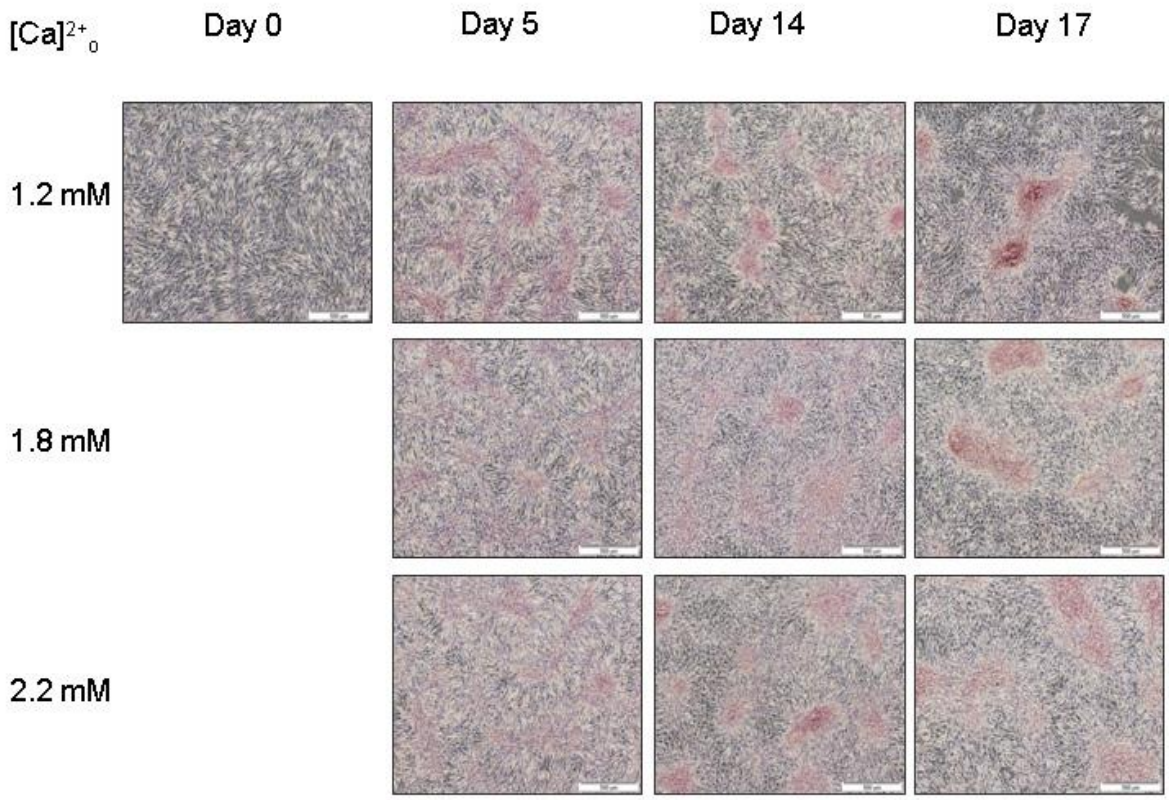


**Figure 3.6 $Ca^{2+}$-induced mineralisation requires the presence of BGP.** BAoSMC (prep C; passage 5) were treated upon confluence with increasing concentrations of $Ca^{2+}$ in the absence of BGP. Images show cells stained with alizarin red at indicated time points (staining in the presence of BGP from the same experiment is shown in Figure 3.7A). Images depict a single experiment, however similar results were obtained in two independent experiments performed on different BAoSMC isolates (see figure 6. 3). Bar = 500 µm.

However in the presence of 5 mM BGP, BAoSMC treated with different concentrations of $Ca^{2+}$ (1.2 mM, 1.8 mM and 2.2 mM) showed a dose- and time-dependent increase in mineral deposition (Figure 3.7). $Ca^{2+}$

accumulation was quantified using cresolphthalein method and alizarin red dye elution. Increases in $Ca^{2+}$ accumulation were detected using both methods, with each showing significant increases with each elevation of $[Ca^{2+}]$ (Figure 3.7B & C).

The potential for $Ca^{2+}$ to promote osteogenic differentiation alongside $Ca^{2+}$ deposition was also investigated. Alkaline phosphatase is an early indicator of SMC osteogenic conversion, and its activity was measured in BAoSMC incubated with 1.2 and 1.8 mM $Ca^{2+}$ in the presence of BGP. On day 3 no difference in alkaline phosphatase activity was detected, however on day 5, alkaline phsophatase activity was shown to be significantly elevated in cells incubated with 1.8 mM $Ca^{2+}$ compared to cells incubated with 1.2 mM $Ca^{2+}$ (Figure 3.8A). No signs of mineralisation were observed on day 5 (Figure 3.8B), however by day 14 alizarin red staining confirmed mineral deposition, with greater mineralisation detected in BAoSMCs incubated with 1.8 mM $Ca^{2+}$ compared to 1.2 mM (Figure 3.8C).

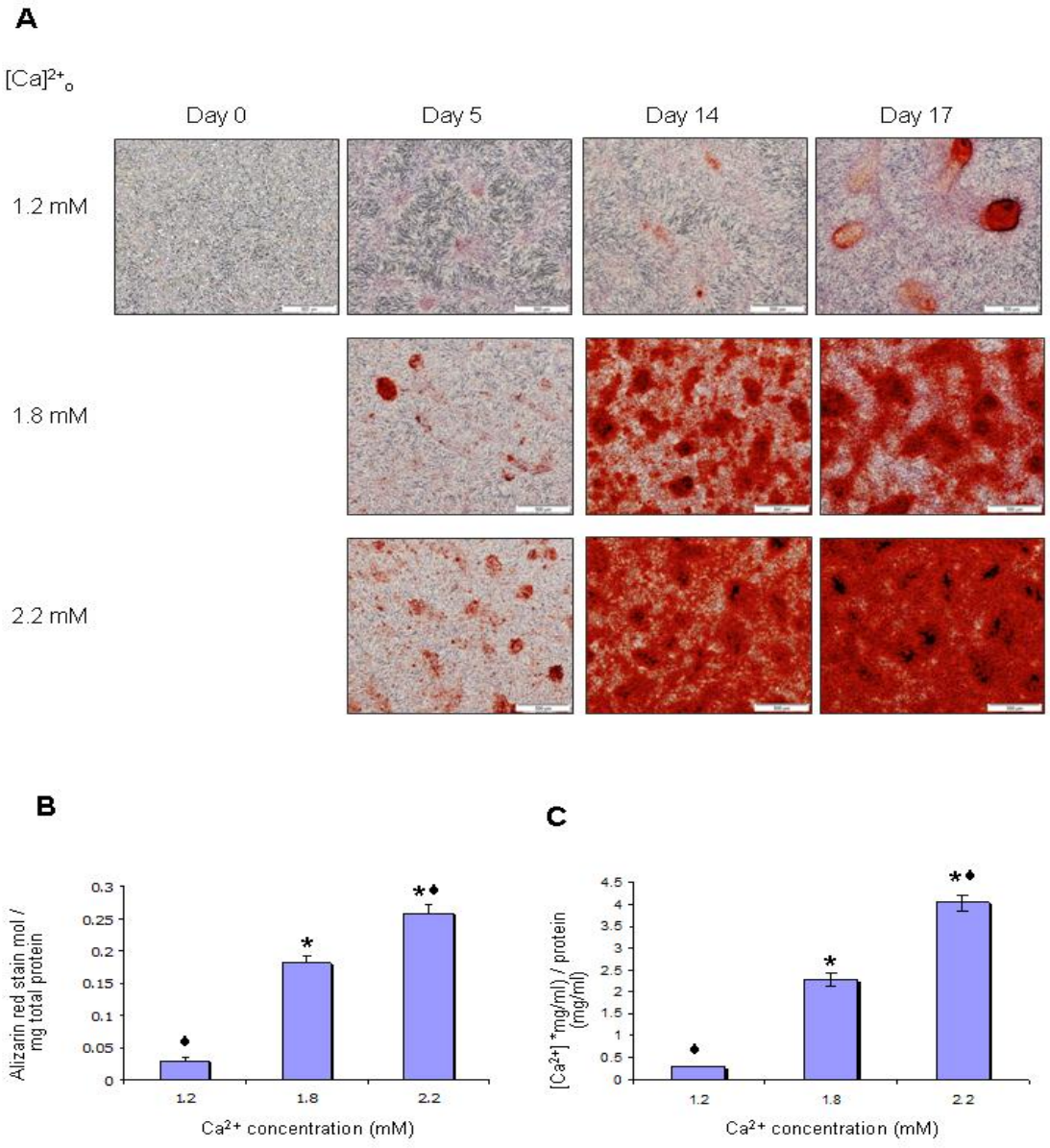


**Figure 3.7 Concentration-dependent effects of $Ca^{2+}_o$ on SMC mineral deposition** A: BAoSMC (prep C; passage 5) were treated upon confluence with increasing concentrations of $Ca^{2+}$ alongside 5 mM BGP. Images show BAoSMCs stained with alizarin red at indicated time points (staining in the absence of BGP from the same experiment is shown in Figure 3.6). Images shown were captured from a single experiments, however $Ca^{2+}$-induced increases in mineralisation were shown in 2 additional experiments (Figure 6.4). Bar = 500 µm. B: Mineralisation quantified by elution of alizarin red stain from stained mineral deposits on day 14. Results are expressed as moles of alizarin red stain per mg of total cellular protein. Data are from a single mineralisation experiment conducted in triplicate. Data represent the mean ± SEM. * $P < 0.05$ vs. 1.2 mM $Ca^{2+}$; ♦ $P < 0.05$ vs. 1.8 mM $Ca^{2+}$. C: $Ca^{2+}$ accumulation was quantified on day 14 using the cresolphthalein method.
Data are represented as mean ± SEM from a single experiment (n=3). * $P < 0.05$ vs. 1.2 mM $Ca^{2+}$; ♦ $P < 0.05$ vs. 1.8 mM $Ca^{2+}$

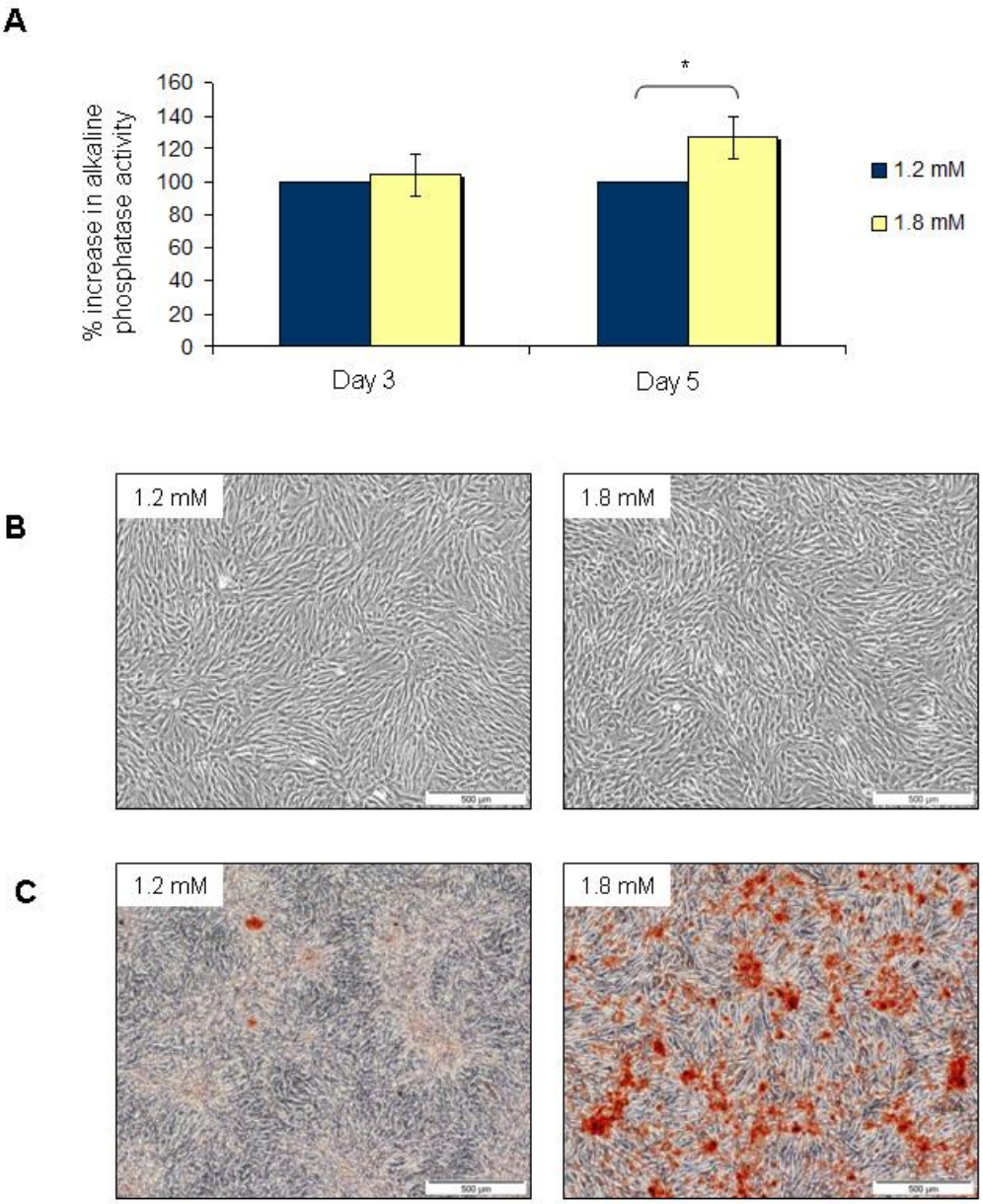


**Figure 3.8 Alkaline phosphatase activity in BAoSMC is $Ca^{2+}$-dependent.** A: BAoSMC (prep C; passage 7-9) were incubated with 5% FCS-DMEM and 5 mM BGP in the presence of 1.2 mM or 1.8 mM $Ca^{2+}$ for the indicated period of time. BAoSMC lysates were extracted and ALP activity measured using the colorimetric conversion of p-nitrophenol phosphate to p-nitrophenol and absorbance measured at 405 nm. P-nitrophenol concentrations was normalised to protein content. Data presented are expressed as % change versus control and combine results from n=3 independent experiments. *$P < 0.05$ versus 1.2 mM $Ca^{2+}$. B: BAoSMCs (prep C; passage 9) were plated in parallel to those used in an alkaline phophatase experiment and treated with 1.2 and 1.8 mM $Ca^{2+}$ in the presence of 5 mM BGP. Images were captured on day 5. Bar = 500 µm. C: BAoSMCs (prep C; passage 9) were plated in parallel to those used in an alkaline phophatase experiment and treated with 1.2 and 1.8 mM $Ca^{2+}$ in the presence of 5 mM BGP. Cells were stained with alizarin red dye on day 14. Bar = 500 µm.

### 3.5 $Ca^{2+}$-induced mineralisation may, at least in part, be independent of the CaSR

Alam et al. (2009) first implicated the SMC CaSR in the local calcification process, reporting enhanced mineralisation with overexpression of a dominant negative form of the CaSR[84]. To expand on these findings, preliminary experiments using an adenovirus expressing a dominant negative (R185Q) variant of the CaSR were used to evaluate the role of the CaSR in $Ca^{2+}$-induced mineralisation. BAoSMC transfected with the adenovirus in the presence of 1.2 mM $Ca^{2+}$, showed markedly increased expression of the receptor at 48 and then 96 hrs compared to cells with no infection (Figure 3.9A) in the absence of cell toxicity.

Despite transfection with dnCaSR, BAoSMCs incubated in 1.8 mM $Ca^{2+}$ and 5 mM BGP produced an increase in BAoSMC mineralisation, compared to BAoSMCs incubated in 1.2 mM $Ca^{2+}$ (Figure 3.9B). Without the appropriate controls cautious interpretation is required however, if validated, these results suggest that $Ca^{2+}$ may have an additional role in the calcification process, independent of the CaSR.

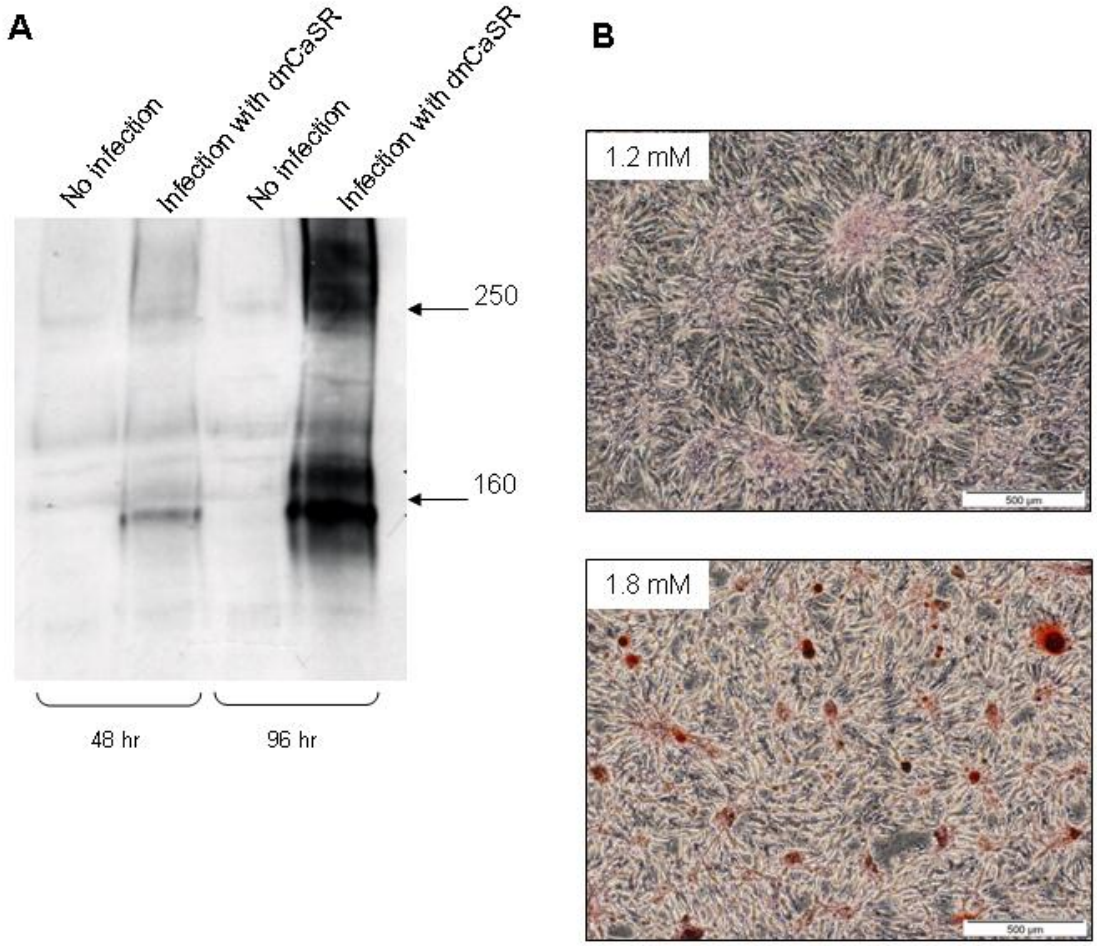


**Figure 3.9 Effect of overexpressing a dominant negative adenoviral CaSR on $Ca^{2+}$-induced mineralisation in BAoSMC.** A: Cell lysates (20 µg) from BAoSMC with no infection or infected with dnCaSR construct (MOI 150 pfu/cell) were taken at 48 and 96 hours examined for successful transfection using Western blotting with anti-CaSR antibody (1:5000). B: BAoSMC (prep C; passage 9) were cultured in 10 % FCS-DMEM containing 1.2 mM $Ca^{2+}$. Upon reaching 80% confluence (day 4), cells were infected with dnCaSR recombinant adenovirus (pacAd5CMV/dnCaSR). 48 hr later (day 6) cells were treated with 5% FCS-DMEM containing 5 mM BGP and 1.2 mM or 1.8 mM $Ca^{2+}$. Cells were subsequently re-infected at day 8 to maintain high transgene expression and mineralisation assessed qualitatively at day 12 with alizarin red staining. Images are representative of a single preliminary experiment performed in duplicate. Bar = 500 µm.

## 3.6 The effect of calcimimetics on mineral deposition by BAoSMC

To further investigate the possible protective effects of local CaSR activation the effect of three calcimimetic compounds on $Ca^{2+}$-induced mineralisation was examined in the presence of BGP. The effect of AMG641(10 pM – 1 nM), a potent calcimimetic, was evaluated in BAoSMC incubated with 5 mM BGP and 1.8 mM $Ca^{2+}$. AMG641 evoked a dose-dependent decrease in BAoSMC mineralisation, however when quantified statistical significance was achieved with the higher dose, 1 nM, only (Figure 3.10).

A second calcimimetic, R-568 (1 nM), also reduced mineral deposition by BAoSMC in cells incubated with 1.8 and 2.2 mM $Ca^{2+}$ (Figure 3.11A). Quantification of these effects showed a significant reduction in $Ca^{2+}$ accumulation in the matrix with 1 nM R-568 at 1.8 mM $Ca^{2+}$ (Figure 3.11B). However, at higher $Ca^{2+}$ concentrations (i.e. 2.2 mM), despite a trend towards decreased $Ca^{2+}$ accumulation being observed, R-568 failed to significantly reduce $Ca^{2+}$ accumulation.

To account for the possibility of non-CaSR mediated effects of the calcimimetics, S-568, an isomer of R-568 which has 10-100 times less potency to activate the CaSR[252] was evaluated for its ability to delay mineralisation. Little/no difference in mineralisation is seen between BAoSMCs treated with S-568 (1 nM) in the presence of 2.2 mM $Ca^{2+}$ and those treated with 2.2 mM $Ca^{2+}$ only (Figure 3.12). Furthermore, when examined quantitatively no significant difference was detected.

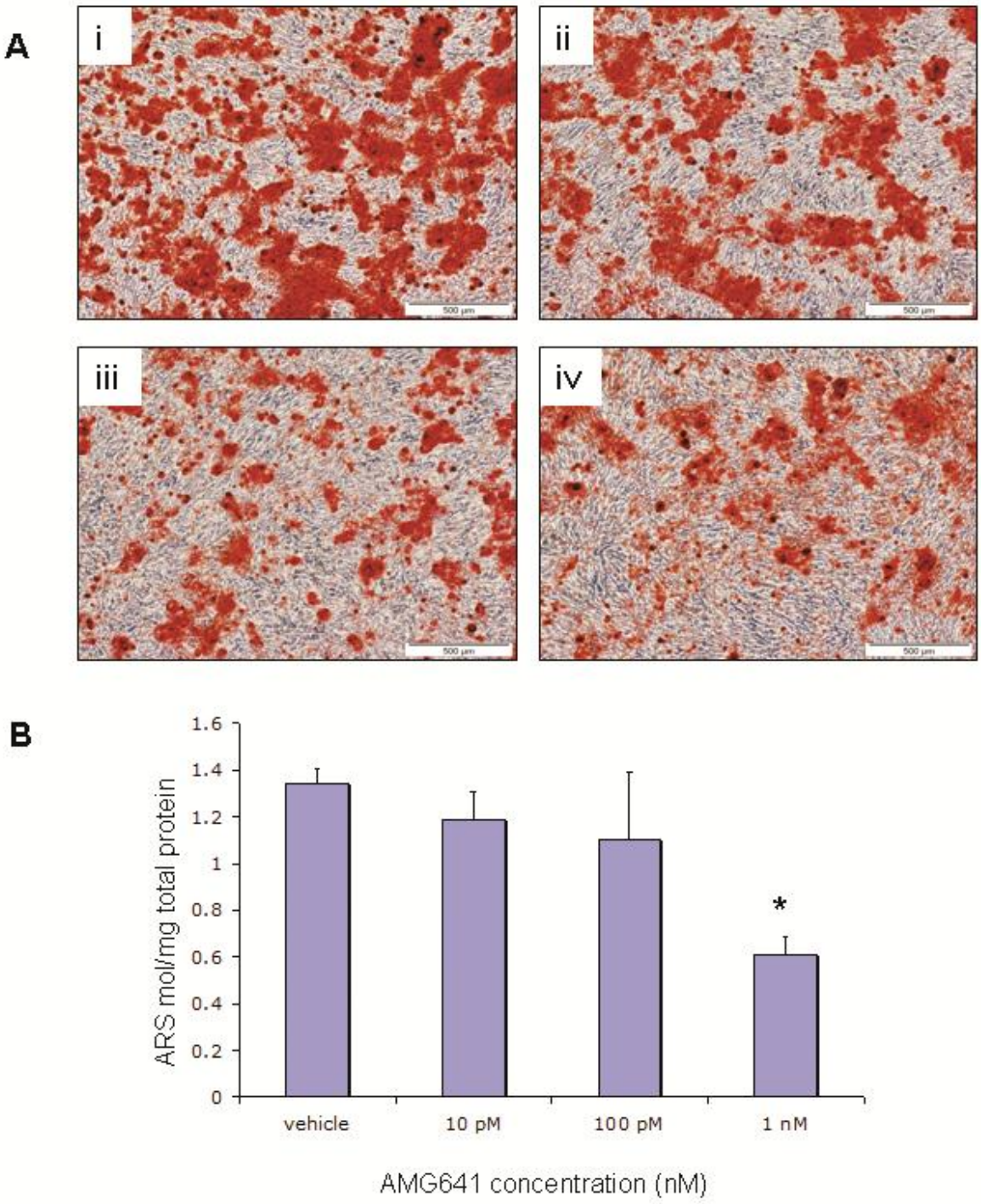


**Figure 3.10 Effect of AMG641 on $Ca^{2+}$-induced mineralisation.** A: BAoSMC (prep C; passage 7) were treated upon confluence with 1.8 mM $Ca^{2+}$ and 5 mM BGP in the presence of vehicle (1:1000 DMSO) (i) or AMG641 at 10 pM (ii), 100 pM (iii) and 1 nM (iv). On day 19 alizarin red staining was performed to visualise mineralisation. Images represent a single experiment performed in triplicate. Similar results were obtained in 2 independent experiments (shown in Figure 6.5). Bar = 500 µm. B: Mineralisation was quantified on day 19 using ARS elution. Data are represented as mean ± SEM from one experiment (n=3). *P < 0.05 compared to vehicle control.

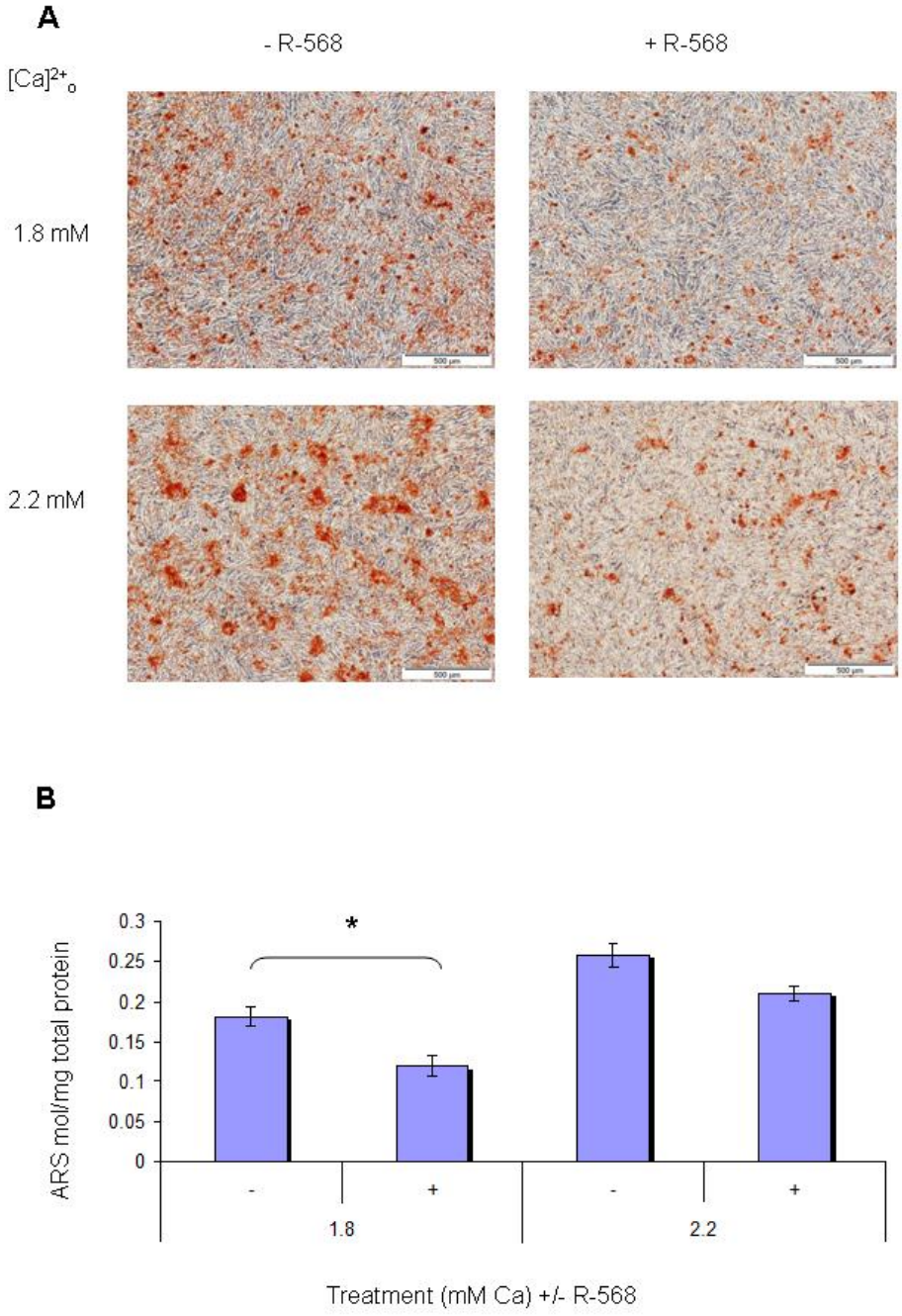


**Figure 3.11 Protective actions of R-568 on $Ca^{2+}$-induced mineralisation.** A: BAoSMCs (prep C; passage 9) were cultured in 5% FCS-DMEM and 5 mM BGP with 1.8 or 2.2 mM $Ca^{2+}$ in the presence or absence of R-568 (1nM). Cells were stained with alizarin red at day 9. Images shown were obtained from a singular experiment but indicative of 2 independent experiments although time of onset and progression of mineralisation varied (images are shown in Figure 6.6). Bar = 500 µm. B: Mineralisation was quantified on day 9 using ARS elution from a single experiment with n=3.

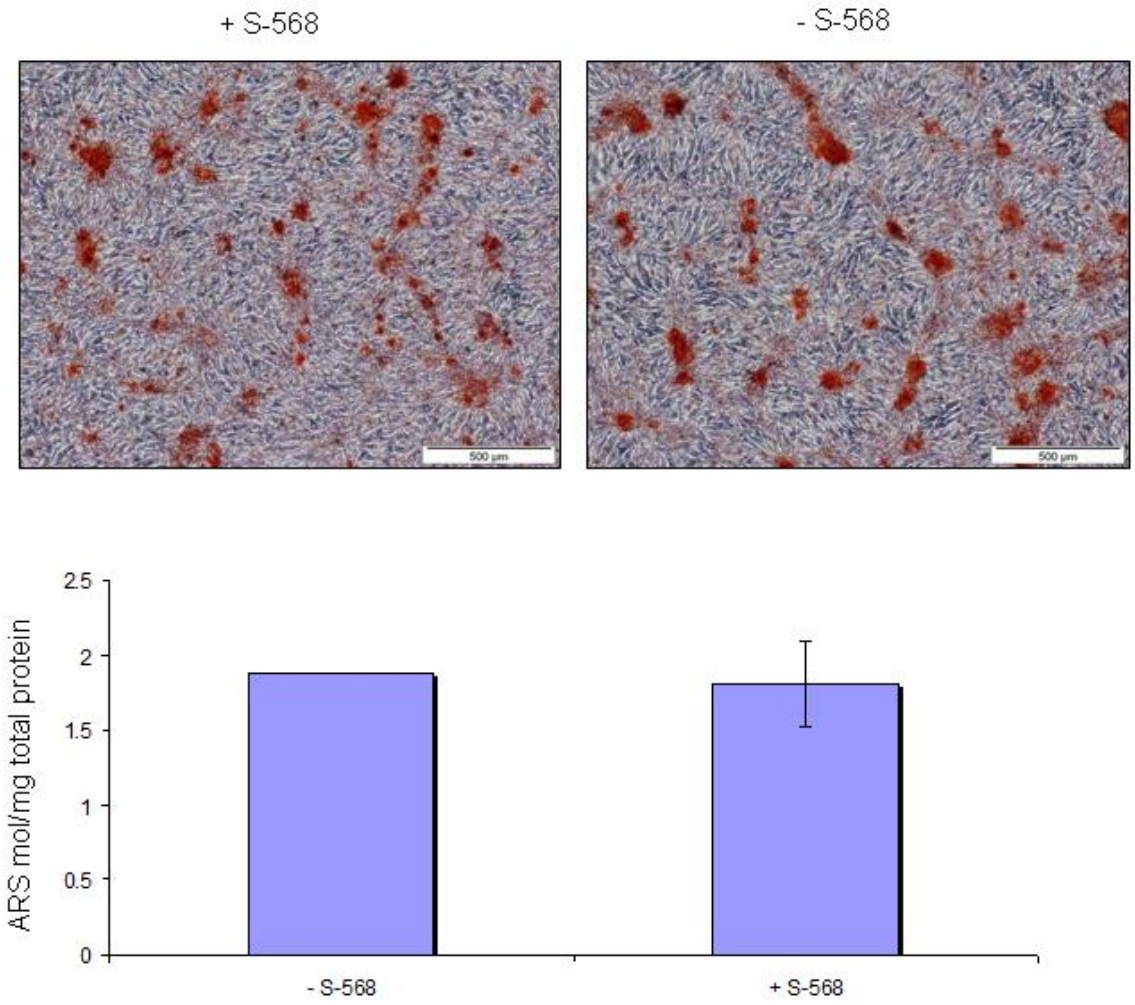


**Figure 3.12 S-568 does not delay $Ca^{2+}$-induced mineralisation.** A: BAoSMCs (prep C; passage 6) were incubated with 2.2 mM $Ca^{2+}$ in the presence or absence of S-568 (1nM). BAoSMCs were stained with alizarin red at day 10. Images shown were obtained from a single experiment performed in triplicate but are indicative of 2 independent experiments although time of onset and progression of mineralisation varied (images from repeat experiments are shown in Figure 6.7). Bar = 500 µm. B: Mineralisation was quantified on day 10 using ARS elution. Data are represented as mean ± SEM from a single experiment (n=3).

## 3.7 Signalling profile(s) induced by acute $Ca^{2+}$ and calcimimetic incubation

To evaluate the activated signalling pathways in SMCs upon $Ca^{2+}$ incubation, a multiplexable assay was used to assess the modulation of 19 phosphoproteins (methodology explained in section 2.9). Previous studies have reported ERK signalling in human, bovine and rat SMC stimulated with elevated $Ca^{2+}_o$ [84, 242-244]. In this study a broader range of signalling molecules were examined simultaneously (a list of the phosphoproteins targeted is shown in table 1).

HAoSMC were used to ensure maximum cross-reactivity with human antibodies. Firstly, CaSR expression was confirmed in these cells. Membrane preparations of HAoSMCs assessed by Western blotting exhibited three prominent bands at ~160, ~200 and ~250 kDa (Figure 3.13A). The band at ~160 kDa is consistent with the fully glycosylated form of CaSR, also observed in BAoSMC (Figure 3.4B) and CaSR-HEKs (3.4C).

Immunofluorescent staining was also used to verify the presence of a CaSR-like protein in HAoSMC. Initial experiments using a polyclonal CaSR antibody and anti-mouse FITC showed positive staining, however removal of the primary antibody did not abolish all staining and reveals non-specific staining produced by the secondary antibody (Figure 3.13B). Therefore the experiment was repeated with alternative secondary antibodies; goat anti-mouse Alexa Fluor 468 (Figure 3.13C) and Alexa Fluor 488 (Figure 3.13D). With both antibodies some non-specific staining was observed, however more prominent staining is detected in HAoSMCs treated with anti-CaSR.

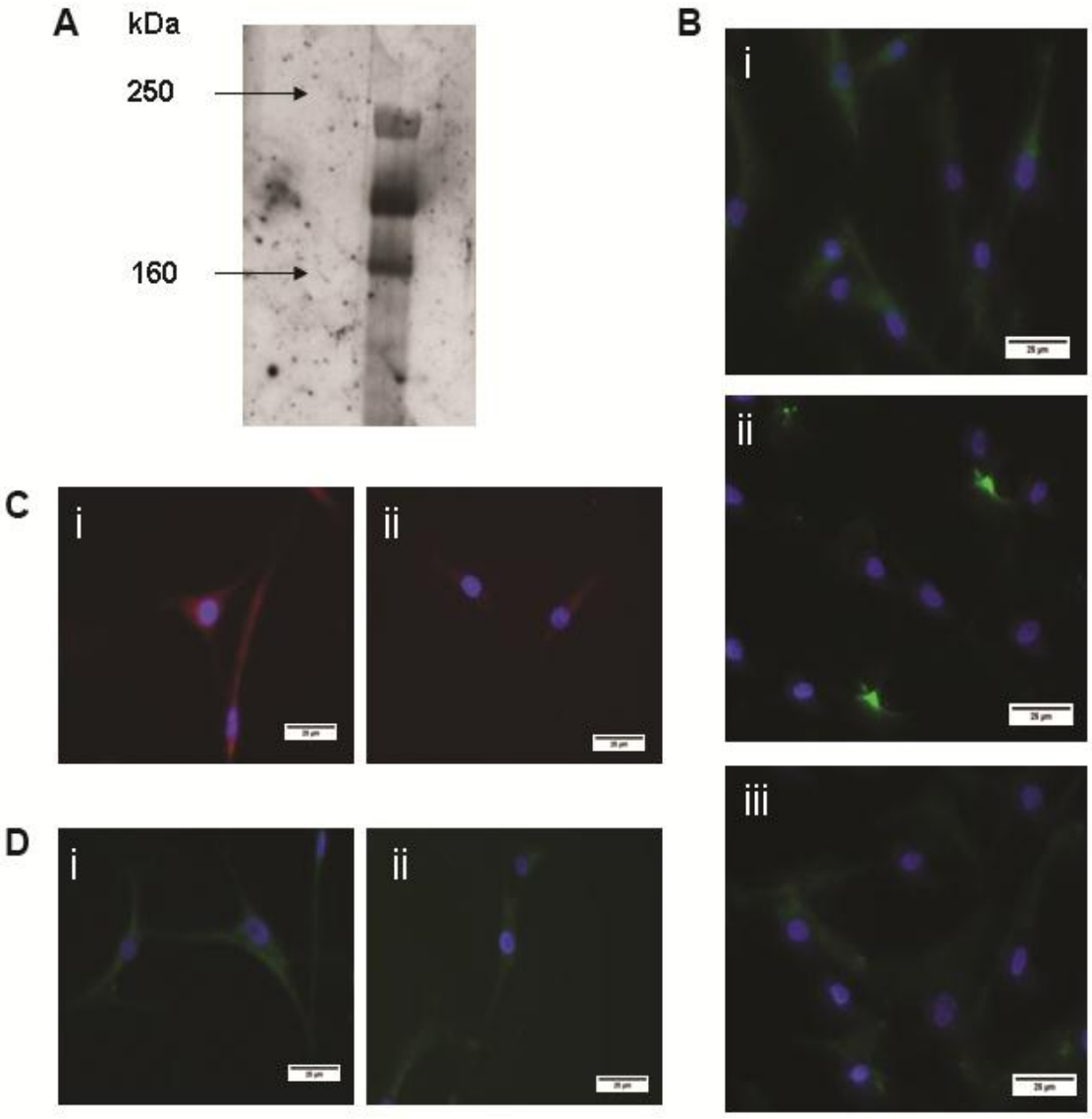


**Figure 3.13 CaSR like immunoreactivity in human aortic SMCs.** A: Membrane preparations of primary HAoSMC (passage 5) were separated on a 5% acrylamide gel and Western blotted with anti-CaSR (1:5000). Sizes (in kDa) of molecular weight markers are indicated on the left. B/C/D: Primary HAoSMC cells (passage 5) were cultured for 24 hr before fixing with 4% formaldehyde and incubation with a polyclonal antibody against human CaSR (1:100). FITC (B), Alexa Flour 568 (red) (C) and Alexa Flour 488 (green) (D) were used as the secondary antibodies (1:40). Cell nuclei were stained using the DNA-specific dye DAPI (blue). B: (i) nuclear (DAPI) and CaSR immunostaining. Control cells were stained with either mouse IgG2a (ii) or secondary antibody alone (iii). C&D: Nuclear and CaSR immunostaining (i) and negative control for which the primary antibody was omitted (ii). Bar = 25 µm.

As a positive control, cell signalling in CaSR-HEKs exposed to 5 mM $Ca^{2+}$ was evaluated (lysates provided by Donald T. Ward). Compared to CaSR-HEKs incubated with 0.5 mM $Ca^{2+}$, cells incubated with 5 mM $Ca^{2+}$ showed elevations in the phosphorylation of signalling components of the MAPK signalling cascades (Table 3.1). Typical of CaSR signalling, significant elevations in phosphorylated MEK, p90RSK and CREB were detected. Furthermore, activation of the phosphoinositide 3-kinase pathway, typically elicited by CaSR agonists, was suggested with increased phosphorylation of p70S6K kinase in cells incubated with 5 mM $Ca^{2+}$ versus control (0.5 mM $Ca^{2+}$).

**Table 3.1. $Ca^{2+}$-induced signalling in CaSR-HEK cells.** CaSR-HEKs were seeded in 10% FCS-DMEM and allowed to reach 70% confluence. CaSR-HEKs were incubated in the presence of 0.5 mM or 5 mM $Ca^{2+}_o$ for 10 min before lysates were prepared as described in the methods section (section 2.7). CaSR-HEK lysates were provided by Donald Ward, University of Manchester. Lysates were ran on a multiplex phospho-protein bead array, which allow for detection of phosphorylation levels of 19 phosphoproteins (a technical error prevented calculation of ERK phosphorylation status). Values are the results of n=4 samples and expressed as % of control (0.5 mM $Ca^{2+}$) ± SEM. * $P < 0.05$

| Phosphoprotein | % change in phosphorylation status with 5mM $Ca^{2+}$ compared to 0.5 mM $Ca^{2+}$ |
|---|---|
| Akt | 224.3 ± 72 |
| BCR-Abl | 148.6 ± 44 |
| c-Jun | 191.5 ± 30 |
| CREB | 792.7 ± 82 * |
| ERK | - |
| GSK-3α/ß | 612.4 ± 288 * |
| HSP27 | 155.8 ± 38 |
| IGF-1R | 525.9 ± 203 |
| I-κB | 303.9 ± 72 * |
| JNK | 164.8 ± 40 |
| MEK | 989.7 ± 233 * |
| PDGF | 203.7 ± 48 |
| p38 | 213.1 ± 53 |
| p53 | 153.3 ± 23 |
| p70 S6K | 482.0 ± 89 * |
| p90RSK | 545.3 ± 173 * |
| Src | 160.5 ± 40 |
| Stat3 | 311.8 ± 91 |
| Tyk2 | 179.0 ± 36 |

### 3.7.1 $Ca^{2+}$-induced signalling in HAoSMC

**Table 3.2 $Ca^{2+}$-induced signalling in SMCs.** HAoSMCs (passages 4-6) were seeded in 10% FCS-DMEM and cultured overnight in serum free medium. To assess $Ca^{2+}$-induced signalling, upon reaching 70% confluence HAoSMCs were incubated with either 0.5 mM (control) or 5 mM $Ca^{2+}$ for 5 minutes. Cell lysates were prepared as described in the methods section (section 2.7) and ran on a multiplex phospho-protein bead array, which allow for detection of phosphorylation levels of 19 phosphoproteins (indicated below). Values are the results of n=6 samples expressed as % of control (0.5 mM $Ca^{2+}$) ± SEM. * $P < 0.05$

| Phosphoprotein | % change in phosphorylation status with 5mM $Ca^{2+}$ compared to 0.5 mM $Ca^{2+}$ in SMC |
|---|---|
| Akt | 92.5 ± 14 |
| BCR-Abl | 69.7 ± 8 * |
| c-Jun | 66.7 ± 14 |
| CREB | 91.6 ± 16 |
| ERK | 89.4 ± 13 |
| GSK-3α/ß | 96.5 ± 20 |
| HSP27 | 75.0 ± 9 |
| IGF-1R | 54.4 ± 11 * |
| I-κB | 75.5 ± 12 |
| JNK | 75.2 ± 9 |
| MEK | 82.7 ± 14 |
| PDGF | 56.0 ± 11 * |
| p38 | 76.5 ± 11 |
| p53 | 70.7 ± 7 * |
| p70 S6K | 74.9 ± 13 |
| p90RSK | 80.9 ± 8 |
| Src | 68.3 ± 8 * |
| Stat3 | 87.5 ± 11 |
| Tyk2 | 65.1 ± 11 * |

When examining signalling in HAoSMCs, cells were incubated for 5 minutes in line with the time-dependent elevation in $Ca^{2+}$-induced signalling in HAoSMC demonstrated by Molostvov et al. (2007). Compared to 0.5 mM $Ca^{2+}$, incubation of HAoSMC with 5 mM $Ca^{2+}$ for 5 minutes produced decreases in the phosphorylation status of all tested phosphoproteins, and these reductions reached statistical significance for BCR-Abl, IGF-1R, PDGF, p53, Src and Tyk2 (Table 3.2.) ($P<0.05$). Surprisingly, no significant change was detected in ERK phosphorylation, or its upstream activator MEK inconsistent with previous studies in SMCs[84, 242-244].

To verify these findings, ERK phosphorylation was investigated using a second method, western blotting with a phospho-ERK antibody. Consistent with the data from Table 3.2 no change in ERK phosphorylation was demonstrated in BAoSMC incubated with 5 mM $Ca^{2+}$, compared to BAoSMCs incubated with 0.5 mM $Ca^{2+}$, despite clear increases detected in CaSR-HEK cells (Figure 3.14).

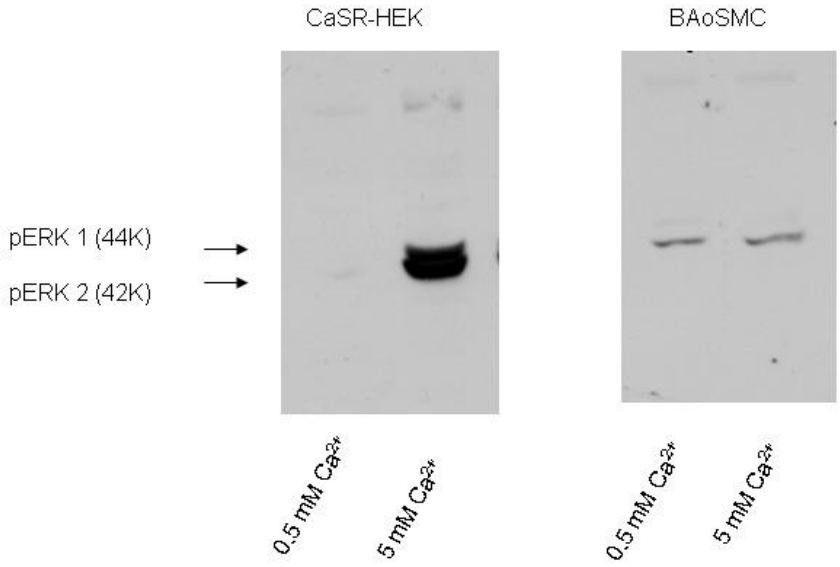


**Figure 3.14. ERK phosphorylation in the presence of 0.5 mM or 5.0 mM $Ca^{2+}$ in CaSR-HEK and BAoSMC.**

CaSR-HEK cells (left; passage 12) and BAoSMC (right; prep C, passage 6) were exposed to 5 mM $Ca^{2+}$ for 5 minutes. Cell lysates (20 µg) were separated on a 10% acrylamide gel and analysed by Western blotting with anti phospho-ERK 1/2. MW markers of ERK 1 and 2 are demonstrated on the left. Results are representative of n=4 experiments.

### 3.7.2 Calcimimetic-induced signalling in HAoSMC

The signalling pathways involved in response to calcimimetic treatment were also assessed. HAoSMC were treated with 2.5 mM $Ca^{2+}$ in the presence and absence of R-568. In the presence of R-568 (1 nM), increases in the phosphorylation status of all phosphoproteins were observed, and significant elevations in MEK (21.9 ± 4%) and p90RSK (8.0 ± 1%) detected, compared to those incubated with $Ca^{2+}$ alone (Table 3.3).

**Table 3.3 R-568-induced signalling in SMCs.** HAoSMCs (passages 4-6) were seeded in 10% FCS-DMEM and cultured overnight in serum free medium. To assess R-568 (1 nM) signalling cells were incubated with 2.5 mM $Ca^{2+}$ in the presence and absence (control) of R-568. Cell lysates were prepared as described in the methods section (section 2.7) and ran on a multiplex phospho-protein bead array, which allow for detection of phosphorylation levels of 19 phosphoproteins. Values are the results of n=3 samples both expressed as % of control (2.5 mM $Ca^{2+}$ alone) ± SEM. * $P < 0.05$

| **Phosphoprotein** | **% change in phosphorylation status with R-568 compared to 2.5 mM $Ca^{2+}$ alone** |
|---|---|
| Akt | 100.6 ± 13 |
| BCR-Abl | 124.8 ± 22 |
| c-Jun | 103.2 ± 11 |
| CREB | 105.8 ± 12 |
| ERK | 122.6 ± 23 |
| GSK-3α/ß | 126.9 ± 37 |
| HSP27 | 107.1 ± 4 |
| IGF-1R | 134.3 ± 27 |
| I-κB | 113.7 ± 13 |
| JNK | 119.0 ± 19 |
| MEK | 121.9 ± 4 * |
| PDGF | 126.5 ± 18 |
| p38 | 122.9 ± 8 |
| p53 | 121.8 ± 34 |
| p70 S6K | 107.5 ± 6 |
| p90RSK | 108.0 ± 1 * |
| Src | 117.9 ± 24 |
| Stat3 | 117.3 ± 10 |
| Tyk2 | 116.0 ± 10 |

# 4.0 Discussion

The effects of hypercalcaemia and calcimimetics on vascular calcification have been studied *in vivo* [236-240] and *in vitro* [82-84, 240]. The parathyroid CaSR[238, 239], and the SMC CaSR[84, 240] have been implicated in the actions of $Ca^{2+}$ and calcimimetics on the mineralisation process. This research supports previous findings suggesting calcimimetics can act directly on SMCs to protect against the mineralisation process[84, 240] and identifies the downstream signalling pathways activated by calcimimetic treatment in SMCs. Furthermore we provide additional insight into the respective role of the SMC CaSR in the promotion and protection of mineralisation produced by $Ca^{2+}$ and calcimimetics respectively.

## 4.1 Characterisation of explant cultures

### 4.1.1. α-sma expression and mineralisation potential

Firstly, primary cultures were assessed for α-sma expression. α-sma is predominantly expressed within SMC. Whilst its expression is relatively restricted to SMCs, α-sma has also been shown to be present in fibroblasts. In most reports fibroblasts only express α-sma in response to tissue injury[253], although α-sma expression has been detected in the absence of injury also[254]. As cells were characterised with α-sma only, the possibility of contaminating cells cannot be excluded, however the method used is a well-established method for isolating SMCs from aorta involving removal of the adventita and endothelial layer.

It is a well accepted principle that SMC preparations can behave differently in regards to their mineralisation potential. Early experiments showed that not all SMC cultures mineralise[255] and the rate of mineralisation is variable across individual preparations and experiments[70, 255-257]. Therefore, initially, each preparation of cells was assessed for their ability to calcify. All preparations showed mineralisation following incubation with 1.8 mM $Ca^{2+}$ and 5 mM BGP, albeit in different patterns. Preparation A and C formed multicellular nodular structures, typical of the calcified vascular cells initially described by Prof.

Demer's group[255]. Although, with increasing passages the pattern of mineralisation observed with preparation C changed and in later experiments more diffuse and widespread calcification was detected. This may reflect a change in SMC as they move from a more contractile phenotype to a synthetic phenotype. The change in SMC phenotype can be characterised by differing morphology, with contractile SMCs possessing an elongated spindle shape vs. synthetic cells with a cobblestone morphology, differing proliferative and migratory characteristics, with synthetic SMCs showing a higher growth rates and higher migratory activity, and expression of protein markers including α-sma, smooth muscle-myosin heavy chain (SMMHC) and smoothelin- A/B [258], however expression of these protein markers was not monitored in this research. While senescence of SMC, classified as passage 11 onwards, has been shown to increase SMC calcification[259], in the present study cells were not used at passage 10 or above.

### 4.1.2 CaSR expression in BAoSMC

The major objective of this work was to further understand the role of the CaSR in SMC mineralisation. Expression of the CaSR in SMC is now well established[84, 240, 242-244], although previously has been a controversial topic, with some groups failing to detect the CaSR[245, 246] and others detecting a CaSR-like protein but that is molecularly distinct[91]. However, the first step was to confirm CaSR expression in the cell population to be tested (i.e. preparation C BAoSMC and HAoSMC). In this study we detected the presence of a CaSR-like protein in BAoSMC (prep C) via Western blotting and immunofluorescence using a CaSR-specifc antibody raised against a region within the extracellular domain of the protein. Positive staining was observed throughout the cell reflecting the pattern of localisation of the CaSR reported in rat SMC[244] and other cell types[260, 261], although in contrast to the punctate staining shown by Alam et al. (2009)[84]. A few cells failed to show CaSR expression, although this represented the minority with majority showing positive expression.

Positive staining was also detected in HAoSMC, although some immunoreactivity was also observed in cells incubated with secondary antibody alone suggesting non-specific staining of the secondary antibody. Similar findings were reported by Molostvov et al (2007), who detected positive CaSR staining intracellularly and at the plasma membrane, however some immunoreactivity was shown with the secondary antibody alone or when the CaSR antibody was pre-absorbed with the immunising peptide[243]. However, in support of current findings, more prominent staining was detected in cells treated with anti-CaSR[243].

Western analysis of membrane preparations from both HAoSMC and BAoSMC revealed immunoreactivities at ~160 kDa, ~200 kDa and ~250kDa. The ~160 kDa band, was observed in SMCs and CaSR-HEKs (see Figure 3.4B, 3.4C and 3.13A) and corresponds to the glycosylated form of the full length CaSR monomer. These findings are consistent with findings from Molostvov et al. (2007), where SMC CaSR immunoreactivity was identified at 160kDa, aligned with CaSR immunoreactivities observed in HKC-8 cells, a human renal proximal tubular cell line (positive control)[243]. The lower molecular weight band (~140 kDa), representing the unglycosylated form of CaSR[262] was absent from membrane preparations of SMCs. Previous reports confirm the absence of the 140 kDa band in cultured SMCs[243], however lysates from freshly dissected renal and epigastric arteries from transplant patients, reveals immunoreactive species including a 140 kDa band[243].

CaSR immunoreactivities were also observed at ~200 and 250 kDa with BAoSMC and HAoSMC. Whilst not visible on lower exposure blots, these bands to appear to align with immunoreactivities detected with CaSR-HEK cells (see Figure 6.2A). Previous reports have identified two bands major between 200 and 300 kDa in CaSR-HEK cells, which are believed to represent the dimeric forms of the receptor[263]. Therefore, the 250 kDa band observed in SMCs may represent a dimeric form of the receptor, however this is not anticipated under reducing conditions. Although, bands of 250 kDa and above, are also detected in CaSR-HEKs, suggesting some dimeric forms of

the receptors may remain. Whilst not presented in Figure 3.4 or 3.13 SMCs also show the traditional dimer doublet at ~280 kDa (shown in Figure 6.2A).

Despite confirmation of protein expression of the CaSR, no CaSR messenger RNA was detected in cultured BAoSMC contrary to previous reports[243, 244], but supported by Farzaneh-Far et al. (2001) who failed to identify CaSR mRNA expression[24]. This may, in part, reflect the sensitivities of our methods, as despite a clear CaSR signal detected from parathyroid gland tissue, the level of CaSR mRNA expression in smooth muscle cells is significantly lower than those observed in the parathyroid gland. However, it may also, additionally, suggest that there is little generation of new CaSR in cultured cells, supported by the absence of the immature unglycosylated form in cultured cells[243].

## 4.2 The effect of CaSR activation on SMC mineralisation

Strong *in vitro* data supports a role for the CaSR, independent of systemic changes in calciotropic hormones. Alam et al. (2009) first proposed a relationship between SMC CaSR and SMC mineralisation, demonstrating increased mineralisation when cells were treated with a dominant negative CaSR construct[84]. The reported effects of CaSR agonists on SMC mineralisation were variable with $Ca^{2+}$ and $Gd^{3+}$, promoting SMC mineralisation, whilst R-568, delayed the onset of mineralisation[84]. The aim of this research was to expand our knowledge of how CaSR agonists modulate SMC mineralisation and the relative involvement of the CaSR in these actions.

### 4.2.1 The effect of $Ca^{2+}$ on SMC mineralisation

Data presented as part of this study support the findings of Alam et al. (2009) showing increased mineralisation with increased $[Ca^{2+}]_o$ in the presence of an external source of phosphate[84]. Increasing $[Ca^{2+}]_o$ alone was not sufficient to trigger mineralisation suggesting that the resulting mineralisation is a reflection of the final Ca x P rather than the $Ca^{2+}$ concentration alone. Additional reports of $Ca^{2+}$-induced mineralisation exist, however in these reports increased mineralisation is detected in the absence of an external

phosphate source[82, 83], in contrast to results presented. A species difference may underlie the differential response as Yang et al. (2004) and Reynolds et al. (2004) both used human SMCs, compared to the current report, and Alam et al. (2009), which used bovine SMCs.

Increasing $[Ca^{2+}]_o$ also resulted in a significant elevation in alkaline phosphatase (ALP) activity, supporting previous findings of $Ca^{2+}$-induced mRNA expression of ALP[82]. ALP is among one of the first functional genes expressed in the process of calcification in osteogenesis[264] and current findings suggest it may also be an early step in vascular calcification with significant elevations detected on day 5, in advance of mineralisation.

The role of $Ca^{2+}$ in the induction of ALP has more recently been questioned as interestingly it has been found that applying high $Ca^{2+}/PO_4^{3-}$ medium (i.e. 2.7 mM $Ca^{2+}$ / 2 mM $PO_4^{3-}$) to vessel rings from humans decreases ALP activity compared to both baseline medium (low $Ca^{2+}/PO_4^{3-}$) [86]. This is in contrast to applying high $PO_4^{3-}$ medium (1.8 mM $Ca^{2+}$ / 2 mM $PO_4^{3-}$) where significant elevations in ALP activity are observed in pre-dialysis and dialysis vessels[86]. In opposition to current findings these findings suggest that $Ca^{2+}$-induced calcification in humans occurs in the absence of elevated ALP activity[86].

It is well accepted that increases in extracellular $Ca^{2+}$ can contribute to increased SMC mineralisation[82-84]. However, an intriguing question unanswered from the findings of Alam et al. (2009) was how $Ca^{2+}$ and $Gd^{3+}$, typical agonists of CaSR, enhance mineralisation whilst R-568, an allosteric modulator, inhibits mineralisation[84]. The authors reported that increasing extracellular $Ca^{2+}$ concentrations from 1.2 mM $Ca^{2+}$ to 1.8 or 2.5 mM resulted in reduced CaSR expression[84], although the effect of $Gd^{3+}$ or calcimimetic treatment on the expression of the SMC CaSR was not reported. Given the available data one could hypothesize that a possible mechanism for $Ca^{2+}$-induced mineralisation is by downregulation of the SMC CaSR, thus reducing the level of protection afforded by its presence. Furthermore it was suggested that calcimimetics may oppose this action by increasing SMC CaSR

expression[84], an action that has been observed in the parathyroid glands[265, 266] and HEK-293 cells[228]. Whilst only a hypothesis at the time, recently Mendoza et al. (2011) has presented evidence to confirm this suggestion; showing that AMG641 can significantly increase CaSR mRNA in SMCs[92].

#### 4.2.1.1 Understanding the process of $Ca^{2+}$-induced mineralisation

Whilst data support CaSR downregulation as one of the likely steps in $Ca^{2+}$-induced mineralisation[84], this study also reports preliminary results suggesting additional mechanisms contributing to the promotion of mineralisation, independent of CaSR-mediated events. Mechanisms for $Ca^{2+}$-induced mineralisation, independent of the CaSR are well reported and have recently been reviewed[78]. Whilst the experimental data presented require cautious interpretation and further validation, we showed that despite treatment with the dominant negative adenoviral construct of CaSR (R185Q), $Ca^{2+}$ maintains the ability to dose-dependently induce SMC mineralisation.

One of the major limitations of this experiment is that the extent of residual CaSR activity by the endogenous receptor was not investigated. Residual activity of the endogenous CaSR may account for the modest increase in mineralisation detected with increased extracellular $Ca^{2+}$ (1.8 mM vs. 1.2 mM $Ca^{2+}$). Additionally this experiment lacked the appropriate controls. Without the inclusion of an empty virus control the relative importance of CaSR-dependent and CaSR-independent actions on local $Ca^{2+}$-induced mineralisation cannot be commented upon.

Although very preliminary at the time, evidence supporting these findings have since emerged[247]. Caudriller et al. reported that $Ca^{2+}$-induced mineralisation occurs in the absence of CaSR and that cells treated with CaSR-SiRNA became more sensitive to the calcifying actions of $Ca^{2+}$[247]. This finding reinforces that CaSR has a protective role in SMCs and also proposes the question of whether $Ca^{2+}$ acts in a protective capacity through the CaSR, but its effects are outweighed by other calcifying activities.

The signalling activities induced in SMC by $Ca^{2+}$, appear to be distinct from previously reported CaSR-mediated actions. $Ca^{2+}$ evoked signalling in CaSR-HEKs showed elevations in a number of protein kinases involved in MAPK signalling (i.e. MEK/p90RSK/p70 s6K), consistent with previous reports in CaSR-HEK[198, 267, 268] and CaSR mediated signalling in other cell types[269-273]. Whereas, no elevation in components of MAPK signaling were detected when SMC were incubated with 5 mM $Ca^{2+}$, compared to 0.5 mM $Ca^{2+}$. These data contradict a number of previous reports in SMC which have shown ERK activation in response to CaSR agonists[92, 242-244], and have shown these changes to be CaSR-dependent[242, 243]. No definitive conclusions can be drawn from the comparison between $Ca^{2+}$-induced signalling in CaSR-HEKs and SMCs as CaSR interactions may be cell specific and different durations of incubation were used between experiments. However, these results open up the possibility that the $Ca^{2+}$-induced signalling events reported in SMCs are not CaSR mediated, although without further work using dominant negative CaSR this remains conjecture.

Instead, $Ca^{2+}$ incubation (5 mM) of SMC evoked significant depressions in a number of signalling pathways; BCR-Abl, IGF-1R, PDGF, p53, Src, Tyk2 compared to 0.5 mM $Ca^{2+}$. Of interest within this group is IGF-1R, which has been suggested to be involved in SMC mineralisation[274, 275]. Loss of IGF-1R signalling, or inhibition of its downstream signalling molecules, promotes mineralisation[274, 275]. Therefore it may be possible that by attenuating IGF-1R signalling, $Ca^{2+}$ reduces the protection afforded by the active IGF-1R receptor.

Furthermore, incubation of SMCs with elevated levels of extracellular $Ca^{2+}$ modulates components of apoptotic pathways. Acute incubation with 5 mM $Ca^{2+}$ suppresses levels of activated BCR-Abl, an apoptosis inhibitor, and p53, which has been reported to protect SMCs from apoptosis, both *in vivo* and *in vitro*[276]. Supporting this hypothesis, extracellular $Ca^{2+}$ (5.4 mM) has been shown to induce apoptosis[83] compared to 1.8 mM $Ca^{2+}$. However these results need to be interpreted cautiously with recent reports showing that extracellular $Ca^{2+}$ at 1.36 – 3.3 mM can be protective of apoptosis[275]

suggesting that the actions of extracellular $Ca^{2+}$ on apoptosis may be dose specific.

### 4.2.2 The effect of calcimimetics on SMC mineralisation

Previous studies have reported that R-568[84, 240] can delay the onset of SMC mineralisation induced by $Ca^{2+}$ *in vitro.* In the present study we expanded on these findings demonstrating that, a second calcimimetic, AMG641 also delays mineral deposition by BAoSMC *in vitro*, in a dose dependent manner. Additionally, as a control for the effect of R-568, its isomer S-568 which shows little/no activity at the CaSR was investigated. Unlike R-568, S-568 produced no protection against the onset of mineralisation, suggesting that the protective actions of calcimimetics are mediated through the CaSR. Consistent with previous reports, calcimimetics did not inhibit the process of calcification but slowed the development / progression of mineralisation[84].

To conclusively report that the actions of AMG641 and R-568 are mediated via the CaSR, knockout studies would be required. The dominant negative adenoviral construct, used in this research, was not suitable for verification of this finding as recent data have shown that calcimimetics can act as pharmacochaperone and increase membrane expression and activity of mutant receptors, including the R185Q receptor used in this research[228, 277]. However, further evidence that the local protective actions of R-568 are mediated through the CaSR came from Ivanovski et al. (2009) who demonstrated that knockout of the CaSR, *in vitro*, by siRNA technology attenuates the protective role of calcimimetics[240].

#### 4.2.2.1 Calcimimetic-induced signalling in SMC

Acute treatment of SMCs with R-568 in the presence of 2.5 mM $Ca^{2+}$ evoked increased phosphorylation of MEK and p90RSK compared to $Ca^{2+}$ alone. Activation of the MEK/ERK pathway is consistent with existing reports that treatment with CaSR agonists increased ERK phosphorylation in SMCs[84, 242, 244]. Furthermore use of CaSR siRNA abolishes ERK phosphorylation induced

by neomycin[234], confirming CaSR specific activation of MEK / ERK pathways. Lending additional support to these findings, Mendoza et al. (2011) recently reported increased ERK phosphorylation with AMG641 treatment in SMCs[92]. However, confirmation that the reported the observed elevations in MEK and p90RSK produced by R-568 are CaSR-dependent will require knockout studies.

Strangely this study failed to show a significant activation of ERK despite activation of signalling components up- and down-stream of ERK. In CaSR-HEK cells, $Ca^{2+}$-induced MEK / ERK pathway activation has been linked to $G\alpha_{q/11}$, $G\alpha_{i/o}$ , P13K, as well as PKC and filamin[278]. Limited data exists to understand how these molecules interact with the SMC CaSR to elicit activation of MEK / ERK pathways. Smajilovic et al. (2006) reported no or very little $IP_3$ accumulation in the presence of neomycin and high concentration $Ca^{2+}$ (20–30 mM), respectively, with no mobilisation of intracellular $Ca^{2+}$[244]. However, Molostvov et al. (2008) showed that the PLC inhibitor, U73122, could attenuate ERK phosphorylation and observed $IP_3$ production in response to neomycin and gentamicin, suggesting a mechanism dependent on the PLC pathway[242]. This group also showed that ERK phosphorylation was independent of PI3K[242]. Findings from this research support that observation showing that elevations in phosphorylated MEK and p90RSK were not accompanied by increased Akt phosphorylation.

Activation of MEK / ERK can trigger a large number of signalling molecules. Downstream of MEK activation, phosphorylation of a number of the tested phosphoproteins may be expected (e.g. c-Jun, IκB, p53, p70s6k, Stat3, CREB), however this research only showed significant elevations on p90RSK. Furthermore, no other MAPK pathways (i.e. p38 or JNK) were shown to be activated by calcimimetics in SMCs, as have been shown in CaSR-HEKs and other cell types[198, 267, 279].

#### 4.2.2.2 Implications for mineralisation

The roles of MEK and p90RSK in the process of calcification were not examined as part of this research although do warrant further investigation. To understand the impact of each of these pathways and their potential as mediators of the protective actions of the calcimimetics we would need to examine signalling pathways following chronic calcimimetic treatment with and without their respective inhibitors (MEK; UO126, PD98059 / p90RSK; BI-D1870, SL0101).

Among the molecules identified that can induce/delay BAoSMC mineralisation, a number of authors have identified MEK / ERK signalling as playing a key role in this process[29, 274, 280-282]. Speer et al. (2009) speculated a role for extracellular signal-regulated kinases (ERKs)[29], as ERK signalling had been implicated in osteoblastic differentiation[283-285], and they found levels of phosphorylated ERK1/2 increased prior to a decrease in the levels of SMC lineage markers[29]. The role of ERK in osteoblastic differentiation in SMC was confirmed using the MEK inhibitor U0126 which prevented down regulation of SMC lineage markers and the SMC-specific transcription coactivator myocardin in calcifying SMCs[29]. Interestingly, ERK has also been reported to be involved in the upregulation of smooth muscle myosin heavy chain[286] and thus may help protect against SMC transdifferentiation. However discrepancies in the current literature exist as to whether MEK / ERK signalling provides a protective role[274, 280] or its activation is one of the steps promoting mineralisation[29, 281, 282, 287]. A large degree of substrate dependence appears to exist as a result of the cross talk among the downstream signalling pathways and the different microenvironments created by each group.

p90RSK (p90 ribosomal S6 kinase) lies immediately downstream from ERK and while a lot of research interest has surrounded ERK signalling, less is known about the role of p90RSK in the process of vascular calcification. In its inactive form, p90RSK resides in the cytoplasm, however upon stimulation is transported to the nucleus complexed with ERK. p90RSK has a number of

cytosolic substrates, including Iκ-B[288] and also regulates a number of transcription factors including c-Fos[289], CREB[290] and Nur77[291].

Of interest to the process of SMC mineralisation, p90RSK has the potential to antagonise apoptosis through neutralizing BAD, a pro-apoptotic member of the Bcl family of proteins[288, 292, 293]. This opposes the signalling activities observed in SMC upon acute incubation with 5 mM $Ca^{2+}$, where reduced activation of apoptosis inhibitors were detected. Therefore, calcimimetics may help delay mineralisation by increasing survival of SMC. Molostvov et al. (2008) have already demonstrated that CaSR-mediated PLC activation is important for SMC survival and protection against apoptosis and reported on the importance of MEK / ERK signalling in this process[242], however more direct association to the mineralisation process is required.

## 4.5 Conclusions

This work advances our understanding of the current role of the CaSR in SMC mineralisation. I have shown that treatment with calcimimetics can delay SMC mineralisation and hypothesise that this protection is mediated via a CaSR-dependent mechanism. Additionally I demonstrated that the role of $Ca^{2+}$ as a promoter of SMC mineralisation is, in part, independent of its actions on the CaSR. MAPK signalling pathways are reported to be activated after acute stimulation with calcimimetics in SMCs and the literature supports a hypothetical role for these signalling molecules in the mineralisation process.

## 4.6 Limitations of current work

1. The cell population used in these experiments were identified as smooth muscle cells on the basis of positive α-smooth muscle actin (α-sma) staining uniformly across the cell culture, however α-sma is not exclusive to SMCs alone. α-sma has also been identified in fibroblasts[294], which are similar in morphology to SMCs; therefore the possibility of cross-contamination cannot be excluded.

2. Whilst the presence of the CaSR in SMC is now widely accepted, the current data do not provide definitive evidence.
    a. Methods used to asses CaSR mRNA expression were no optimised to detect low abundance mRNA transcripts, previously observed in bovine SMCs[92].
    b. Immunfluorescence experiments could have been performed under more stringent conditions with stronger controls (i.e. pre-incubation of the CaSR antibody with immunising peptide). Protocols for immunostaining of the CaSR in HAoSMC should have been further optimised using different blocking agents and dilutions of antibodies.
    c. Assessment of CaSR mRNA and protein expression from freshly isolated bovine SMCs may have yielded better results, but were not investigated in this research.
3. This research reports preliminary findings that $Ca^{2+}$-induced mineralisation can occur independently of CaSR. However, no empty virus control was included in this preliminary research and therefore the relative role played by CaSR cannot be inferred. As part of future work we would expect confirmation that cells treated with the dominant negative RAd produce a dose dependent increase in mineralisation with increasing concentrations of $Ca^{2+}$ (vs. empty virus control).
4. The bioplex allowed for an initial screen of 19 phosphoproteins in a time efficient manner, however, limitations to exist which may have led to the generation of false positives / negatives and thus results require validation
    a. Total phosphoprotein was not assessed in parallel to phosphorylation status and therefore effects could have been masked or amplified. Positive results require confirmation with western blot for both the phosphorylated form and total phosphoprotein.
    b. $Ca^{2+}$-treated CaSR-HEKs were used as a positive control, however, positive controls showing activation of each phosphoprotein were not included, and therefore results may contain false negatives

c. Methods used required that the average of control values for individual experiments were used in statistical analysis incorporating a false uniformity within the data set.

5. Finally, the current research utilised pharmacological tools to suggest that calcimimetic effects are mediated through the CaSR. Calcimimetic, however, have been shown to effect $Ca^{2+}$ channels at high doses[295], therefore for confirmation of these findings knockout studies are necessary, which have recently been published[240]. Similarly the signalling pathways found to be activated by CaSR cannot be conclusively attributed to the CaSR activation without KO being used.

### 4.7 Future research questions and directions

We know, through this research and that of others, that calcimimetics can act on SMC to prevent mineralisation. However it is still unknown how they produce their protective actions, whether their protective actions can reverse established mineralisation and the relative contribution of activation of SMC CaSR vs parathyroid CaSR.

1. Reported data suggest that calcimimetics may enhance signalling through MAPK pathways, in particular MEK and p90RSK. Firstly, to expand on current findings, confirmation that enhanced MAPK signalling results from CaSR activation is necessary, using CaSR siRNA. Secondly, the potential contribution of the activation of these signalling molecules to the mineralisation process, and apoptosis, should be investigated, using pharmacological manipulation of each of these pathways independently. Therefore, in vitro calcification experiments assessing the degree of protection afforded by calcimimetics in the presence and absence of MEK (UO126 / PD98059) and p90RSK (BI-D1870 and SL0101) inhibitors should be performed.

2. (i) To further evaluate the current hypothesis that the loss of CaSR is associated with SMC mineralisation we need to better understand at

what stage in the mineralisation process CaSR is downregulated. Alam et al. (2009) reported CaSR downregulation in response to high levels of $[Ca^{2+}]_o$ as early as 24 hours after a change in culture conditions. However whether this occurs prior to changes in gene expression of osteoblast / smooth muscle markers is unknown. Using qPCR, expression levels of osteoblastic (e.g. osterix, Runx2, osteonectin) and SM markers (α-sma, SM22α, myocardin) will be analysed alongside CaSR expression.

(ii) In parallel, the ability of calcimimetics to promote CaSR expression and correct for CaSR down regulation in high $Ca^{2+}$ environments should be examined. Reports by Mendoza et al. (2011) reported the ability of AMG641 to increase CaSR expression in cells incubated in 1.8 mM $Ca^{2+}$, a concentration which has been reported to result in receptor down regulation[84]. However the length of time cells were incubated in this environment and the extent of down regulation prior to treatment with AMG641 are unknown.

3. As a potential therapeutic strategy for calcification, it is important to understand the extent of protection afforded by calcimimetics and whether calcimimetics are also capable of reversing / slowing the progression of established calcification. This can be investigated in vitro, staggering the introduction of calcimimetic therapy to SMCs cultured with pro-calcifying stimulus (i.e. 5mM BGP + 1.8 mM $Ca^{2+}$) ie day 0, day 3, day 6, day 9… This should accompany ex vivo work in which cells isolated from calcifying arterial medias of matrix Gla-protein knockout (MGP -/-) mice are treated with calcimimetics and the progression of mineralisation monitored.

4. Finally, despite the accumulating in vitro evidence, the physiological role of SMC CaSR remains largely unknown. Severe hyperparathyroidism, premature death, and incomplete gene excision in CaSR–/– mice have precluded the assessment of CaSR function in SMCs, thus a tissue specific knockout is required. Dr. Shoback and colleagues have recently generated mice with tissue specific deletions

in the parathyroid gland, bone and cartilage[296]. As part of a collaborative effort with our group, the floxed animals with exon 7 of the CaSR 'knocked out' (equating to the 7TMD and 4 intracellular loops of the receptor protein) are being bred with a SM22α-Cre transgenic mouse to remove CaSR in a tissue specific manner. This will allow us to assess the relative contribution of the SMC CaSR in calcification i.e. does loss of SMC CaSR in vivo predispose animals to the development of calcification and to what extent are the protective effects of calcimimetics dependent on the presence of CaSR SMC?

## Chapter 5: References


1. Goodman WG, Goldin J, Kuizon BD, Yoon C, Gales B, Sider D, Wang Y, Chung J, Emerick A, Greaser L, Elashoff RM, Salusky IB. Coronary-artery calcification in young adults with end-stage renal disease who are undergoing dialysis. *The New England journal of medicine*. 2000;342:1478-1483
2. Braun J, Oldendorf M, Moshage W, Heidler R, Zeitler E, Luft FC. Electron beam computed tomography in the evaluation of cardiac calcification in chronic dialysis patients. *American journal of kidney diseases : the official journal of the National Kidney Foundation*. 1996;27:394-401
3. Raggi P, Boulay A, Chasan-Taber S, Amin N, Dillon M, Burke SK, Chertow GM. Cardiac calcification in adult hemodialysis patients. A link between end-stage renal disease and cardiovascular disease? *Journal of the American College of Cardiology*. 2002;39:695-701
4. Gross ML, Meyer HP, Ziebart H, Rieger P, Wenzel U, Amann K, Berger I, Adamczak M, Schirmacher P, Ritz E. Calcification of coronary intima and media: Immunohistochemistry, backscatter imaging, and x-ray analysis in renal and nonrenal patients. *Clinical journal of the American Society of Nephrology : CJASN*. 2007;2:121-134
5. de Jager DJ, Grootendorst DC, Jager KJ, van Dijk PC, Tomas LM, Ansell D, Collart F, Finne P, Heaf JG, De Meester J, Wetzels JF, Rosendaal FR, Dekker FW. Cardiovascular and noncardiovascular mortality among patients starting dialysis. *JAMA : the journal of the American Medical Association*. 2009;302:1782-1789
6. Nakamura S, Ishibashi-Ueda H, Niizuma S, Yoshihara F, Horio T, Kawano Y. Coronary calcification in patients with chronic kidney disease and coronary artery disease. *Clinical journal of the American Society of Nephrology : CJASN*. 2009;4:1892-1900
7. Temmar M, Liabeuf S, Renard C, Czernichow S, Esper NE, Shahapuni I, Presne C, Makdassi R, Andrejak M, Tribouilloy C, Galan P, Safar ME, Choukroun G, Massy Z. Pulse wave velocity and vascular calcification at different stages of chronic kidney disease. *Journal of hypertension*. 2010;28:163-169
8. McCullough PA, Sandberg KR, Dumler F, Yanez JE. Determinants of coronary vascular calcification in patients with chronic kidney disease and end-stage renal disease: A systematic review. *Journal of nephrology*. 2004;17:205-215
9. Shroff RC, McNair R, Skepper JN, Figg N, Schurgers LJ, Deanfield J, Rees L, Shanahan CM. Chronic mineral dysregulation promotes vascular smooth muscle cell adaptation and extracellular matrix calcification. *Journal of the American Society of Nephrology : JASN*. 2010;21:103-112
10. Goodman WG. Vascular calcification in chronic renal failure. *Lancet*. 2001;358:1115-1116
11. Blacher J, Guerin AP, Pannier B, Marchais SJ, London GM. Arterial calcifications, arterial stiffness, and cardiovascular risk in end-stage renal disease. *Hypertension*. 2001;38:938-942

12. London GM, Marchais SJ, Safar ME, Genest AF, Guerin AP, Metivier F, Chedid K, London AM. Aortic and large artery compliance in end-stage renal failure. *Kidney international*. 1990;37:137-142
13. Jeziorska M, McCollum C, Wooley DE. Observations on bone formation and remodelling in advanced atherosclerotic lesions of human carotid arteries. *Virchows Archiv : an international journal of pathology*. 1998;433:559-565
14. Shanahan CM. Inflammation ushers in calcification: A cycle of damage and protection? *Circulation*. 2007;116:2782-2785
15. Aikawa E, Nahrendorf M, Figueiredo JL, Swirski FK, Shtatland T, Kohler RH, Jaffer FA, Aikawa M, Weissleder R. Osteogenesis associates with inflammation in early-stage atherosclerosis evaluated by molecular imaging in vivo. *Circulation*. 2007;116:2841-2850
16. London GM, Guerin AP, Marchais SJ, Metivier F, Pannier B, Adda H. Arterial media calcification in end-stage renal disease: Impact on all-cause and cardiovascular mortality. *Nephrology, dialysis, transplantation : official publication of the European Dialysis and Transplant Association - European Renal Association*. 2003;18:1731-1740
17. Amann K. Media calcification and intima calcification are distinct entities in chronic kidney disease. *Clinical journal of the American Society of Nephrology : CJASN*. 2008;3:1599-1605
18. Dao HH, Essalihi R, Bouvet C, Moreau P. Evolution and modulation of age-related medial elastocalcinosis: Impact on large artery stiffness and isolated systolic hypertension. *Cardiovascular research*. 2005;66:307-317
19. Haydar AA, Covic A, Colhoun H, Rubens M, Goldsmith DJ. Coronary artery calcification and aortic pulse wave velocity in chronic kidney disease patients. *Kidney international*. 2004;65:1790-1794
20. London GM. Cardiovascular disease in chronic renal failure: Pathophysiologic aspects. *Seminars in dialysis*. 2003;16:85-94
21. Burke AP, Taylor A, Farb A, Malcom GT, Virmani R. Coronary calcification: Insights from sudden coronary death victims. *Zeitschrift fur Kardiologie*. 2000;89 Suppl 2:49-53
22. Schwarz U, Buzello M, Ritz E, Stein G, Raabe G, Wiest G, Mall G, Amann K. Morphology of coronary atherosclerotic lesions in patients with end-stage renal failure. *Nephrology, dialysis, transplantation : official publication of the European Dialysis and Transplant Association - European Renal Association*. 2000;15:218-223
23. Giachelli CM. Ectopic calcification: Gathering hard facts about soft tissue mineralization. *The American journal of pathology*. 1999;154:671-675
24. Farzaneh-Far A, Proudfoot D, Shanahan C, Weissberg PL. Vascular and valvar calcification: Recent advances. *Heart*. 2001;85:13-17
25. Moe SM, Duan D, Doehle BP, O'Neill KD, Chen NX. Uremia induces the osteoblast differentiation factor cbfa1 in human blood vessels. *Kidney international*. 2003;63:1003-1011
26. Aikawa E, Nahrendorf M, Sosnovik D, Lok VM, Jaffer FA, Aikawa M, Weissleder R. Multimodality molecular imaging identifies proteolytic

and osteogenic activities in early aortic valve disease. *Circulation*. 2007;115:377-386
27. Tyson KL, Reynolds JL, McNair R, Zhang Q, Weissberg PL, Shanahan CM. Osteo/chondrocytic transcription factors and their target genes exhibit distinct patterns of expression in human arterial calcification. *Arteriosclerosis, thrombosis, and vascular biology*. 2003;23:489-494
28. Bobryshev YV. Transdifferentiation of smooth muscle cells into chondrocytes in atherosclerotic arteries in situ: Implications for diffuse intimal calcification. *The Journal of pathology*. 2005;205:641-650
29. Speer MY, Yang HY, Brabb T, Leaf E, Look A, Lin WL, Frutkin A, Dichek D, Giachelli CM. Smooth muscle cells give rise to osteochondrogenic precursors and chondrocytes in calcifying arteries. *Circulation research*. 2009;104:733-741
30. Speer MY, Li X, Hiremath PG, Giachelli CM. Runx2/cbfa1, but not loss of myocardin, is required for smooth muscle cell lineage reprogramming toward osteochondrogenesis. *Journal of cellular biochemistry*. 2010;110:935-947
31. Shen J, Yang M, Jiang H, Ju D, Zheng JP, Xu Z, Liao TD, Li L. Arterial injury promotes medial chondrogenesis in sm22 knockout mice. *Cardiovascular research*. 2011;90:28-37
32. Mathew S, Lund RJ, Strebeck F, Tustison KS, Geurs T, Hruska KA. Reversal of the adynamic bone disorder and decreased vascular calcification in chronic kidney disease by sevelamer carbonate therapy. *Journal of the American Society of Nephrology : JASN*. 2007;18:122-130
33. Pai A, Leaf EM, El-Abbadi M, Giachelli CM. Elastin degradation and vascular smooth muscle cell phenotype change precede cell loss and arterial medial calcification in a uremic mouse model of chronic kidney disease. *The American journal of pathology*. 2011;178:764-773
34. Adeney KL, Siscovick DS, Ix JH, Seliger SL, Shlipak MG, Jenny NS, Kestenbaum BR. Association of serum phosphate with vascular and valvular calcification in moderate ckd. *Journal of the American Society of Nephrology : JASN*. 2009;20:381-387
35. Sexton PM, Findlay DM, Martin TJ. Calcitonin. *Current medicinal chemistry*. 1999;6:1067-1093
36. Bergwitz C, Juppner H. Regulation of phosphate homeostasis by pth, vitamin d, and fgf23. *Annual review of medicine*. 2010;61:91-104
37. Renkema KY, Alexander RT, Bindels RJ, Hoenderop JG. Calcium and phosphate homeostasis: Concerted interplay of new regulators. *Annals of medicine*. 2008;40:82-91
38. Larsson T, Nisbeth U, Ljunggren O, Juppner H, Jonsson KB. Circulating concentration of fgf-23 increases as renal function declines in patients with chronic kidney disease, but does not change in response to variation in phosphate intake in healthy volunteers. *Kidney international*. 2003;64:2272-2279
39. Imanishi Y, Inaba M, Nakatsuka K, Nagasue K, Okuno S, Yoshihara A, Miura M, Miyauchi A, Kobayashi K, Miki T, Shoji T, Ishimura E, Nishizawa Y. Fgf-23 in patients with end-stage renal disease on hemodialysis. *Kidney international*. 2004;65:1943-1946

40. Fliser D, Kollerits B, Neyer U, Ankerst DP, Lhotta K, Lingenhel A, Ritz E, Kronenberg F, Kuen E, Konig P, Kraatz G, Mann JF, Muller GA, Kohler H, Riegler P. Fibroblast growth factor 23 (fgf23) predicts progression of chronic kidney disease: The mild to moderate kidney disease (mmkd) study. *Journal of the American Society of Nephrology : JASN*. 2007;18:2600-2608
41. Isakova T, Wahl P, Vargas GS, Gutierrez OM, Scialla J, Xie H, Appleby D, Nessel L, Bellovich K, Chen J, Hamm L, Gadegbeku C, Horwitz E, Townsend RR, Anderson CA, Lash JP, Hsu CY, Leonard MB, Wolf M. Fibroblast growth factor 23 is elevated before parathyroid hormone and phosphate in chronic kidney disease. *Kidney international*. 2011
42. Hasegawa H, Nagano N, Urakawa I, Yamazaki Y, Iijima K, Fujita T, Yamashita T, Fukumoto S, Shimada T. Direct evidence for a causative role of fgf23 in the abnormal renal phosphate handling and vitamin d metabolism in rats with early-stage chronic kidney disease. *Kidney international*. 2010;78:975-980
43. Lavi-Moshayoff V, Wasserman G, Meir T, Silver J, Naveh-Many T. Pth increases fgf23 gene expression and mediates the high-fgf23 levels of experimental kidney failure: A bone parathyroid feedback loop. *American journal of physiology. Renal physiology*. 2010;299:F882-889
44. Saito H, Kusano K, Kinosaki M, Ito H, Hirata M, Segawa H, Miyamoto K, Fukushima N. Human fibroblast growth factor-23 mutants suppress na+-dependent phosphate co-transport activity and 1alpha,25-dihydroxyvitamin d3 production. *The Journal of biological chemistry*. 2003;278:2206-2211
45. Bai X, Miao D, Li J, Goltzman D, Karaplis AC. Transgenic mice overexpressing human fibroblast growth factor 23 (r176q) delineate a putative role for parathyroid hormone in renal phosphate wasting disorders. *Endocrinology*. 2004;145:5269-5279
46. Shimada T, Kakitani M, Yamazaki Y, Hasegawa H, Takeuchi Y, Fujita T, Fukumoto S, Tomizuka K, Yamashita T. Targeted ablation of fgf23 demonstrates an essential physiological role of fgf23 in phosphate and vitamin d metabolism. *The Journal of clinical investigation*. 2004;113:561-568
47. Shimada T, Urakawa I, Yamazaki Y, Hasegawa H, Hino R, Yoneya T, Takeuchi Y, Fujita T, Fukumoto S, Yamashita T. Fgf-23 transgenic mice demonstrate hypophosphatemic rickets with reduced expression of sodium phosphate cotransporter type iia. *Biochemical and biophysical research communications*. 2004;314:409-414
48. Levin A, Bakris GL, Molitch M, Smulders M, Tian J, Williams LA, Andress DL. Prevalence of abnormal serum vitamin d, pth, calcium, and phosphorus in patients with chronic kidney disease: Results of the study to evaluate early kidney disease. *Kidney international*. 2007;71:31-38
49. De Boer IH, Gorodetskaya I, Young B, Hsu CY, Chertow GM. The severity of secondary hyperparathyroidism in chronic renal insufficiency is gfr-dependent, race-dependent, and associated with cardiovascular disease. *Journal of the American Society of Nephrology : JASN*. 2002;13:2762-2769

50. Korkor AB. Reduced binding of [3h]1,25-dihydroxyvitamin d3 in the parathyroid glands of patients with renal failure. *The New England journal of medicine*. 1987;316:1573-1577
51. Kifor O, Moore FD, Jr., Wang P, Goldstein M, Vassilev P, Kifor I, Hebert SC, Brown EM. Reduced immunostaining for the extracellular ca2+-sensing receptor in primary and uremic secondary hyperparathyroidism. *The Journal of clinical endocrinology and metabolism*. 1996;81:1598-1606
52. Gogusev J, Duchambon P, Hory B, Giovannini M, Goureau Y, Sarfati E, Drueke TB. Depressed expression of calcium receptor in parathyroid gland tissue of patients with hyperparathyroidism. *Kidney international*. 1997;51:328-336
53. Drueke TB. Klotho, fgf23, and fgf receptors in chronic kidney disease: A yin-yang situation? *Kidney international*. 2010;78:1057-1060
54. Komaba H, Goto S, Fujii H, Hamada Y, Kobayashi A, Shibuya K, Tominaga Y, Otsuki N, Nibu K, Nakagawa K, Tsugawa N, Okano T, Kitazawa R, Fukagawa M, Kita T. Depressed expression of klotho and fgf receptor 1 in hyperplastic parathyroid glands from uremic patients. *Kidney international*. 2010;77:232-238
55. Goodman WG. Medical management of secondary hyperparathyroidism in chronic renal failure. *Nephrology, dialysis, transplantation : official publication of the European Dialysis and Transplant Association - European Renal Association*. 2003;18 Suppl 3:iii2-8
56. Kestenbaum B, Sampson JN, Rudser KD, Patterson DJ, Seliger SL, Young B, Sherrard DJ, Andress DL. Serum phosphate levels and mortality risk among people with chronic kidney disease. *Journal of the American Society of Nephrology : JASN*. 2005;16:520-528
57. Ganesh SK, Stack AG, Levin NW, Hulbert-Shearon T, Port FK. Association of elevated serum po(4), ca x po(4) product, and parathyroid hormone with cardiac mortality risk in chronic hemodialysis patients. *Journal of the American Society of Nephrology : JASN*. 2001;12:2131-2138
58. Block GA. Prevalence and clinical consequences of elevated ca x p product in hemodialysis patients. *Clinical nephrology*. 2000;54:318-324
59. Block GA, Hulbert-Shearon TE, Levin NW, Port FK. Association of serum phosphorus and calcium x phosphate product with mortality risk in chronic hemodialysis patients: A national study. *American journal of kidney diseases : the official journal of the National Kidney Foundation*. 1998;31:607-617
60. Lowrie EG, Lew NL. Death risk in hemodialysis patients: The predictive value of commonly measured variables and an evaluation of death rate differences between facilities. *American journal of kidney diseases : the official journal of the National Kidney Foundation*. 1990;15:458-482
61. Young EW, Albert JM, Satayathum S, Goodkin DA, Pisoni RL, Akiba T, Akizawa T, Kurokawa K, Bommer J, Piera L, Port FK. Predictors and consequences of altered mineral metabolism: The dialysis outcomes and practice patterns study. *Kidney international*. 2005;67:1179-1187
62. Dhingra R, Sullivan LM, Fox CS, Wang TJ, D'Agostino RB, Sr., Gaziano JM, Vasan RS. Relations of serum phosphorus and calcium

levels to the incidence of cardiovascular disease in the community. *Archives of internal medicine*. 2007;167:879-885
63. Tonelli M, Sacks F, Pfeffer M, Gao Z, Curhan G. Relation between serum phosphate level and cardiovascular event rate in people with coronary disease. *Circulation*. 2005;112:2627-2633
64. Stubbs J, Liu S, Quarles LD. Role of fibroblast growth factor 23 in phosphate homeostasis and pathogenesis of disordered mineral metabolism in chronic kidney disease. *Seminars in dialysis*. 2007;20:302-308
65. Stubbs JR, Liu S, Tang W, Zhou J, Wang Y, Yao X, Quarles LD. Role of hyperphosphatemia and 1,25-dihydroxyvitamin d in vascular calcification and mortality in fibroblastic growth factor 23 null mice. *Journal of the American Society of Nephrology : JASN*. 2007;18:2116-2124
66. Kuro-o M, Matsumura Y, Aizawa H, Kawaguchi H, Suga T, Utsugi T, Ohyama Y, Kurabayashi M, Kaname T, Kume E, Iwasaki H, Iida A, Shiraki-Iida T, Nishikawa S, Nagai R, Nabeshima YI. Mutation of the mouse klotho gene leads to a syndrome resembling ageing. *Nature*. 1997;390:45-51
67. Son BK, Kozaki K, Iijima K, Eto M, Kojima T, Ota H, Senda Y, Maemura K, Nakano T, Akishita M, Ouchi Y. Statins protect human aortic smooth muscle cells from inorganic phosphate-induced calcification by restoring gas6-axl survival pathway. *Circulation research*. 2006;98:1024-1031
68. Proudfoot D, Skepper JN, Hegyi L, Bennett MR, Shanahan CM, Weissberg PL. Apoptosis regulates human vascular calcification in vitro: Evidence for initiation of vascular calcification by apoptotic bodies. *Circulation research*. 2000;87:1055-1062
69. Melaragno MG, Cavet ME, Yan C, Tai LK, Jin ZG, Haendeler J, Berk BC. Gas6 inhibits apoptosis in vascular smooth muscle: Role of axl kinase and akt. *Journal of molecular and cellular cardiology*. 2004;37:881-887
70. Jono S, McKee MD, Murry CE, Shioi A, Nishizawa Y, Mori K, Morii H, Giachelli CM. Phosphate regulation of vascular smooth muscle cell calcification. *Circulation research*. 2000;87:E10-17
71. Steitz SA, Speer MY, Curinga G, Yang HY, Haynes P, Aebersold R, Schinke T, Karsenty G, Giachelli CM. Smooth muscle cell phenotypic transition associated with calcification: Upregulation of cbfa1 and downregulation of smooth muscle lineage markers. *Circulation research*. 2001;89:1147-1154
72. Shioi A, Nishizawa Y, Jono S, Koyama H, Hosoi M, Morii H. Beta-glycerophosphate accelerates calcification in cultured bovine vascular smooth muscle cells. *Arteriosclerosis, thrombosis, and vascular biology*. 1995;15:2003-2009
73. Chen NX, O'Neill KD, Duan D, Moe SM. Phosphorus and uremic serum up-regulate osteopontin expression in vascular smooth muscle cells. *Kidney international*. 2002;62:1724-1731
74. El-Abbadi MM, Pai AS, Leaf EM, Yang HY, Bartley BA, Quan KK, Ingalls CM, Liao HW, Giachelli CM. Phosphate feeding induces arterial medial calcification in uremic mice: Role of serum phosphorus,

fibroblast growth factor-23, and osteopontin. *Kidney international*. 2009;75:1297-1307
75. Li X, Yang HY, Giachelli CM. Role of the sodium-dependent phosphate cotransporter, pit-1, in vascular smooth muscle cell calcification. *Circulation research*. 2006;98:905-912
76. Zhao MM, Xu MJ, Cai Y, Zhao G, Guan Y, Kong W, Tang C, Wang X. Mitochondrial reactive oxygen species promote p65 nuclear translocation mediating high-phosphate-induced vascular calcification in vitro and in vivo. *Kidney international*. 2011;79:1071-1079
77. Mathew S, Tustison KS, Sugatani T, Chaudhary LR, Rifas L, Hruska KA. The mechanism of phosphorus as a cardiovascular risk factor in ckd. *Journal of the American Society of Nephrology : JASN*. 2008;19:1092-1105
78. Shanahan CM, Crouthamel MH, Kapustin A, Giachelli CM. Arterial calcification in chronic kidney disease: Key roles for calcium and phosphate. *Circulation research*. 2011;109:697-711
79. Block GA, Spiegel DM, Ehrlich J, Mehta R, Lindbergh J, Dreisbach A, Raggi P. Effects of sevelamer and calcium on coronary artery calcification in patients new to hemodialysis. *Kidney international*. 2005;68:1815-1824
80. Chertow GM, Burke SK, Raggi P. Sevelamer attenuates the progression of coronary and aortic calcification in hemodialysis patients. *Kidney international*. 2002;62:245-252
81. West SL, Swan VJ, Jamal SA. Effects of calcium on cardiovascular events in patients with kidney disease and in a healthy population. *Clinical journal of the American Society of Nephrology : CJASN*. 2010;5 Suppl 1:S41-47
82. Yang H, Curinga G, Giachelli CM. Elevated extracellular calcium levels induce smooth muscle cell matrix mineralization in vitro. *Kidney international*. 2004;66:2293-2299
83. Reynolds JL, Joannides AJ, Skepper JN, McNair R, Schurgers LJ, Proudfoot D, Jahnen-Dechent W, Weissberg PL, Shanahan CM. Human vascular smooth muscle cells undergo vesicle-mediated calcification in response to changes in extracellular calcium and phosphate concentrations: A potential mechanism for accelerated vascular calcification in esrd. *Journal of the American Society of Nephrology : JASN*. 2004;15:2857-2867
84. Alam MU, Kirton JP, Wilkinson FL, Towers E, Sinha S, Rouhi M, Vizard TN, Sage AP, Martin D, Ward DT, Alexander MY, Riccardi D, Canfield AE. Calcification is associated with loss of functional calcium-sensing receptor in vascular smooth muscle cells. *Cardiovascular research*. 2009;81:260-268
85. Lomashvili K, Garg P, O'Neill WC. Chemical and hormonal determinants of vascular calcification in vitro. *Kidney international*. 2006;69:1464-1470
86. Shroff RC, McNair R, Skepper JN, Figg N, Schurgers LJ, Deanfield J, Rees L, Shanahan CM. Chronic mineral dysregulation promotes vascular smooth muscle cell adaptation and extracellular matrix calcification. *Journal of the American Society of Nephrology : JASN*. 2010;21:103-112

87. Anderson HC, Garimella R, Tague SE. The role of matrix vesicles in growth plate development and biomineralization. *Frontiers in bioscience : a journal and virtual library*. 2005;10:822-837
88. Moe SM, Reslerova M, Ketteler M, O'Neill K, Duan D, Koczman J, Westenfeld R, Jahnen-Dechent W, Chen NX. Role of calcification inhibitors in the pathogenesis of vascular calcification in chronic kidney disease (ckd). *Kidney international*. 2005;67:2295-2304
89. Reynolds JL, Skepper JN, McNair R, Kasama T, Gupta K, Weissberg PL, Jahnen-Dechent W, Shanahan CM. Multifunctional roles for serum protein fetuin-a in inhibition of human vascular smooth muscle cell calcification. *Journal of the American Society of Nephrology : JASN*. 2005;16:2920-2930
90. Chen NX, O'Neill KD, Chen X, Moe SM. Annexin-mediated matrix vesicle calcification in vascular smooth muscle cells. *Journal of bone and mineral research : the official journal of the American Society for Bone and Mineral Research*. 2008;23:1798-1805
91. Farzaneh-Far A, Proudfoot D, Weissberg PL, Shanahan CM. Matrix gla protein is regulated by a mechanism functionally related to the calcium-sensing receptor. *Biochemical and biophysical research communications*. 2000;277:736-740
92. Mendoza FJ, Martinez-Moreno J, Almaden Y, Rodriguez-Ortiz ME, Lopez I, Estepa JC, Henley C, Rodriguez M, Aguilera-Tejero E. Effect of calcium and the calcimimetic amg 641 on matrix-gla protein in vascular smooth muscle cells. *Calcified tissue international*. 2011;88:169-178
93. Kapustin AN, Davies JD, Reynolds JL, McNair R, Jones GT, Sidibe A, Schurgers LJ, Skepper JN, Proudfoot D, Mayr M, Shanahan CM. Calcium regulates key components of vascular smooth muscle cell-derived matrix vesicles to enhance mineralization. *Circulation research*. 2011;109:e1-12
94. Schinke T, Amendt C, Trindl A, Poschke O, Muller-Esterl W, Jahnen-Dechent W. The serum protein alpha2-hs glycoprotein/fetuin inhibits apatite formation in vitro and in mineralizing calvaria cells. A possible role in mineralization and calcium homeostasis. *The Journal of biological chemistry*. 1996;271:20789-20796
95. Heiss A, DuChesne A, Denecke B, Grotzinger J, Yamamoto K, Renne T, Jahnen-Dechent W. Structural basis of calcification inhibition by alpha 2-hs glycoprotein/fetuin-a. Formation of colloidal calciprotein particles. *The Journal of biological chemistry*. 2003;278:13333-13341
96. Heiss A, Eckert T, Aretz A, Richtering W, van Dorp W, Schafer C, Jahnen-Dechent W. Hierarchical role of fetuin-a and acidic serum proteins in the formation and stabilization of calcium phosphate particles. *The Journal of biological chemistry*. 2008;283:14815-14825
97. Chen NX, O'Neill KD, Chen X, Duan D, Wang E, Sturek MS, Edwards JM, Moe SM. Fetuin-a uptake in bovine vascular smooth muscle cells is calcium dependent and mediated by annexins. *American journal of physiology. Renal physiology*. 2007;292:F599-606
98. Jahnen-Dechent W, Schinke T, Trindl A, Muller-Esterl W, Sablitzky F, Kaiser S, Blessing M. Cloning and targeted deletion of the mouse

fetuin gene. *The Journal of biological chemistry*. 1997;272:31496-31503
99. Schafer C, Heiss A, Schwarz A, Westenfeld R, Ketteler M, Floege J, Muller-Esterl W, Schinke T, Jahnen-Dechent W. The serum protein alpha 2-heremans-schmid glycoprotein/fetuin-a is a systemically acting inhibitor of ectopic calcification. *The Journal of clinical investigation*. 2003;112:357-366
100. Westenfeld R, Schafer C, Kruger T, Haarmann C, Schurgers LJ, Reutelingsperger C, Ivanovski O, Drueke T, Massy ZA, Ketteler M, Floege J, Jahnen-Dechent W. Fetuin-a protects against atherosclerotic calcification in ckd. *Journal of the American Society of Nephrology : JASN*. 2009;20:1264-1274
101. Ketteler M, Bongartz P, Westenfeld R, Wildberger JE, Mahnken AH, Bohm R, Metzger T, Wanner C, Jahnen-Dechent W, Floege J. Association of low fetuin-a (ahsg) concentrations in serum with cardiovascular mortality in patients on dialysis: A cross-sectional study. *Lancet*. 2003;361:827-833
102. Hermans MM, Brandenburg V, Ketteler M, Kooman JP, van der Sande FM, Boeschoten EW, Leunissen KM, Krediet RT, Dekker FW. Association of serum fetuin-a levels with mortality in dialysis patients. *Kidney international*. 2007;72:202-207
103. Verduijn M, Prein RA, Stenvinkel P, Carrero JJ, le Cessie S, Witasp A, Nordfors L, Krediet RT, Boeschoten EW, Dekker FW. Is fetuin-a a mortality risk factor in dialysis patients or a mere risk marker? A mendelian randomization approach. *Nephrology, dialysis, transplantation : official publication of the European Dialysis and Transplant Association - European Renal Association*. 2011;26:239-245
104. Stenvinkel P, Wang K, Qureshi AR, Axelsson J, Pecoits-Filho R, Gao P, Barany P, Lindholm B, Jogestrand T, Heimburger O, Holmes C, Schalling M, Nordfors L. Low fetuin-a levels are associated with cardiovascular death: Impact of variations in the gene encoding fetuin. *Kidney international*. 2005;67:2383-2392
105. Lehtinen AB, Burdon KP, Lewis JP, Langefeld CD, Ziegler JT, Rich SS, Register TC, Carr JJ, Freedman BI, Bowden DW. Association of alpha2-heremans-schmid glycoprotein polymorphisms with subclinical atherosclerosis. *The Journal of clinical endocrinology and metabolism*. 2007;92:345-352
106. Ix JH, Chertow GM, Shlipak MG, Brandenburg VM, Ketteler M, Whooley MA. Association of fetuin-a with mitral annular calcification and aortic stenosis among persons with coronary heart disease: Data from the heart and soul study. *Circulation*. 2007;115:2533-2539
107. Luo G, Ducy P, McKee MD, Pinero GJ, Loyer E, Behringer RR, Karsenty G. Spontaneous calcification of arteries and cartilage in mice lacking matrix gla protein. *Nature*. 1997;386:78-81
108. Murshed M, Schinke T, McKee MD, Karsenty G. Extracellular matrix mineralization is regulated locally; different roles of two gla-containing proteins. *The Journal of cell biology*. 2004;165:625-630
109. Schurgers LJ, Spronk HM, Skepper JN, Hackeng TM, Shanahan CM, Vermeer C, Weissberg PL, Proudfoot D. Post-translational

modifications regulate matrix gla protein function: Importance for inhibition of vascular smooth muscle cell calcification. *Journal of thrombosis and haemostasis : JTH*. 2007;5:2503-2511
110. Price PA, Urist MR, Otawara Y. Matrix gla protein, a new gamma-carboxyglutamic acid-containing protein which is associated with the organic matrix of bone. *Biochemical and biophysical research communications*. 1983;117:765-771
111. Proudfoot D, Skepper JN, Shanahan CM, Weissberg PL. Calcification of human vascular cells in vitro is correlated with high levels of matrix gla protein and low levels of osteopontin expression. *Arteriosclerosis, thrombosis, and vascular biology*. 1998;18:379-388
112. Schurgers LJ, Dissel PE, Spronk HM, Soute BA, Dhore CR, Cleutjens JP, Vermeer C. Role of vitamin k and vitamin k-dependent proteins in vascular calcification. *Zeitschrift fur Kardiologie*. 2001;90 Suppl 3:57-63
113. Spronk HM, Soute BA, Schurgers LJ, Cleutjens JP, Thijssen HH, De Mey JG, Vermeer C. Matrix gla protein accumulates at the border of regions of calcification and normal tissue in the media of the arterial vessel wall. *Biochemical and biophysical research communications*. 2001;289:485-490
114. Schurgers LJ, Teunissen KJ, Knapen MH, Kwaijtaal M, van Diest R, Appels A, Reutelingsperger CP, Cleutjens JP, Vermeer C. Novel conformation-specific antibodies against matrix gamma-carboxyglutamic acid (gla) protein: Undercarboxylated matrix gla protein as marker for vascular calcification. *Arteriosclerosis, thrombosis, and vascular biology*. 2005;25:1629-1633
115. Hackeng TM, Rosing J, Spronk HM, Vermeer C. Total chemical synthesis of human matrix gla protein. *Protein science : a publication of the Protein Society*. 2001;10:864-870
116. Zebboudj AF, Imura M, Bostrom K. Matrix gla protein, a regulatory protein for bone morphogenetic protein-2. *The Journal of biological chemistry*. 2002;277:4388-4394
117. Sweatt A, Sane DC, Hutson SM, Wallin R. Matrix gla protein (mgp) and bone morphogenetic protein-2 in aortic calcified lesions of aging rats. *Journal of thrombosis and haemostasis : JTH*. 2003;1:178-185
118. Wallin R, Cain D, Hutson SM, Sane DC, Loeser R. Modulation of the binding of matrix gla protein (mgp) to bone morphogenetic protein-2 (bmp-2). *Thrombosis and haemostasis*. 2000;84:1039-1044
119. Yao Y, Zebboudj AF, Shao E, Perez M, Bostrom K. Regulation of bone morphogenetic protein-4 by matrix gla protein in vascular endothelial cells involves activin-like kinase receptor 1. *The Journal of biological chemistry*. 2006;281:33921-33930
120. Zebboudj AF, Shin V, Bostrom K. Matrix gla protein and bmp-2 regulate osteoinduction in calcifying vascular cells. *Journal of cellular biochemistry*. 2003;90:756-765
121. Koos R, Krueger T, Westenfeld R, Kuhl HP, Brandenburg V, Mahnken AH, Stanzel S, Vermeer C, Cranenburg EC, Floege J, Kelm M, Schurgers LJ. Relation of circulating matrix gla-protein and anticoagulation status in patients with aortic valve calcification. *Thrombosis and haemostasis*. 2009;101:706-713

122. Jono S, Ikari Y, Vermeer C, Dissel P, Hasegawa K, Shioi A, Taniwaki H, Kizu A, Nishizawa Y, Saito S. Matrix gla protein is associated with coronary artery calcification as assessed by electron-beam computed tomography. *Thrombosis and haemostasis*. 2004;91:790-794
123. Munroe PB, Olgunturk RO, Fryns JP, Van Maldergem L, Ziereisen F, Yuksel B, Gardiner RM, Chung E. Mutations in the gene encoding the human matrix gla protein cause keutel syndrome. *Nature genetics*. 1999;21:142-144
124. Hur DJ, Raymond GV, Kahler SG, Riegert-Johnson DL, Cohen BA, Boyadjiev SA. A novel mgp mutation in a consanguineous family: Review of the clinical and molecular characteristics of keutel syndrome. *American journal of medical genetics. Part A*. 2005;135:36-40
125. Hermans MM, Vermeer C, Kooman JP, Brandenburg V, Ketteler M, Gladziwa U, Rensma PL, Leunissen KM, Schurgers LJ. Undercarboxylated matrix gla protein levels are decreased in dialysis patients and related to parameters of calcium-phosphate metabolism and aortic augmentation index. *Blood purification*. 2007;25:395-401
126. Cranenburg EC, Vermeer C, Koos R, Boumans ML, Hackeng TM, Bouwman FG, Kwaijtaal M, Brandenburg VM, Ketteler M, Schurgers LJ. The circulating inactive form of matrix gla protein (ucmgp) as a biomarker for cardiovascular calcification. *Journal of vascular research*. 2008;45:427-436
127. Cranenburg EC, Brandenburg VM, Vermeer C, Stenger M, Muhlenbruch G, Mahnken AH, Gladziwa U, Ketteler M, Schurgers LJ. Uncarboxylated matrix gla protein (ucmgp) is associated with coronary artery calcification in haemodialysis patients. *Thrombosis and haemostasis*. 2009;101:359-366
128. Schurgers LJ, Barreto DV, Barreto FC, Liabeuf S, Renard C, Magdeleyns EJ, Vermeer C, Choukroun G, Massy ZA. The circulating inactive form of matrix gla protein is a surrogate marker for vascular calcification in chronic kidney disease: A preliminary report. *Clinical journal of the American Society of Nephrology : CJASN*. 2010;5:568-575
129. Ross FP, Chappel J, Alvarez JI, Sander D, Butler WT, Farach-Carson MC, Mintz KA, Robey PG, Teitelbaum SL, Cheresh DA. Interactions between the bone matrix proteins osteopontin and bone sialoprotein and the osteoclast integrin alpha v beta 3 potentiate bone resorption. *The Journal of biological chemistry*. 1993;268:9901-9907
130. Boskey AL, Maresca M, Ullrich W, Doty SB, Butler WT, Prince CW. Osteopontin-hydroxyapatite interactions in vitro: Inhibition of hydroxyapatite formation and growth in a gelatin-gel. *Bone and mineral*. 1993;22:147-159
131. Okamoto H. Osteopontin and cardiovascular system. *Molecular and cellular biochemistry*. 2007;300:1-7
132. Speer MY, McKee MD, Guldberg RE, Liaw L, Yang HY, Tung E, Karsenty G, Giachelli CM. Inactivation of the osteopontin gene enhances vascular calcification of matrix gla protein-deficient mice: Evidence for osteopontin as an inducible inhibitor of vascular calcification in vivo. *The Journal of experimental medicine*. 2002;196:1047-1055

133. Jono S, Peinado C, Giachelli CM. Phosphorylation of osteopontin is required for inhibition of vascular smooth muscle cell calcification. *The Journal of biological chemistry*. 2000;275:20197-20203
134. Giachelli CM, Bae N, Almeida M, Denhardt DT, Alpers CE, Schwartz SM. Osteopontin is elevated during neointima formation in rat arteries and is a novel component of human atherosclerotic plaques. *The Journal of clinical investigation*. 1993;92:1686-1696
135. Giachelli CM, Liaw L, Murry CE, Schwartz SM, Almeida M. Osteopontin expression in cardiovascular diseases. *Annals of the New York Academy of Sciences*. 1995;760:109-126
136. O'Brien ER, Garvin MR, Stewart DK, Hinohara T, Simpson JB, Schwartz SM, Giachelli CM. Osteopontin is synthesized by macrophage, smooth muscle, and endothelial cells in primary and restenotic human coronary atherosclerotic plaques. *Arteriosclerosis and thrombosis : a journal of vascular biology / American Heart Association*. 1994;14:1648-1656
137. Ikeda T, Shirasawa T, Esaki Y, Yoshiki S, Hirokawa K. Osteopontin mrna is expressed by smooth muscle-derived foam cells in human atherosclerotic lesions of the aorta. *The Journal of clinical investigation*. 1993;92:2814-2820
138. Hirota S, Imakita M, Kohri K, Ito A, Morii E, Adachi S, Kim HM, Kitamura Y, Yutani C, Nomura S. Expression of osteopontin messenger rna by macrophages in atherosclerotic plaques. A possible association with calcification. *The American journal of pathology*. 1993;143:1003-1008
139. Fitzpatrick LA, Severson A, Edwards WD, Ingram RT. Diffuse calcification in human coronary arteries. Association of osteopontin with atherosclerosis. *The Journal of clinical investigation*. 1994;94:1597-1604
140. Mohler ER, 3rd, Adam LP, McClelland P, Graham L, Hathaway DR. Detection of osteopontin in calcified human aortic valves. *Arteriosclerosis, thrombosis, and vascular biology*. 1997;17:547-552
141. Aryan M, Kepez A, Atalar E, Hazirolan T, Haznedaroglu I, Akata D, Ozer N, Aksoyek S, Ovunc K, Ozmen F. Association of plasma osteopontin levels with coronary calcification evaluated by tomographic coronary calcium scoring. *Journal of bone and mineral metabolism*. 2009;27:591-597
142. Shanahan CM, Cary NR, Metcalfe JC, Weissberg PL. High expression of genes for calcification-regulating proteins in human atherosclerotic plaques. *The Journal of clinical investigation*. 1994;93:2393-2402
143. Ohmori R, Momiyama Y, Taniguchi H, Takahashi R, Kusuhara M, Nakamura H, Ohsuzu F. Plasma osteopontin levels are associated with the presence and extent of coronary artery disease. *Atherosclerosis*. 2003;170:333-337
144. Chiba S, Okamoto H, Kon S, Kimura C, Murakami M, Inobe M, Matsui Y, Sugawara T, Shimizu T, Uede T, Kitabatake A. Development of atherosclerosis in osteopontin transgenic mice. *Heart and vessels*. 2002;16:111-117

145. Schibler D, Russell RG, Fleisch H. Inhibition by pyrophosphate and polyphosphate of aortic calcification induced by vitamin d3 in rats. *Clinical science*. 1968;35:363-372
146. Lomashvili KA, Cobbs S, Hennigar RA, Hardcastle KI, O'Neill WC. Phosphate-induced vascular calcification: Role of pyrophosphate and osteopontin. *Journal of the American Society of Nephrology : JASN*. 2004;15:1392-1401
147. Fleisch H, Russell RG, Straumann F. Effect of pyrophosphate on hydroxyapatite and its implications in calcium homeostasis. *Nature*. 1966;212:901-903
148. Johnson K, Polewski M, van Etten D, Terkeltaub R. Chondrogenesis mediated by ppi depletion promotes spontaneous aortic calcification in npp1-/- mice. *Arteriosclerosis, thrombosis, and vascular biology*. 2005;25:686-691
149. Villa-Bellosta R, Wang X, Millan JL, Dubyak GR, O'Neill WC. Extracellular pyrophosphate metabolism and calcification in vascular smooth muscle. *American journal of physiology. Heart and circulatory physiology*. 2011
150. Ho AM, Johnson MD, Kingsley DM. Role of the mouse ank gene in control of tissue calcification and arthritis. *Science*. 2000;289:265-270
151. Rutsch F, Vaingankar S, Johnson K, Goldfine I, Maddux B, Schauerte P, Kalhoff H, Sano K, Boisvert WA, Superti-Furga A, Terkeltaub R. Pc-1 nucleoside triphosphate pyrophosphohydrolase deficiency in idiopathic infantile arterial calcification. *The American journal of pathology*. 2001;158:543-554
152. Lorenz-Depiereux B, Schnabel D, Tiosano D, Hausler G, Strom TM. Loss-of-function enpp1 mutations cause both generalized arterial calcification of infancy and autosomal-recessive hypophosphatemic rickets. *American journal of human genetics*. 2010;86:267-272
153. Lomashvili KA, Garg P, Narisawa S, Millan JL, O'Neill WC. Upregulation of alkaline phosphatase and pyrophosphate hydrolysis: Potential mechanism for uremic vascular calcification. *Kidney international*. 2008;73:1024-1030
154. Lomashvili KA, Khawandi W, O'Neill WC. Reduced plasma pyrophosphate levels in hemodialysis patients. *Journal of the American Society of Nephrology : JASN*. 2005;16:2495-2500
155. O'Neill WC, Sigrist MK, McIntyre CW. Plasma pyrophosphate and vascular calcification in chronic kidney disease. *Nephrology, dialysis, transplantation : official publication of the European Dialysis and Transplant Association - European Renal Association*. 2010;25:187-191
156. O'Neill WC, Lomashvili KA, Malluche HH, Faugere MC, Riser BL. Treatment with pyrophosphate inhibits uremic vascular calcification. *Kidney international*. 2011;79:512-517
157. Bucay N, Sarosi I, Dunstan CR, Morony S, Tarpley J, Capparelli C, Scully S, Tan HL, Xu W, Lacey DL, Boyle WJ, Simonet WS. Osteoprotegerin-deficient mice develop early onset osteoporosis and arterial calcification. *Genes & development*. 1998;12:1260-1268
158. Orita Y, Yamamoto H, Kohno N, Sugihara M, Honda H, Kawamata S, Mito S, Soe NN, Yoshizumi M. Role of osteoprotegerin in arterial

calcification: Development of new animal model. *Arteriosclerosis, thrombosis, and vascular biology*. 2007;27:2058-2064
159. Bennett BJ, Scatena M, Kirk EA, Rattazzi M, Varon RM, Averill M, Schwartz SM, Giachelli CM, Rosenfeld ME. Osteoprotegerin inactivation accelerates advanced atherosclerotic lesion progression and calcification in older apoe-/- mice. *Arteriosclerosis, thrombosis, and vascular biology*. 2006;26:2117-2124
160. Morony S, Tintut Y, Zhang Z, Cattley RC, Van G, Dwyer D, Stolina M, Kostenuik PJ, Demer LL. Osteoprotegerin inhibits vascular calcification without affecting atherosclerosis in ldlr(-/-) mice. *Circulation*. 2008;117:411-420
161. Price PA, June HH, Buckley JR, Williamson MK. Osteoprotegerin inhibits artery calcification induced by warfarin and by vitamin d. *Arteriosclerosis, thrombosis, and vascular biology*. 2001;21:1610-1616
162. Nitta K, Akiba T, Uchida K, Otsubo S, Takei T, Yumura W, Kabaya T, Nihei H. Serum osteoprotegerin levels and the extent of vascular calcification in haemodialysis patients. *Nephrology, dialysis, transplantation : official publication of the European Dialysis and Transplant Association - European Renal Association*. 2004;19:1886-1889
163. Shroff RC, Shah V, Hiorns MP, Schoppet M, Hofbauer LC, Hawa G, Schurgers LJ, Singhal A, Merryweather I, Brogan P, Shanahan C, Deanfield J, Rees L. The circulating calcification inhibitors, fetuin-a and osteoprotegerin, but not matrix gla protein, are associated with vascular stiffness and calcification in children on dialysis. *Nephrology, dialysis, transplantation : official publication of the European Dialysis and Transplant Association - European Renal Association*. 2008;23:3263-3271
164. Barreto DV, Barreto FC, Carvalho AB, Cuppari L, Cendoroglo M, Draibe SA, Moyses RM, Neves KR, Jorgetti V, Blair A, Guiberteau R, Fernandes Canziani ME. Coronary calcification in hemodialysis patients: The contribution of traditional and uremia-related risk factors. *Kidney international*. 2005;67:1576-1582
165. Kiechl S, Werner P, Knoflach M, Furtner M, Willeit J, Schett G. The osteoprotegerin/rank/rankl system: A bone key to vascular disease. *Expert review of cardiovascular therapy*. 2006;4:801-811
166. Van Campenhout A, Golledge J. Osteoprotegerin, vascular calcification and atherosclerosis. *Atherosclerosis*. 2009;204:321-329
167. Brown EM, Vassilev PM, Quinn S, Hebert SC. G-protein-coupled, extracellular ca(2+)-sensing receptor: A versatile regulator of diverse cellular functions. *Vitamins and hormones*. 1999;55:1-71
168. Naveh-Many T, Silver J. Regulation of parathyroid hormone gene expression by hypocalcemia, hypercalcemia, and vitamin d in the rat. *The Journal of clinical investigation*. 1990;86:1313-1319
169. Riccardi D, Hall AE, Chattopadhyay N, Xu JZ, Brown EM, Hebert SC. Localization of the extracellular ca2+/polyvalent cation-sensing protein in rat kidney. *The American journal of physiology*. 1998;274:F611-622
170. Garrett JE, Tamir H, Kifor O, Simin RT, Rogers KV, Mithal A, Gagel RF, Brown EM. Calcitonin-secreting cells of the thyroid express an

extracellular calcium receptor gene. *Endocrinology*. 1995;136:5202-5211
171. Riccardi D, Brown EM. Physiology and pathophysiology of the calcium-sensing receptor in the kidney. *American journal of physiology. Renal physiology*. 2010;298:F485-499
172. Brown EM. Anti-parathyroid and anti-calcium sensing receptor antibodies in autoimmune hypoparathyroidism. *Endocrinology and metabolism clinics of North America*. 2009;38:437-445, x
173. Kifor O, Moore FD, Jr., Delaney M, Garber J, Hendy GN, Butters R, Gao P, Cantor TL, Kifor I, Brown EM, Wysolmerski J. A syndrome of hypocalciuric hypercalcemia caused by autoantibodies directed at the calcium-sensing receptor. *The Journal of clinical endocrinology and metabolism*. 2003;88:60-72
174. Pallais JC, Kifor O, Chen YB, Slovik D, Brown EM. Acquired hypocalciuric hypercalcemia due to autoantibodies against the calcium-sensing receptor. *The New England journal of medicine*. 2004;351:362-369
175. Oda Y, Tu CL, Pillai S, Bikle DD. The calcium sensing receptor and its alternatively spliced form in keratinocyte differentiation. *The Journal of biological chemistry*. 1998;273:23344-23352
176. Cheng I, Klingensmith ME, Chattopadhyay N, Kifor O, Butters RR, Soybel DI, Brown EM. Identification and localization of the extracellular calcium-sensing receptor in human breast. *The Journal of clinical endocrinology and metabolism*. 1998;83:703-707
177. Bradbury RA, Sunn KL, Crossley M, Bai M, Brown EM, Delbridge L, Conigrave AD. Expression of the parathyroid ca(2+)-sensing receptor in cytotrophoblasts from human term placenta. *The Journal of endocrinology*. 1998;156:425-430
178. Brauner-Osborne H, Wellendorph P, Jensen AA. Structure, pharmacology and therapeutic prospects of family c g-protein coupled receptors. *Current drug targets*. 2007;8:169-184
179. Kunishima N, Shimada Y, Tsuji Y, Sato T, Yamamoto M, Kumasaka T, Nakanishi S, Jingami H, Morikawa K. Structural basis of glutamate recognition by a dimeric metabotropic glutamate receptor. *Nature*. 2000;407:971-977
180. Tsuchiya D, Kunishima N, Kamiya N, Jingami H, Morikawa K. Structural views of the ligand-binding cores of a metabotropic glutamate receptor complexed with an antagonist and both glutamate and gd3+. *Proceedings of the National Academy of Sciences of the United States of America*. 2002;99:2660-2665
181. Hu J, Hauache O, Spiegel AM. Human ca2+ receptor cysteine-rich domain. Analysis of function of mutant and chimeric receptors. *The Journal of biological chemistry*. 2000;275:16382-16389
182. Ray K, Clapp P, Goldsmith PK, Spiegel AM. Identification of the sites of n-linked glycosylation on the human calcium receptor and assessment of their role in cell surface expression and signal transduction. *The Journal of biological chemistry*. 1998;273:34558-34567
183. Saidak Z, Brazier M, Kamel S, Mentaverri R. Agonists and allosteric modulators of the calcium-sensing receptor and their therapeutic applications. *Molecular pharmacology*. 2009;76:1131-1144

184. Huang Y, Zhou Y, Castiblanco A, Yang W, Brown EM, Yang JJ. Multiple ca(2+)-binding sites in the extracellular domain of the ca(2+)-sensing receptor corresponding to cooperative ca(2+) response. *Biochemistry*. 2009;48:388-398
185. Petrel C, Kessler A, Maslah F, Dauban P, Dodd RH, Rognan D, Ruat M. Modeling and mutagenesis of the binding site of calhex 231, a novel negative allosteric modulator of the extracellular ca(2+)-sensing receptor. *The Journal of biological chemistry*. 2003;278:49487-49494
186. Miedlich SU, Gama L, Seuwen K, Wolf RM, Breitwieser GE. Homology modeling of the transmembrane domain of the human calcium sensing receptor and localization of an allosteric binding site. *The Journal of biological chemistry*. 2004;279:7254-7263
187. Petrel C, Kessler A, Dauban P, Dodd RH, Rognan D, Ruat M. Positive and negative allosteric modulators of the ca2+-sensing receptor interact within overlapping but not identical binding sites in the transmembrane domain. *The Journal of biological chemistry*. 2004;279:18990-18997
188. Fan GF, Ray K, Zhao XM, Goldsmith PK, Spiegel AM. Mutational analysis of the cysteines in the extracellular domain of the human ca2+ receptor: Effects on cell surface expression, dimerization and signal transduction. *FEBS letters*. 1998;436:353-356
189. Pidasheva S, Grant M, Canaff L, Ercan O, Kumar U, Hendy GN. Calcium-sensing receptor dimerizes in the endoplasmic reticulum: Biochemical and biophysical characterization of casr mutants retained intracellularly. *Human molecular genetics*. 2006;15:2200-2209
190. Zhang Z, Sun S, Quinn SJ, Brown EM, Bai M. The extracellular calcium-sensing receptor dimerizes through multiple types of intermolecular interactions. *The Journal of biological chemistry*. 2001;276:5316-5322
191. Ray K, Hauschild BC, Steinbach PJ, Goldsmith PK, Hauache O, Spiegel AM. Identification of the cysteine residues in the amino-terminal extracellular domain of the human ca(2+) receptor critical for dimerization. Implications for function of monomeric ca(2+) receptor. *The Journal of biological chemistry*. 1999;274:27642-27650
192. Gama L, Wilt SG, Breitwieser GE. Heterodimerization of calcium sensing receptors with metabotropic glutamate receptors in neurons. *The Journal of biological chemistry*. 2001;276:39053-39059
193. Chang W, Tu C, Cheng Z, Rodriguez L, Chen TH, Gassmann M, Bettler B, Margeta M, Jan LY, Shoback D. Complex formation with the type b gamma-aminobutyric acid receptor affects the expression and signal transduction of the extracellular calcium-sensing receptor. Studies with hek-293 cells and neurons. *The Journal of biological chemistry*. 2007;282:25030-25040
194. Wellendorph P, Johansen LD, Brauner-Osborne H. The emerging role of promiscuous 7tm receptors as chemosensors for food intake. *Vitamins and hormones*. 2010;84:151-184
195. Ward DT. Calcium receptor-mediated intracellular signalling. *Cell calcium*. 2004;35:217-228
196. Kifor O, Diaz R, Butters R, Brown EM. The ca2+-sensing receptor (car) activates phospholipases c, a2, and d in bovine parathyroid and car-

transfected, human embryonic kidney (hek293) cells. *Journal of bone and mineral research : the official journal of the American Society for Bone and Mineral Research*. 1997;12:715-725
197. Mamillapalli R, Wysolmerski J. The calcium-sensing receptor couples to galpha(s) and regulates pthrp and acth secretion in pituitary cells. *The Journal of endocrinology*. 2010;204:287-297
198. Kifor O, MacLeod RJ, Diaz R, Bai M, Yamaguchi T, Yao T, Kifor I, Brown EM. Regulation of map kinase by calcium-sensing receptor in bovine parathyroid and car-transfected hek293 cells. *American journal of physiology. Renal physiology*. 2001;280:F291-302
199. Kimoto K, Nakatsuka K, Matsuo N, Yoshioka H. P38 mapk mediates the expression of type i collagen induced by tgf-beta 2 in human retinal pigment epithelial cells arpe-19. *Investigative ophthalmology & visual science*. 2004;45:2431-2437
200. Varela-Rey M, Montiel-Duarte C, Oses-Prieto JA, Lopez-Zabalza MJ, Jaffrezou JP, Rojkind M, Iraburu MJ. P38 mapk mediates the regulation of alpha1(i) procollagen mrna levels by tnf-alpha and tgf-beta in a cell line of rat hepatic stellate cells(1). *FEBS letters*. 2002;528:133-138
201. Keeton AB, Bortoff KD, Bennett WL, Franklin JL, Venable DY, Messina JL. Insulin-regulated expression of egr-1 and krox20: Dependence on erk1/2 and interaction with p38 and pi3-kinase pathways. *Endocrinology*. 2003;144:5402-5410
202. Hao F, Tan M, Xu X, Cui MZ. Histamine induces egr-1 expression in human aortic endothelial cells via the h1 receptor-mediated protein kinase cdelta-dependent erk activation pathway. *The Journal of biological chemistry*. 2008;283:26928-26936
203. Oldenhof AD, Shynlova OP, Liu M, Langille BL, Lye SJ. Mitogen-activated protein kinases mediate stretch-induced c-fos mrna expression in myometrial smooth muscle cells. *American journal of physiology. Cell physiology*. 2002;283:C1530-1539
204. Luo S, Lee AS. Requirement of the p38 mitogen-activated protein kinase signalling pathway for the induction of the 78 kda glucose-regulated protein/immunoglobulin heavy-chain binding protein by azetidine stress: Activating transcription factor 6 as a target for stress-induced phosphorylation. *The Biochemical journal*. 2002;366:787-795
205. Hirade K, Kozawa O, Tanabe K, Niwa M, Matsuno H, Oiso Y, Akamatsu S, Ito H, Kato K, Katagiri Y, Uematsu T. Thrombin stimulates dissociation and induction of hsp27 via p38 mapk in vascular smooth muscle cells. *American journal of physiology. Heart and circulatory physiology*. 2002;283:H941-948
206. Weiss C, Faust D, Durk H, Kolluri SK, Pelzer A, Schneider S, Dietrich C, Oesch F, Gottlicher M. Tcdd induces c-jun expression via a novel ah (dioxin) receptor-mediated p38-mapk-dependent pathway. *Oncogene*. 2005;24:4975-4983
207. Chanprasert S, Geddis AE, Barroga C, Fox NE, Kaushansky K. Thrombopoietin (tpo) induces c-myc expression through a pi3k- and mapk-dependent pathway that is not mediated by akt, pkczeta or mtor in tpo-dependent cell lines and primary megakaryocytes. *Cellular signalling*. 2006;18:1212-1218

208. Garrett JE, Capuano IV, Hammerland LG, Hung BC, Brown EM, Hebert SC, Nemeth EF, Fuller F. Molecular cloning and functional expression of human parathyroid calcium receptor cdnas. *The Journal of biological chemistry*. 1995;270:12919-12925
209. Bosel J, John M, Freichel M, Blind E. Signaling of the human calcium-sensing receptor expressed in hek293-cells is modulated by protein kinases a and c. *Experimental and clinical endocrinology & diabetes : official journal, German Society of Endocrinology [and] German Diabetes Association*. 2003;111:21-26
210. Racke FK, Nemeth EF. Protein kinase c modulates hormone secretion regulated by extracellular polycations in bovine parathyroid cells. *The Journal of physiology*. 1993;468:163-176
211. Racke FK, Nemeth EF. Cytosolic calcium homeostasis in bovine parathyroid cells and its modulation by protein kinase c. *The Journal of physiology*. 1993;468:141-162
212. Bai M, Trivedi S, Lane CR, Yang Y, Quinn SJ, Brown EM. Protein kinase c phosphorylation of threonine at position 888 in ca2+o-sensing receptor (car) inhibits coupling to ca2+ store release. *The Journal of biological chemistry*. 1998;273:21267-21275
213. Davies SL, Ozawa A, McCormick WD, Dvorak MM, Ward DT. Protein kinase c-mediated phosphorylation of the calcium-sensing receptor is stimulated by receptor activation and attenuated by calyculin-sensitive phosphatase activity. *The Journal of biological chemistry*. 2007;282:15048-15056
214. Awata H, Huang C, Handlogten ME, Miller RT. Interaction of the calcium-sensing receptor and filamin, a potential scaffolding protein. *The Journal of biological chemistry*. 2001;276:34871-34879
215. Huang C, Wu Z, Hujer KM, Miller RT. Silencing of filamin a gene expression inhibits ca2+ -sensing receptor signaling. *FEBS letters*. 2006;580:1795-1800
216. Hjalm G, MacLeod RJ, Kifor O, Chattopadhyay N, Brown EM. Filamin-a binds to the carboxyl-terminal tail of the calcium-sensing receptor, an interaction that participates in car-mediated activation of mitogen-activated protein kinase. *The Journal of biological chemistry*. 2001;276:34880-34887
217. Pi M, Spurney RF, Tu Q, Hinson T, Quarles LD. Calcium-sensing receptor activation of rho involves filamin and rho-guanine nucleotide exchange factor. *Endocrinology*. 2002;143:3830-3838
218. Rey O, Young SH, Yuan J, Slice L, Rozengurt E. Amino acid-stimulated ca2+ oscillations produced by the ca2+-sensing receptor are mediated by a phospholipase c/inositol 1,4,5-trisphosphate-independent pathway that requires g12, rho, filamin-a, and the actin cytoskeleton. *The Journal of biological chemistry*. 2005;280:22875-22882
219. Zhang M, Breitwieser GE. High affinity interaction with filamin a protects against calcium-sensing receptor degradation. *The Journal of biological chemistry*. 2005;280:11140-11146
220. Huang C, Miller RT. The calcium-sensing receptor and its interacting proteins. *Journal of cellular and molecular medicine*. 2007;11:923-934

221. Quinn SJ, Kifor O, Trivedi S, Diaz R, Vassilev P, Brown E. Sodium and ionic strength sensing by the calcium receptor. *The Journal of biological chemistry*. 1998;273:19579-19586
222. Quinn SJ, Bai M, Brown EM. Ph sensing by the calcium-sensing receptor. *The Journal of biological chemistry*. 2004;279:37241-37249
223. Brown EM. The calcium-sensing receptor: Physiology, pathophysiology and car-based therapeutics. *Sub-cellular biochemistry*. 2007;45:139-167
224. Bai M. Structure-function relationship of the extracellular calcium-sensing receptor. *Cell calcium*. 2004;35:197-207
225. Huang Y, Zhou Y, Yang W, Butters R, Lee HW, Li S, Castiblanco A, Brown EM, Yang JJ. Identification and dissection of ca(2+)-binding sites in the extracellular domain of ca(2+)-sensing receptor. *The Journal of biological chemistry*. 2007;282:19000-19010
226. Ray K, Northup J. Evidence for distinct cation and calcimimetic compound (nps 568) recognition domains in the transmembrane regions of the human ca2+ receptor. *The Journal of biological chemistry*. 2002;277:18908-18913
227. Conigrave AD, Quinn SJ, Brown EM. L-amino acid sensing by the extracellular ca2+-sensing receptor. *Proceedings of the National Academy of Sciences of the United States of America*. 2000;97:4814-4819
228. Huang Y, Breitwieser GE. Rescue of calcium-sensing receptor mutants by allosteric modulators reveals a conformational checkpoint in receptor biogenesis. *The Journal of biological chemistry*. 2007;282:9517-9525
229. Zhang Z, Jiang Y, Quinn SJ, Krapcho K, Nemeth EF, Bai M. L-phenylalanine and nps r-467 synergistically potentiate the function of the extracellular calcium-sensing receptor through distinct sites. *The Journal of biological chemistry*. 2002;277:33736-33741
230. Block GA, Martin KJ, de Francisco AL, Turner SA, Avram MM, Suranyi MG, Hercz G, Cunningham J, Abu-Alfa AK, Messa P, Coyne DW, Locatelli F, Cohen RM, Evenepoel P, Moe SM, Fournier A, Braun J, McCary LC, Zani VJ, Olson KA, Drueke TB, Goodman WG. Cinacalcet for secondary hyperparathyroidism in patients receiving hemodialysis. *The New England journal of medicine*. 2004;350:1516-1525
231. Cunningham J. Management of secondary hyperparathyroidism. *Therapeutic apheresis and dialysis : official peer-reviewed journal of the International Society for Apheresis, the Japanese Society for Apheresis, the Japanese Society for Dialysis Therapy*. 2005;9 Suppl 1:S35-40
232. Cunningham J, Danese M, Olson K, Klassen P, Chertow GM. Effects of the calcimimetic cinacalcet hcl on cardiovascular disease, fracture, and health-related quality of life in secondary hyperparathyroidism. *Kidney international*. 2005;68:1793-1800
233. Chertow GM, Pupim LB, Block GA, Correa-Rotter R, Drueke TB, Floege J, Goodman WG, London GM, Mahaffey KW, Moe SM, Wheeler DC, Albizem M, Olson K, Klassen P, Parfrey P. Evaluation of cinacalcet therapy to lower cardiovascular events (evolve): Rationale

and design overview. *Clinical journal of the American Society of Nephrology : CJASN*. 2007;2:898-905
234. Bonet J, Bayes B, Fernandez-Crespo P, Casals M, Lopez-Ayerbe J, Romero R. Cinacalcet may reduce arterial stiffness in patients with chronic renal disease and secondary hyperparathyroidism - results of a small-scale, prospective, observational study. *Clinical nephrology*. 2011;75:181-187
235. Raggi P, Chertow GM, Torres PU, Csiky B, Naso A, Nossuli K, Moustafa M, Goodman WG, Lopez N, Downey G, Dehmel B, Floege J. The advance study: A randomized study to evaluate the effects of cinacalcet plus low-dose vitamin d on vascular calcification in patients on hemodialysis. *Nephrology, dialysis, transplantation : official publication of the European Dialysis and Transplant Association - European Renal Association*. 2011;26:1327-1339
236. Henley C, Davis J, Miller G, Shatzen E, Cattley R, Li X, Martin D, Yao W, Lane N, Shalhoub V. The calcimimetic amg 641 abrogates parathyroid hyperplasia, bone and vascular calcification abnormalities in uremic rats. *European journal of pharmacology*. 2009;616:306-313
237. Kawata T, Nagano N, Obi M, Miyata S, Koyama C, Kobayashi N, Wakita S, Wada M. Cinacalcet suppresses calcification of the aorta and heart in uremic rats. *Kidney international*. 2008;74:1270-1277
238. Lopez I, Aguilera-Tejero E, Mendoza FJ, Almaden Y, Perez J, Martin D, Rodriguez M. Calcimimetic r-568 decreases extraosseous calcifications in uremic rats treated with calcitriol. *Journal of the American Society of Nephrology : JASN*. 2006;17:795-804
239. Lopez I, Mendoza FJ, Guerrero F, Almaden Y, Henley C, Aguilera-Tejero E, Rodriguez M. The calcimimetic amg 641 accelerates regression of extraosseous calcification in uremic rats. *American journal of physiology. Renal physiology*. 2009;296:F1376-1385
240. Ivanovski O, Nikolov IG, Joki N, Caudrillier A, Phan O, Mentaverri R, Maizel J, Hamada Y, Nguyen-Khoa T, Fukagawa M, Kamel S, Lacour B, Drueke TB, Massy ZA. The calcimimetic r-568 retards uremia-enhanced vascular calcification and atherosclerosis in apolipoprotein e deficient (apoe-/-) mice. *Atherosclerosis*. 2009;205:55-62
241. Weston AH, Absi M, Ward DT, Ohanian J, Dodd RH, Dauban P, Petrel C, Ruat M, Edwards G. Evidence in favor of a calcium-sensing receptor in arterial endothelial cells: Studies with calindol and calhex 231. *Circulation research*. 2005;97:391-398
242. Molostvov G, Fletcher S, Bland R, Zehnder D. Extracellular calcium-sensing receptor mediated signalling is involved in human vascular smooth muscle cell proliferation and apoptosis. *Cellular physiology and biochemistry : international journal of experimental cellular physiology, biochemistry, and pharmacology*. 2008;22:413-422
243. Molostvov G, James S, Fletcher S, Bennett J, Lehnert H, Bland R, Zehnder D. Extracellular calcium-sensing receptor is functionally expressed in human artery. *American journal of physiology. Renal physiology*. 2007;293:F946-955
244. Smajilovic S, Hansen JL, Christoffersen TE, Lewin E, Sheikh SP, Terwilliger EF, Brown EM, Haunso S, Tfelt-Hansen J. Extracellular

calcium sensing in rat aortic vascular smooth muscle cells. *Biochemical and biophysical research communications*. 2006;348:1215-1223
245. Klein GL, Enkhbaatar P, Traber DL, Buja LM, Jonkam CC, Poindexter BJ, Bick RJ. Cardiovascular distribution of the calcium sensing receptor before and after burns. *Burns : journal of the International Society for Burn Injuries*. 2008;34:370-375
246. Shalhoub V, Shatzen E, Henley C, Boedigheimer M, McNinch J, Manoukian R, Damore M, Fitzpatrick D, Haas K, Twomey B, Kiaei P, Ward S, Lacey DL, Martin D. Calcification inhibitors and wnt signaling proteins are implicated in bovine artery smooth muscle cell calcification in the presence of phosphate and vitamin d sterols. *Calcified tissue international*. 2006;79:431-442
247. Caudrillier A, Petit L, Boudot Z, Massy Z, Brazier M, Mentaverri R, Kamel S. Involvement of the car in smooth muscle cell mineralisation during atherosclerosis. *Bone*. 2009;44:S294
248. Ashley AE, Niebauer J. Cardiology explained. 2004
249. Shanahan CM, Cary NR, Salisbury JR, Proudfoot D, Weissberg PL, Edmonds ME. Medial localization of mineralization-regulating proteins in association with monckeberg's sclerosis: Evidence for smooth muscle cell-mediated vascular calcification. *Circulation*. 1999;100:2168-2176
250. Tanimura A, McGregor DH, Anderson HC. Calcification in atherosclerosis. I. Human studies. *Journal of experimental pathology*. 1986;2:261-273
251. Rozen S, Skaletsky H. Primer3 on the www for general users and for biologist programmers. *Methods in molecular biology*. 2000;132:365-386
252. Nemeth EF. Summary--calcium receptors: Potential targets for novel treatments for skeletal disease. *Journal of musculoskeletal & neuronal interactions*. 2004;4:416-417
253. Shi Y, Pieniek M, Fard A, O'Brien J, Mannion JD, Zalewski A. Adventitial remodeling after coronary arterial injury. *Circulation*. 1996;93:340-348
254. Storch KN, Taatjes DJ, Bouffard NA, Locknar S, Bishop NM, Langevin HM. Alpha smooth muscle actin distribution in cytoplasm and nuclear invaginations of connective tissue fibroblasts. *Histochemistry and cell biology*. 2007;127:523-530
255. Watson KE, Bostrom K, Ravindranath R, Lam T, Norton B, Demer LL. Tgf-beta 1 and 25-hydroxycholesterol stimulate osteoblast-like vascular cells to calcify. *The Journal of clinical investigation*. 1994;93:2106-2113
256. Tintut Y, Patel J, Parhami F, Demer LL. Tumor necrosis factor-alpha promotes in vitro calcification of vascular cells via the camp pathway. *Circulation*. 2000;102:2636-2642
257. Tintut Y, Parhami F, Bostrom K, Jackson SM, Demer LL. Camp stimulates osteoblast-like differentiation of calcifying vascular cells. Potential signaling pathway for vascular calcification. *The Journal of biological chemistry*. 1998;273:7547-7553
258. Rensen SS, Doevendans PA, van Eys GJ. Regulation and characteristics of vascular smooth muscle cell phenotypic diversity.

*Netherlands heart journal : monthly journal of the Netherlands Society of Cardiology and the Netherlands Heart Foundation*. 2007;15:100-108
259. Nakano-Kurimoto R, Ikeda K, Uraoka M, Nakagawa Y, Yutaka K, Koide M, Takahashi T, Matoba S, Yamada H, Okigaki M, Matsubara H. Replicative senescence of vascular smooth muscle cells enhances the calcification through initiating the osteoblastic transition. *American journal of physiology. Heart and circulatory physiology*. 2009;297:H1673-1684
260. Chattopadhyay N, Yano S, Tfelt-Hansen J, Rooney P, Kanuparthi D, Bandyopadhyay S, Ren X, Terwilliger E, Brown EM. Mitogenic action of calcium-sensing receptor on rat calvarial osteoblasts. *Endocrinology*. 2004;145:3451-3462
261. Yamauchi M, Yamaguchi T, Kaji H, Sugimoto T, Chihara K. Involvement of calcium-sensing receptor in osteoblastic differentiation of mouse mc3t3-e1 cells. *American journal of physiology. Endocrinology and metabolism*. 2005;288:E608-616
262. Bai M, Quinn S, Trivedi S, Kifor O, Pearce SH, Pollak MR, Krapcho K, Hebert SC, Brown EM. Expression and characterization of inactivating and activating mutations in the human ca2+o-sensing receptor. *The Journal of biological chemistry*. 1996;271:19537-19545
263. Bai M, Trivedi S, Kifor O, Quinn SJ, Brown EM. Intermolecular interactions between dimeric calcium-sensing receptor monomers are important for its normal function. *Proceedings of the National Academy of Sciences of the United States of America*. 1999;96:2834-2839
264. Golub EE, Harrison G, Taylor AG, Camper S, Shapiro IM. The role of alkaline phosphatase in cartilage mineralization. *Bone and mineral*. 1992;17:273-278
265. Mendoza FJ, Lopez I, Canalejo R, Almaden Y, Martin D, Aguilera-Tejero E, Rodriguez M. Direct upregulation of parathyroid calcium-sensing receptor and vitamin d receptor by calcimimetics in uremic rats. *American journal of physiology. Renal physiology*. 2009;296:F605-613
266. Mizobuchi M, Hatamura I, Ogata H, Saji F, Uda S, Shiizaki K, Sakaguchi T, Negi S, Kinugasa E, Koshikawa S, Akizawa T. Calcimimetic compound upregulates decreased calcium-sensing receptor expression level in parathyroid glands of rats with chronic renal insufficiency. *Journal of the American Society of Nephrology : JASN*. 2004;15:2579-2587
267. MacLeod RJ, Chattopadhyay N, Brown EM. Pthrp stimulated by the calcium-sensing receptor requires map kinase activation. *American journal of physiology. Endocrinology and metabolism*. 2003;284:E435-442
268. Hobson SA, Wright J, Lee F, McNeil SE, Bilderback T, Rodland KD. Activation of the map kinase cascade by exogenous calcium-sensing receptor. *Molecular and cellular endocrinology*. 2003;200:189-198
269. McNeil SE, Hobson SA, Nipper V, Rodland KD. Functional calcium-sensing receptors in rat fibroblasts are required for activation of src kinase and mitogen-activated protein kinase in response to extracellular calcium. *The Journal of biological chemistry*. 1998;273:1114-1120

270. Huang Z, Cheng SL, Slatopolsky E. Sustained activation of the extracellular signal-regulated kinase pathway is required for extracellular calcium stimulation of human osteoblast proliferation. *The Journal of biological chemistry*. 2001;276:21351-21358
271. Yamaguchi T, Chattopadhyay N, Kifor O, Sanders JL, Brown EM. Activation of p42/44 and p38 mitogen-activated protein kinases by extracellular calcium-sensing receptor agonists induces mitogenic responses in the mouse osteoblastic mc3t3-e1 cell line. *Biochemical and biophysical research communications*. 2000;279:363-368
272. Ward DT, McLarnon SJ, Riccardi D. Aminoglycosides increase intracellular calcium levels and erk activity in proximal tubular ok cells expressing the extracellular calcium-sensing receptor. *Journal of the American Society of Nephrology : JASN*. 2002;13:1481-1489
273. Hobson SA, McNeil SE, Lee F, Rodland KD. Signal transduction mechanisms linking increased extracellular calcium to proliferation in ovarian surface epithelial cells. *Experimental cell research*. 2000;258:1-11
274. Radcliff K, Tang TB, Lim J, Zhang Z, Abedin M, Demer LL, Tintut Y. Insulin-like growth factor-i regulates proliferation and osteoblastic differentiation of calcifying vascular cells via extracellular signal-regulated protein kinase and phosphatidylinositol 3-kinase pathways. *Circulation research*. 2005;96:398-400
275. Di Bartolo BA, Schoppet M, Mattar MZ, Rachner TD, Shanahan CM, Kavurma MM. Calcium and osteoprotegerin regulate igf1r expression to inhibit vascular calcification. *Cardiovascular research*. 2011;91:537-545
276. Mercer J, Figg N, Stoneman V, Braganza D, Bennett MR. Endogenous p53 protects vascular smooth muscle cells from apoptosis and reduces atherosclerosis in apoe knockout mice. *Circulation research*. 2005;96:667-674
277. White E, McKenna J, Cavanaugh A, Breitwieser GE. Pharmacochaperone-mediated rescue of calcium-sensing receptor loss-of-function mutants. *Molecular endocrinology*. 2009;23:1115-1123
278. Ward DT, Riccardi D. New concepts in calcium-sensing receptor pharmacology and signalling. *British journal of pharmacology*. 2011
279. Tfelt-Hansen J, MacLeod RJ, Chattopadhyay N, Yano S, Quinn S, Ren X, Terwilliger EF, Schwarz P, Brown EM. Calcium-sensing receptor stimulates pthrp release by pathways dependent on pkc, p38 mapk, jnk, and erk1/2 in h-500 cells. *American journal of physiology. Endocrinology and metabolism*. 2003;285:E329-337
280. Liao XB, Zhou XM, Li JM, Yang JF, Tan ZP, Hu ZW, Liu W, Lu Y, Yuan LQ. Taurine inhibits osteoblastic differentiation of vascular smooth muscle cells via the erk pathway. *Amino acids*. 2008;34:525-530
281. You H, Yang H, Zhu Q, Li M, Xue J, Gu Y, Lin S, Ding F. Advanced oxidation protein products induce vascular calcification by promoting osteoblastic trans-differentiation of smooth muscle cells via oxidative stress and erk pathway. *Renal failure*. 2009;31:313-319
282. Gu X, Masters KS. Role of the mapk/erk pathway in valvular interstitial cell calcification. *American journal of physiology. Heart and circulatory physiology*. 2009;296:H1748-1757

283. Xiao G, Jiang D, Thomas P, Benson MD, Guan K, Karsenty G, Franceschi RT. Mapk pathways activate and phosphorylate the osteoblast-specific transcription factor, cbfa1. *The Journal of biological chemistry*. 2000;275:4453-4459
284. Wang X, Harimoto K, Liu J, Guo J, Hinshaw S, Chang Z, Wang Z. Spata4 promotes osteoblast differentiation through erk-activated runx2 pathway. *Journal of bone and mineral research : the official journal of the American Society for Bone and Mineral Research*. 2011
285. Gallea S, Lallemand F, Atfi A, Rawadi G, Ramez V, Spinella-Jaegle S, Kawai S, Faucheu C, Huet L, Baron R, Roman-Roman S. Activation of mitogen-activated protein kinase cascades is involved in regulation of bone morphogenetic protein-2-induced osteoblast differentiation in pluripotent c2c12 cells. *Bone*. 2001;28:491-498
286. Schauwienold D, Plum C, Helbing T, Voigt P, Bobbert T, Hoffmann D, Paul M, Reusch HP. Erk1/2-dependent contractile protein expression in vascular smooth muscle cells. *Hypertension*. 2003;41:546-552
287. Simmons CA, Nikolovski J, Thornton AJ, Matlis S, Mooney DJ. Mechanical stimulation and mitogen-activated protein kinase signaling independently regulate osteogenic differentiation and mineralization by calcifying vascular cells. *Journal of biomechanics*. 2004;37:1531-1541
288. Ghoda L, Lin X, Greene WC. The 90-kda ribosomal s6 kinase (pp90rsk) phosphorylates the n-terminal regulatory domain of ikappabalpha and stimulates its degradation in vitro. *The Journal of biological chemistry*. 1997;272:21281-21288
289. Chen RH, Abate C, Blenis J. Phosphorylation of the c-fos transrepression domain by mitogen-activated protein kinase and 90-kda ribosomal s6 kinase. *Proceedings of the National Academy of Sciences of the United States of America*. 1993;90:10952-10956
290. Xing J, Ginty DD, Greenberg ME. Coupling of the ras-mapk pathway to gene activation by rsk2, a growth factor-regulated creb kinase. *Science*. 1996;273:959-963
291. Fisher TL, Blenis J. Evidence for two catalytically active kinase domains in pp90rsk. *Molecular and cellular biology*. 1996;16:1212-1219
292. Zoubeidi A, Zardan A, Wiedmann RM, Locke J, Beraldi E, Fazli L, Gleave ME. Hsp27 promotes insulin-like growth factor-i survival signaling in prostate cancer via p90rsk-dependent phosphorylation and inactivation of bad. *Cancer research*. 2010;70:2307-2317
293. Tan Y, Ruan H, Demeter MR, Comb MJ. P90(rsk) blocks bad-mediated cell death via a protein kinase c-dependent pathway. *The Journal of biological chemistry*. 1999;274:34859-34867
294. Desmouliere A, Rubbia-Brandt L, Abdiu A, Walz T, Macieira-Coelho A, Gabbiani G. Alpha-smooth muscle actin is expressed in a subpopulation of cultured and cloned fibroblasts and is modulated by gamma-interferon. *Experimental cell research*. 1992;201:64-73
295. Nakagawa K, Parekh N, Koleganova N, Ritz E, Schaefer F, Schmitt CP. Acute cardiovascular effects of the calcimimetic r-568 and its enantiomer s-568 in rats. *Pediatr Nephrol*. 2009;24:1385-1389

296. Chang W, Tu C, Chen TH, Bikle D, Shoback D. The extracellular calcium-sensing receptor (casr) is a critical modulator of skeletal development. *Science signaling*. 2008;1:ra1

# Chapter 6: Appendix

## 6.1 Serum batch testing

In vitro, mineralisation of BAoSMC is dependent on the batch of serum used (Prof. Ann Canfield, University of Manchester, personal communication). Therefore prior to experimentation serum is assessed for its ability to induce mineralisation. The figure below (Figure 6.1) illustrates one such experiment.

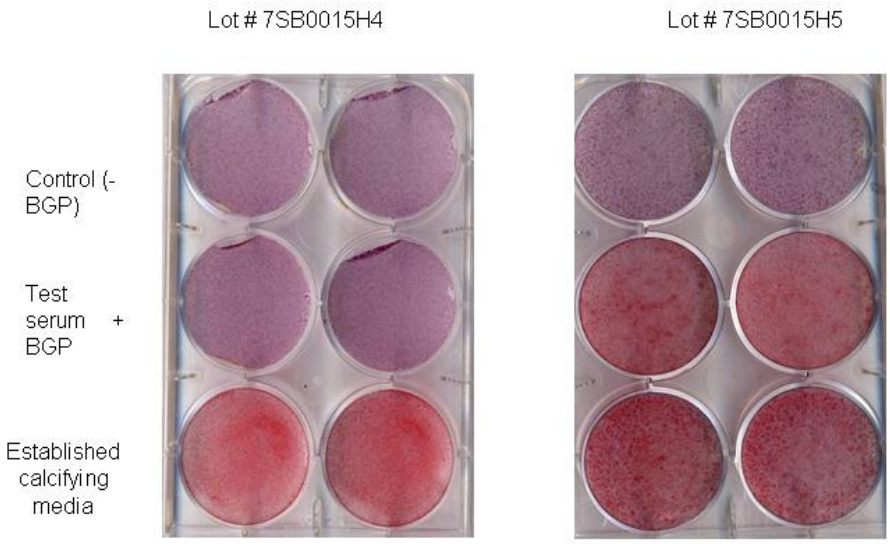


**Figure 6.1 Serum batch testing.** BAoSMC were grown to confluence in 10% FCS–DMEM containing 1.2 mM $Ca^{2+}$. Upon confluence cells were incubated with 1.8 mM $Ca^{2+}$ with (i) established calcifying serum but no BGP (negative control), (ii) test serum in the presence of BGP or (iii) established calcifying serum in the presence of 5 mM BGP (positive control). A lots of serum were tested 7SB0015HA and 7SB0015H5. Cells were treated for 10 days before fixing and staining with ARS, illustrating mineral deposition.

## 6.2. Supplementary figures

The following figures show additional data / repeat experiments from findings presented with the results section (Chapter 3).

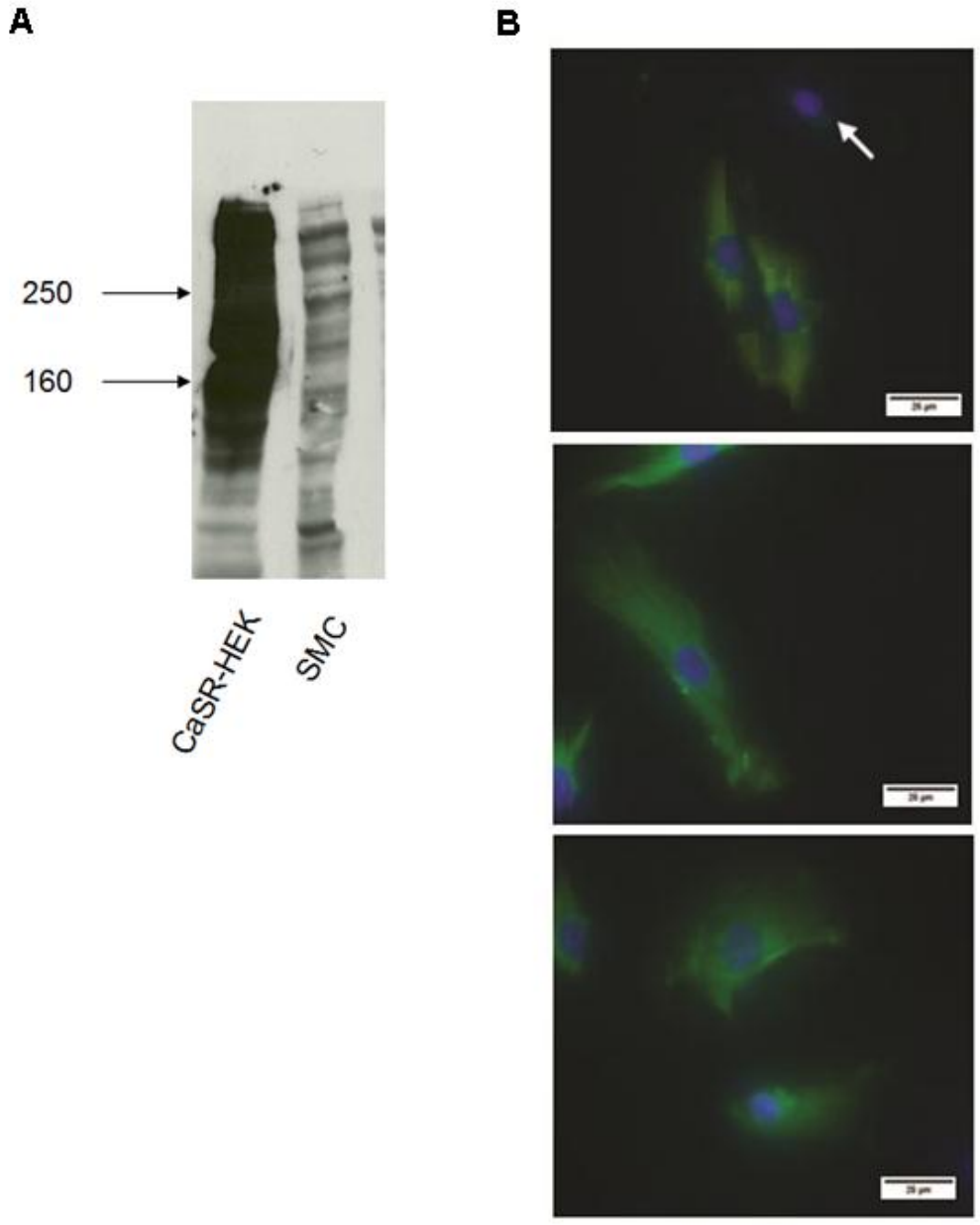


**Figure 6.2 CaSR immunoreactivity in BAoSMC (supplement to Figure 3.4)** A: Membrane preparations from cultured BAoSMC (prep C; passage 4) were separated using 5% SDS-PAGE and CaSR immunoreactivity detected by Western blotting using a CaSR antibody (1:5000). Exposure time 2 min. Original figure (Figure 3.4) shows immunoreactivities at two different exposure times, optimised for visualisation of SMC CaSR and CaSR-HEK CaSR. Size (in kDa) of molecular weight markers is indicated on the left. B: BAosMC (prep C; passage 4) grown on chamber slides for 24 hrs in 10% FCS-DMEM (1.2 mM $Ca^{2+}$) were fixed with 4% formaldehyde before incubation with a polyclonal antibody against human CaSR (1:200). A fluorescein isothiocyanate (FITC)-conjugated secondary antibody (green; 1:40) and DAPI (blue) was used to visualise the CaSR and nuclear staining (i). Arrow used to highlight cells with negative staining. Bar = 25 µm.

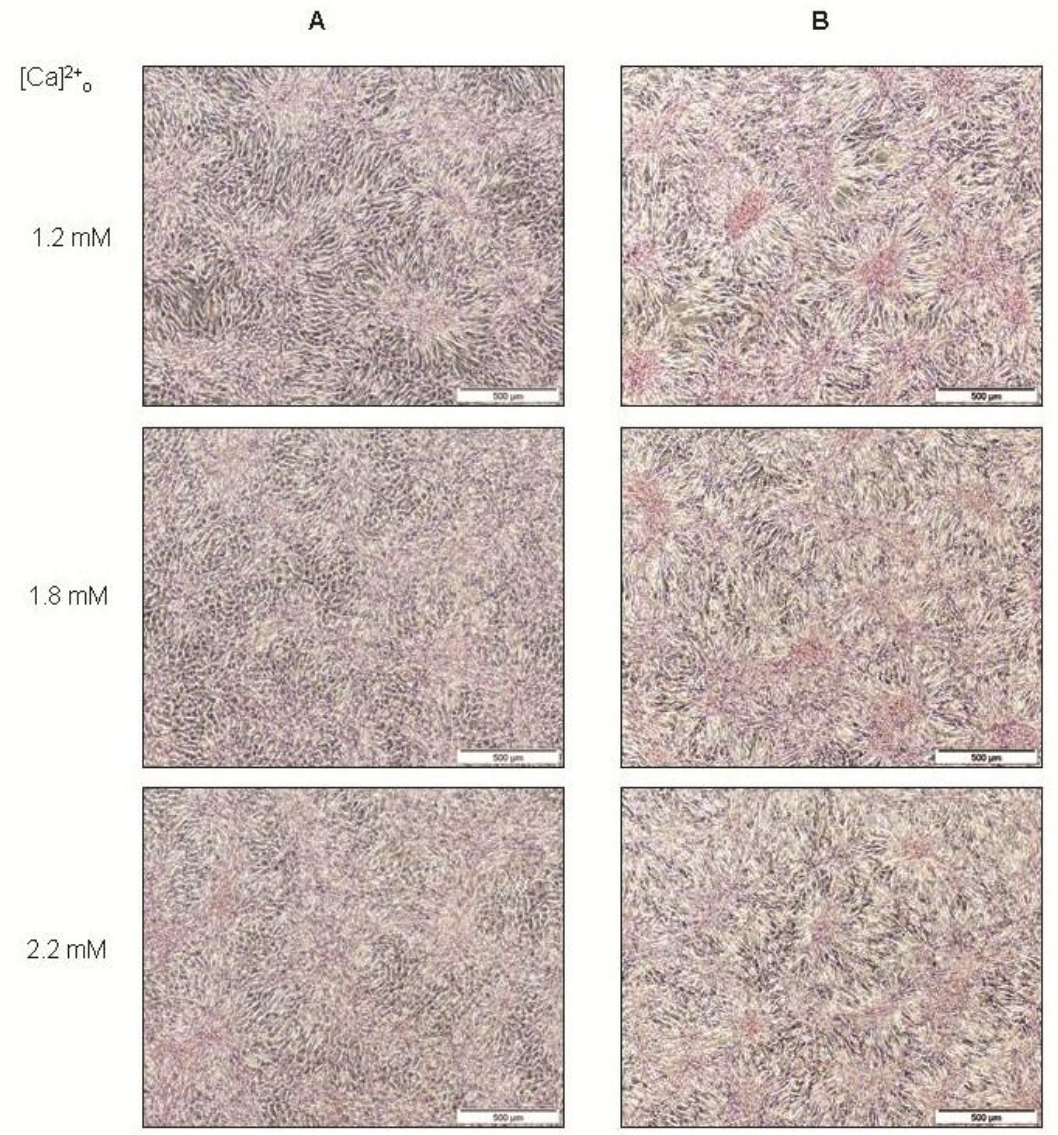


**Figure 6.3 $Ca^{2+}$-induced mineralisation requires the presence of BGP (supplement to Figure 3.6).** A and B represent independent experiments. BAoSMC (prep C; passage 6 and 7) were treated upon confluence with increasing concentrations of $Ca^{2+}$ in the absence of BGP. Images show cells stained with alizarin red at days 17 (experiment A) and 13 (experiment B). Bar = 500 µm.

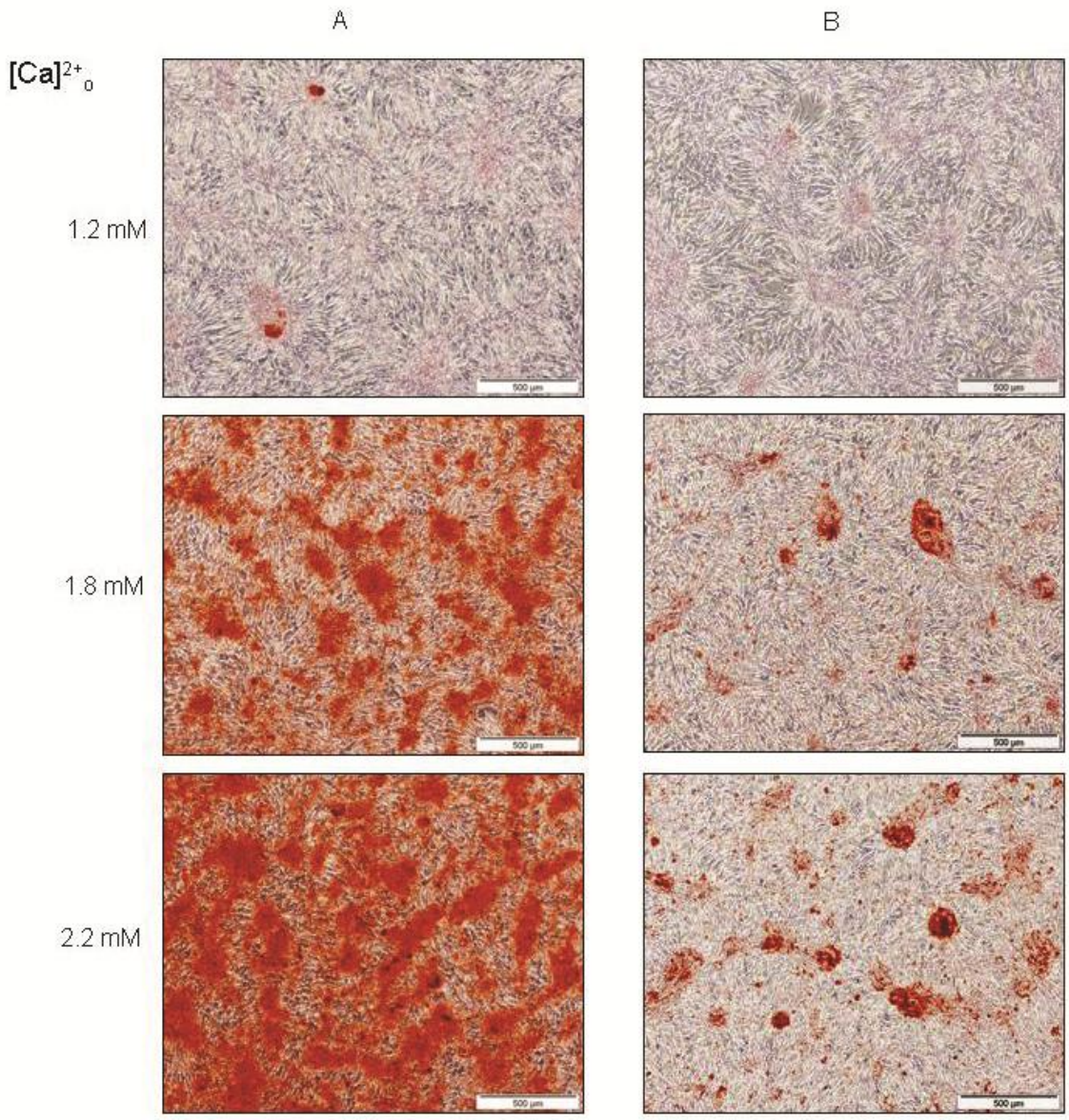


**Figure 6.4 Concentration-dependent effects of $Ca^{2+}_o$ on SMC mineral deposition (supplement to Figure 3.7).** A and B represent independent experiments. BAoSMC (prep C; passage 6 and 7) were treated upon confluence with increasing concentrations of $Ca^{2+}$ alongside 5 mM BGP. Images show cells stained with alizarin red at day 17 (experiment A) and day 13 (experiment B). Bar = 500 µm.

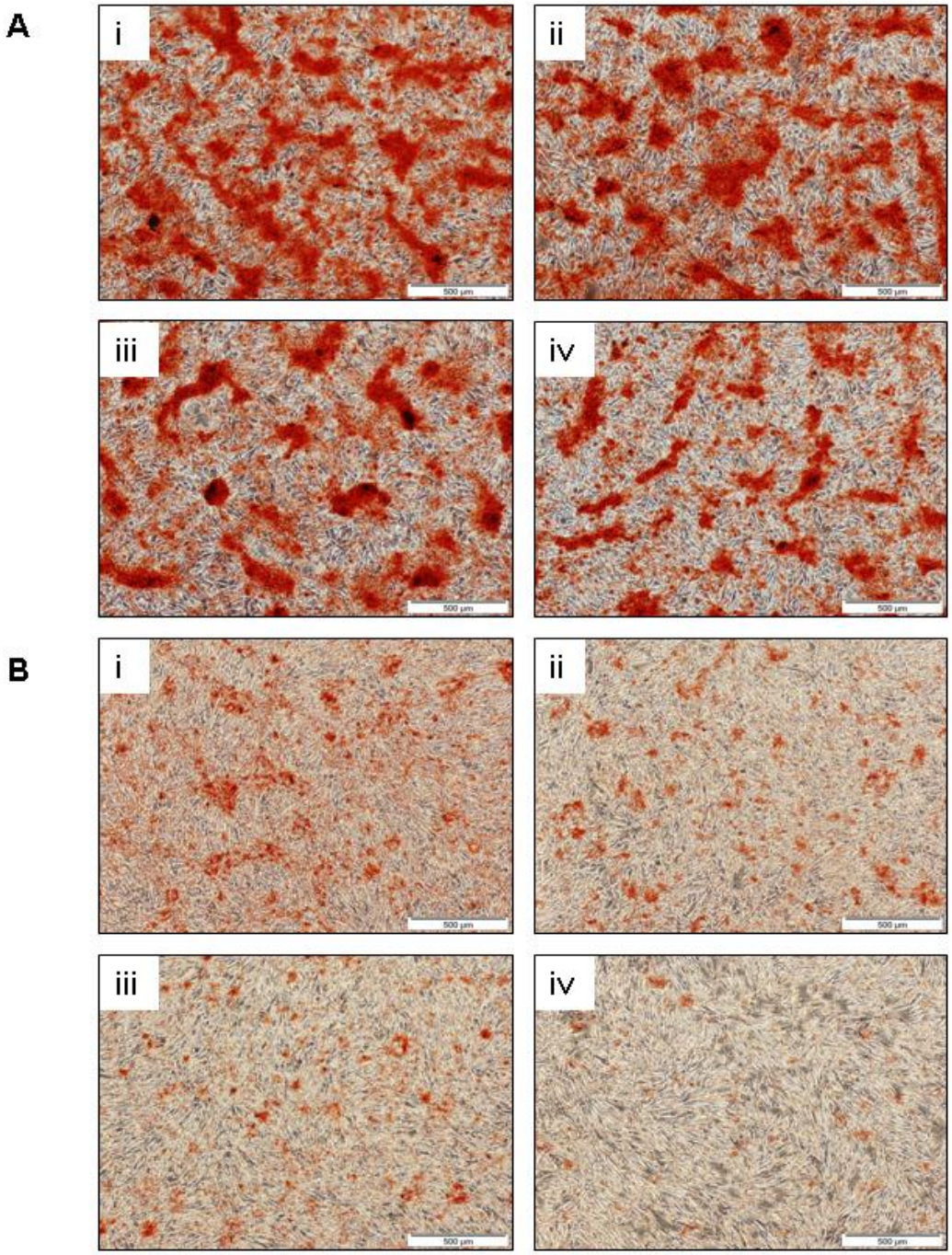


**Figure 6.5 Effect of AMG641 on $Ca^{2+}$-induced mineralisation (supplement to Figure 3.10).**

A and B represent independent experiments. BAoSMC (prep C; passage 8 and 9) were treated upon confluence with 1.8 mM $Ca^{2+}$ and 5 mM BGP in the presence of vehicle (1:1000 DMSO) (i) or AMG641 at 10 pM (ii), 100 pM (iii) and 1 nM (iv). Images show cells stained with alizarin red at day 19 (experiment A) and day 11 (experiment B). Bar = 500 µm.

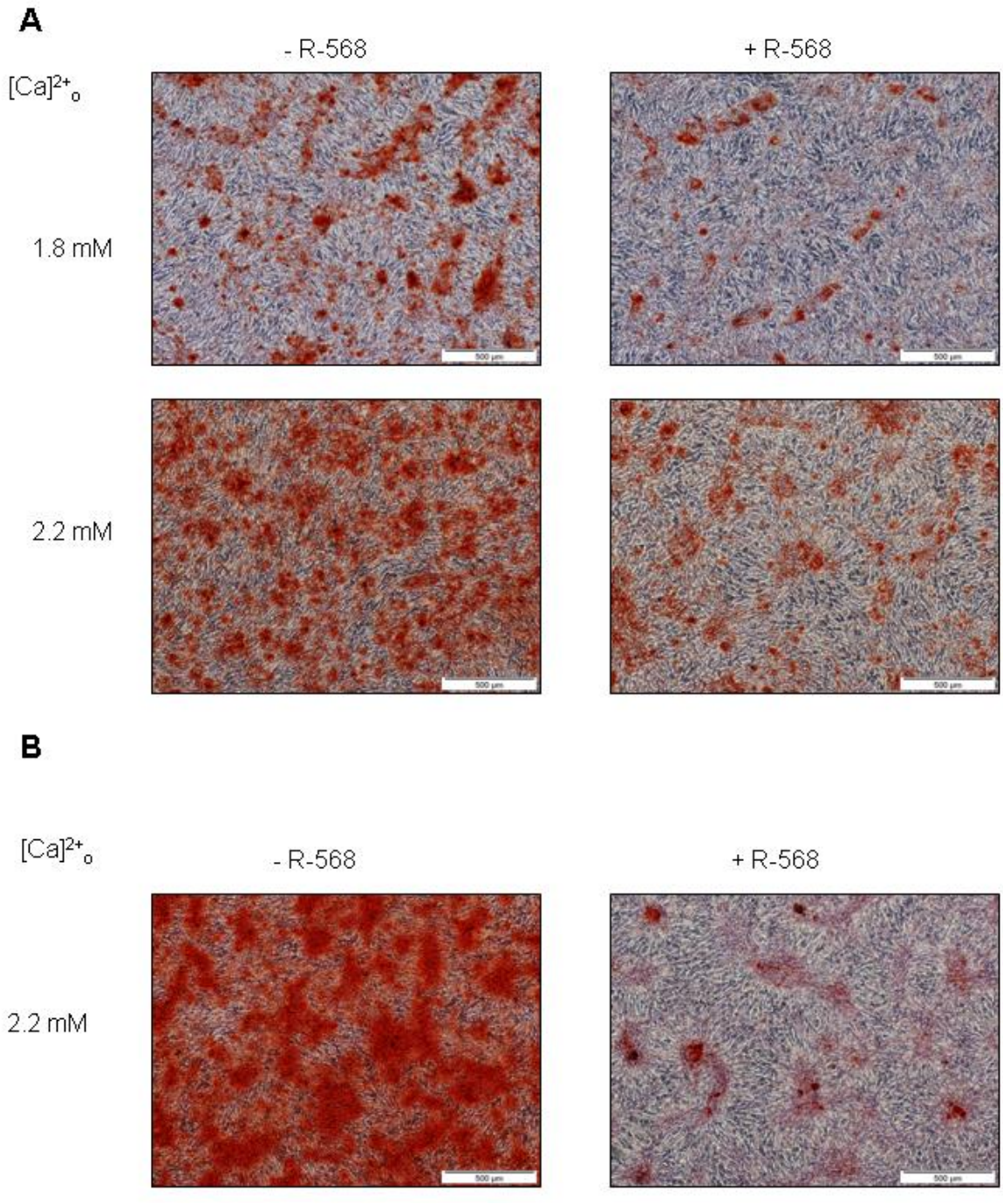


**Figure 6.6 Protective actions of R-568 on $Ca^{2+}$-induced mineralisation (supplement to Figure 3.11).** A & B represent independent experiments. BAoSMCs (prep C; passage 6 and 8) were cultured in 5% FCS-DMEM and 5 mM BGP with 1.8 or 2.2 mM $Ca^{2+}$ in the presence or absence of R-568. Cells were stained with alizarin red at day 15 (experiment A) and day 18 (experiment B). Bar = 500 µm.

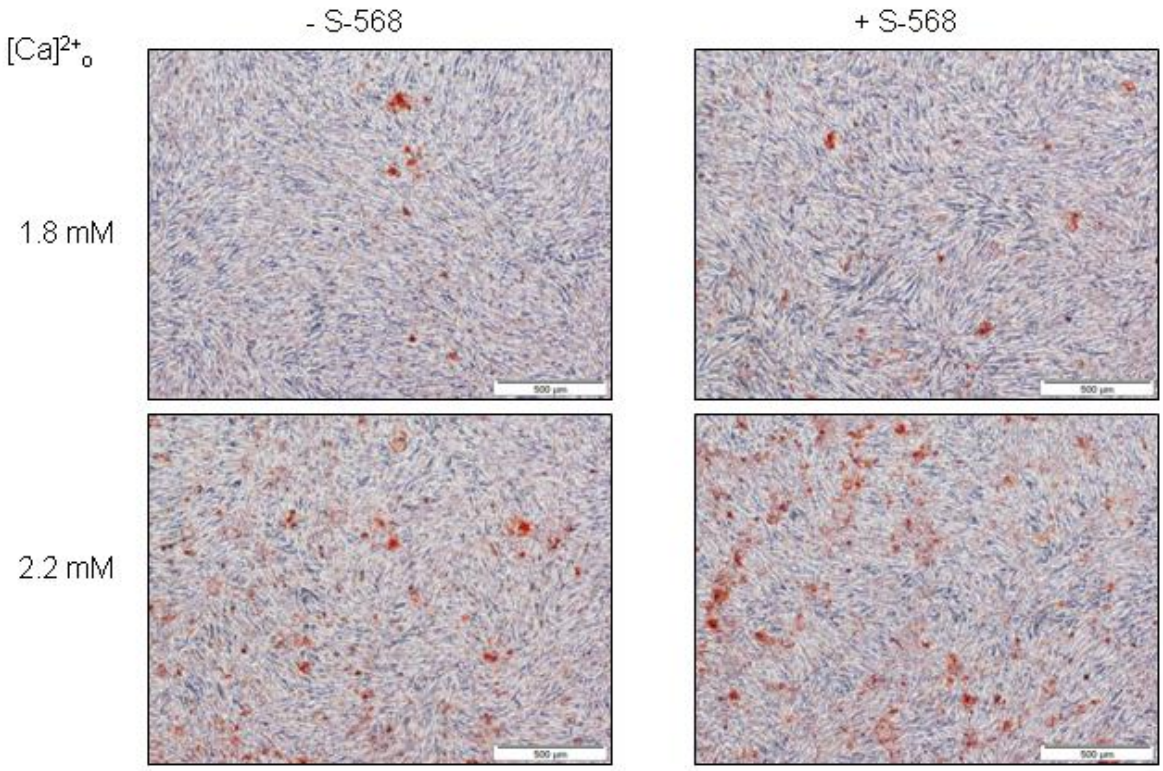


**Figure 6.7 S-568 does not delay $Ca^{2+}$-induced mineralisation (supplement to 3.12).**

BAoSMCs (prep C; passage 9) were incubated with 1.8 mM or 2.2 mM $Ca^{2+}$ in the presence or absence of S-568. Cells were stained with alizarin red at day 10. Bar = 500 µm.